To the Graduate Council:

I am submitting herewith a thesis written by Christopher A. Moniodes entitled "Export Coefficient Modeling of Water Pollutants with Geographic Information Science: An Examination of Geographic Scale." I have examined the final paper copy of this thesis for form and content and recommend that it be accepted in partial fulfillment of the requirements for the degree of Master of Science, with a major in Geography.

Carol P. Harden, Major Professor

We have read this thesis
and recommend its acceptance:

Bruce A. Ralston

Kenneth H. Orvis

Accepted for the Council:

Vice Chancellor and Dean of Graduate Studies

EXPORT COEFFICIENT MODELING OF WATER POLLUTANTS WITH GEOGRAPHIC INFORMATION SCIENCE: AN EXAMINATION OF GEOGRAPHIC SCALE

A Thesis
Presented for the
Master of Science
Degree
The University of Tennessee, Knoxville

Christopher A. Moniodes
May 2004

Thesis
2004
.M66

Copyright © *Chris Moniodes* 2004

All Rights Reserved

ACKNOWLEDGMENTS

There are several people I want to thank for their vision, motivation, support, and interest in this thesis. First, I would like to thank all the members on my advisory committee. I especially want to thank Dr. Carol Harden for motivating me to become a better writer, researcher, and geographer, and for spending the time to help me develop this idea into a thesis topic. I thank Drs. Bruce Ralston and Ken Orvis for their hard work in making sure my writing was understandable, and for their critical thought on the topic. I want to give special thanks to Dr. Anita Drever, who was not part of my committee, but provided some much-needed help with the multiple regression model.

I thank Dr. Roger Tankersley, Jr. and Dennis Yankee from the Tennessee Valley Authority for their critical thought and support, and for their answers to all my "good" questions! I want to also thank Roger and Dennis for giving me the opportunity to work as a research assistant with TVA; the knowledge and "wisdom" they provided me over the last two years will last a lifetime. I thank Tom McDonough from TVA for his interest in and support of this thesis.

I thank Dr. Joanne Logan and Susanna Sutherland for their help in collecting in-stream water quality measurements during summer 2003. I especially want to thank Susanna for her extremely hard work in analyzing and testing all water quality samples.

Lastly, I want to thank my parents, Chris and Peggy Moniodes, who gave me support and motivation through both undergraduate and graduate school. They will be pleased to know that I am now ready to get a job!

ABSTRACT

Land cover data are frequently used as a basis for estimating total phosphorus (TP) and total nitrogen (TN) delivered to surface waters. Nutrients, such as TP and TN, are a leading cause of water quality impairment in the United States. Section 305(b) of the Clean Water Act requires each state to report all impaired surface waters every two years. Ideally, this is accomplished with in-stream measurements; however, the cost and time requirements of such a daunting task are too great for most states to incur. Alternatively, the export coefficient model (ECM) uses commonly available land cover and elevation data to screen watershed areas for high levels of nutrient export quickly and inexpensively. Incorporating the ECM into a GIS architecture allows a watershed manager to visualize nutrient export over large areas and prioritize those areas accordingly. Once specific nutrient-yielding areas have been identified and prioritized, the watershed manager can implement more detailed monitoring and analysis programs.

New developments in GIS have produced a wide range of commonly available broad-scale geospatial data. For example, the United States Geological Survey (USGS) freely distributes National Land Cover Data (NLCD), which identify 21 classes of land cover for the conterminous United States at 30-m resolution. Conversely, fine-scale, fine-resolution geospatial data, such as locally mapped, 10-m resolution land cover data, are not widely available, costly, and usually developed for small areas on a client-by-client basis. In regions where fine-scale, fine-resolution data are not available, watershed managers need information on the performance of water quality models using fine-scale, fine-resolution versus broad-scale, coarse-resolution data (e.g., 30-m NLCD).

The purpose of this thesis is to determine if broad-scale land cover data (e.g., 30-m NLCD), incorporated within a broad-scale hydrologic model, are appropriate for effectively screening county- or smaller-sized areas for excessive nutrient exports, prioritizing those areas, and making management decisions based on the prioritization. I answer five questions for addressing this issue:

1. Can broad-scale, coarse-resolution land cover data capture enough detail to produce usable model results for stream remediation decisions?

2. At what spatial scale do model results produced from fine- and broad-scale land cover datasets become statistically different?

3. At what spatial scale does the prioritization of sub-watersheds for nutrient flux change between simulations that use different land cover data?

4. Within sub-watersheds, is excessive nutrient export more likely to originate in the riparian zone or farther from the stream?

5. Does the prioritization of areas within watersheds for nutrient flux reduction change between simulations using fine- and broad-scale data, such that model results suggest different management scenarios?

Using an ECM, I simulated nutrient loading for Blount County and the Little River watershed (BCLRW), Tennessee. I compare model results produced from an ensemble of model runs that incorporated various land cover datasets (of 10-m, 30-m, and 1-km resolution) at multiple spatial mapping extents, which were represented by 4^{th}, 5^{th}, and 6^{th} order stream contributing areas. Within Arc/Info© GRID©, I constructed an unweighted ECM that simulates cumulative nutrient exports by watershed, and a weighted ECM that considers topographic orientation and nutrient trapping ability for simulating nutrient export within the watershed, allowing the researcher to examine nutrient export on a pixel-by-pixel basis.

Overall, results support the hypothesis that broad-scale land cover data (e.g., 30-m NLCD) are appropriate for prioritizing sub-watershed for nutrient flux remediation at the county-mapping scale in study areas similar to BCLRW. Results from unweighted ECM simulations suggest that cumulative nutrient fluxes of 4th order watershed differ significantly between models based on 30-m and 10-m resolution land cover data. However, as the area of analysis increases from watersheds of 4th order streams to those of 5th and 6th order streams, predictions based on 10-m and 30-m input data are not significantly different.

Weighted ECM simulations using both broad-scale (30-m) and fine-scale (10-m) data suggest that nutrient fluxes originate in non-riparian areas of the Blount County/Little River watershed study area. Simulations based on coarser-resolution (30-m) land cover data produced similar patters of nutrient export within watersheds as simulations based on higher resolution (10-m) data, but the former accounted for 9% (TP) to 19% (TN) of the high nutrient export identified by the latter.

Findings from this research do not suggest that detailed data are unnecessary for modeling the hydrologic processes and water quality of a particular watershed, only that these data are unnecessary for screening and prioritizing risk areas in a county-sized area. This project was confined to BCLRW, therefore, the findings are empirical rather than theoretical. This research is a first step in exploring the effects that geographic scale and geospatial data resolution have on county-wide hydrologic modeling. Future research should expand this study and determine whether nutrient modeling trends observed in this research are similar to those in other places.

TABLE OF CONTENTS

CHAPTER I: INTRODUCTION 1

CHAPTER II: THE STUDY AREA AND LITERATURE SURVEY 9

The Study Area 9
Literature Survey 14
Land Use and Water Quality Problems 14
Geographic Scale in Water Quality Studies 18
Hydrologic Modeling and Geographic Scale 20
The Impact of Geographic Information Science (GIS) on Hydrologic Modeling 22
The Export Coefficient Model 26

CHAPTER III: METHODS: OBJECTIVES AND DATA PREPARATION 31

Project Scope and Objectives 31
GIS and Water Quality Data 32
Land Cover Data 33
Elevation Data 40
Water Quality Data 42
Sub-Watershed Delineation 46

CHAPTER IV: METHODS: THE EXPORT MODEL APPROACH 50

Export Coefficient Value Calculation 51
Background and Methods 51
Results and Discussion of Export Coefficient Value Calculation 56
Export Coefficient Model Calibration 59
The Unweighted Export Coefficient Model 62
The Weighted Export Coefficient Model 64
The Topographic Index (TI) 65
The Buffer Index (BI) 70
Normalization of Topographic and Buffer Indices 76
Weighted Export Coefficient Model Application 78

CHAPTER V: RESULTS 81

Calibration Analysis: Export Coefficient Value Selection 81
The Unweighted Export Coefficient Model Analysis 83
The Weighted Export Coefficient Model Analysis 100

CHAPTER VI: DISCUSSION AND CONCLUSION 109

Research Implications 109
Scale and Data 109
Differences in Nutrient Between Sub-Watersheds 112

Differences in Nutrient Loading Within Sub-Watersheds 114
Model Limitations 118
General Limitations 118
BCLRW-ECMs Limitations 120
Application of BCLRW-ECMs to Other Regions 123
Future Research 125

WORKS CITED 129

APPENDIX 140

VITA 156

LIST OF TABLES

TABLE **PAGE**

1. Reclassified land cover composition 36

2. Riparian land cover composition associated with drainage areas above each sampling site 54

3. Annualized riparian nutrient fluxes associated with drainage areas above each sampling site 55

4. Multiple regression model coefficient estimates for nutrient loadings as a function of land cover percent in BCLRW 57

5. Quartile aggregation of literature reported TP and TN ECVs by land cover. 61

6. Nutrient retention values by land cover class 73

7. Statistical differences in unweighted ECM results between IPSI- and NLCD-based simulations 86

8. Twenty-fifth percentile nutrient loading values 103

9. Percentage of each risk-watershed's total area associated with a high nutrient loading 104

A.1. IPSI and NLCD original land cover classification schemes with generalized and detailed categories 141

A.2. IPSI, NLCD, and LULC-AVHRR reclassification into the six-class scheme 144

A.3. IPSI land cover composition associated with drainage area above each sampling site 147

A.4. Literature survey of TP and TN export coefficient values 149

A.5. Calibration loading values 150

A.6. Categorical breaks in unweighted ECM results produced using all three land cover datasets 151

LIST OF FIGURES

FIGURE		PAGE
1.	The study area	10
2.	The study area and surrounding hydrologic features	11
3.	Land cover reclassification	37
4.	TDEC sampling site locations	43
5.	Ellejoy Creek and Nails Creek sampling sites	45
6.	Sub-watershed mapping extent	47
7.	Topographic index (TI) computation	67
8.	Topographic and buffer indices map	69
9.	Buffer index (BI) computation	71
10.	Unweighted vs. weighted ECM nutrient export map	80
11.	ECM calibration results	82
12.	Difference within and between land cover-based TP simulation results	84
13.	Difference within and between land cover-based TN simulation results	85
14.	4^{th} order watershed prioritization for TP export	88
15.	5^{th} order watershed prioritization for TP export	89
16.	6^{th} order watershed prioritization for TP export	90
17.	4^{th} order watershed prioritization for TN export	91
18.	5^{th} order watershed prioritization for TN export	92
19.	6^{th} order watershed prioritization for TN export	93

20. Correlation between IPSI- and NLCD-based TP simulations 95

21. Correlation between IPSI- and NLCD-based TN simulations.....96

22. Correlation map of watershed prioritization for TP export 97

23. Correlation map of watershed prioritization for TN export.....98

24. The weighted ECM study area.....101

25. High TP export from weighted ECM simulations 106

26. High TN export from weighted ECM simulations 107

27. Detailed map of high TP fluxes produced from 10-m and 30-m data-based simulations.....117

A.1. Logarithmic transformation of TP results produced from ECM simulations 152

A.2. Logarithmic transformation of TN results produced from ECM simulations 153

A.3. TP flux by sub-watershed with natural-break values.....154

A.4. TN flux by sub-watershed with natural-break values 155

CHAPTER I
INTRODUCTION

Land cover data are frequently used in estimating nutrient constituents of total phosphorus (TP) and total nitrogen (TN) delivered to surface waters (Wickham and Wade 2002). Empirical studies have shown a strong relationship between land cover composition and TP and TN exports from watersheds (Haith 1976; Omernik 1976; Hill 1978; Konrad *et al.*1985; Gale *et al.* 1993; Heng and Nikolaidis 1998; Nerbonne and Vondracek 2001; Wang *et al.* 2002). Enhancements in computer technology and geographic information science (GIS) enable researchers to broaden the spatial scale of hydrologic modeling applications. Incorporating land cover information into GIS-based modeling applications allows the watershed manager to conceptualize and visualize current and future trends of surface water impairment by nutrients (Burian *et al.* 2002).

Surface water pollution sources can be categorized as point source or non-point source (NPS). In past years, regulations affecting stream water quality in the United States have been focused on discharges from factories, waste facilities, sewage facilities, and other point sources (Carrubba 2000). By the 1970s, governmental regulations such as the Clean Water Act (1972) compelled industries to address and reduce point source discharges (e.g., the National Pollution Discharge Elimination System) (USEPA 2003a). Although this helped to reduce pollution, surface water quality degradation is now being attributed to NPS water pollution (Sliva and Williams 2000).

NPS pollutants usually originate from upland watershed lands and are transported via overland flow pathways to standing and running surface waters. NPS pollutants may

originate in large contributing areas with complex topography and land cover, thus making their sources hard to identify (Likens and Bormann 1974; Henderson and Harris 1975; Dillon and Kirchner 1975; Haith 1976; Omernik 1976; Hill 1978; Konrad *et al.*1985; Gale *et al.* 1993; Heng and Nikolaidis 1998; Carrubba 2000; Sliva and Williams 2000; Nerbonne and Vondracek 2001; Wang *et al.* 2002). Sediment and nitrogen can contaminate public drinking water supplies and affect aquatic species diversity and abundance (Likens and Bormann 1974; Henderson and Harris 1975). Extensive phosphorus loading accelerates surface water eutrophication (Reckhow *et al.* 1980; Winter and Duthie 2000; Fisher *et al.* 2000). While other NPS pollutant constituents can also be problematic for environmental systems and human use, this research incorporates only TP and TN into the modeling process.

Section 305(b) of the Clean Water Act of 1972 requires each state to identify impaired waters and assess point sources and NPSs of pollution every two years (USEPA 2002). During the 1990s, the United States Environmental Protection Agency's (USEPA) Watershed Initiative broadened the spatial scale of NPS remediation by requiring NPS assessment across entire watersheds rather than in localized areas. Ideally, this is to be done through direct in-stream monitoring programs; however, the time and money required for monitoring make comprehensive sampling prohibitively expensive for most states (McFarland and Hauck 2001; Burt and Johnes 2002).

Alternatively, the export coefficient model (ECM) allows researchers to target areas for stream remediation quickly and inexpensively. ECModeling assumes that, for similar climatic regimes, land cover will export a known amount of nutrients. Using readily available land cover data and export coefficient values (ECVs), which are annual

estimates of pollutant loading per land cover areal unit, it is possible to estimate a watershed's annual nutrient export (Winter and Duthie 2000). When built within a GIS framework, the ECM allows a researcher to evaluate broad-scale areas for management *a priori*, visualizing nutrient-risk areas and prioritizing them accordingly (Johnes 1996; Mattikalli and Richards 1996; Johnes and Heathwaite 1997; Endreny and Wood 2003).

Unlike complex, hourly-time-step, hydrologic models with large data requirements, which are cumbersome and complicated to implement at broad scales (Johnes 1996; Soranno *et al.* 1996; Endreny and Wood 2003), the ECM uses general rules of watershed response from commonly available data, such as land cover, ECVs, and elevation, to estimate real world watershed processes at broad scales (Endreny and Wood 2003). Land cover data and elevation data are available from the United States Geological Survey (USGS), which freely distributes 30-m resolution National Land Cover Data (NLCD) (*ca.* 1992), global 1-km Land Cover/Land Use Data (*ca.* 1992), and digital elevation models (DEM) (of 1-km, 30-m, and 10-m resolution) for the conterminous United States, over the World Wide Web. ECVs are available in the hydrologic literature, where numerous empirical studies report observed nutrient export values and calculated ECVs that can be extrapolated to broader watershed scales (Reckhow *et al.* 1980; Beaulac and Reckhow 1982; Frink 1991; Wickham and Wade 2001).

One significant advantage of ECModeling is the ability to analyze large areas. Watershed managers and county planners often need broad-scale information to quickly evaluate and prioritize nutrient-exporting areas. The use of commonly available data is an economically feasible alternative to fine-scale assessments of in-stream water quality

and land cover patterns (Johnes 1996; Johnes and Heathwaite 1997; Endreny and Wood 2003). While broad-scale data (e.g., 30 m resolution extending across the conterminous U.S.) may introduce uncertainty to particular locations within the watershed (Meentemeyer 1989), the level of uncertainty can be appropriate for broad-scale studies, such as those covering entire counties or watersheds. Once the ECM has identified critical contributing areas, more expensive, detailed in-stream water quality measurements and modeling may be implemented in targeted areas.

BASINS (Better Assessment Science Integrating Point and Nonpoint Sources) (USEPA 2001a)—a collection of hydrologic models, GIS toolsets, and geospatial datasets that operate within the ArcView 3.x computing architecture—includes PLOAD, a lumped annual pollutant load model that emulates ECModeling. Like most ECMs, PLOAD does not model hourly time-step activities, nor does it require extensive meteorological data or atmosphere-vegetation-soil equations; rather, PLOAD uses simple ECM ideology and commonly available data to prioritize sub-watersheds (USEPA 2001b; Endreny and Wood 2003; Endreny *et al.* 2003).

Although accurate ECVs are critical components to ECModeling, the outcome of modeling depends on land cover scale and resolution. Therefore, different model results may be obtained from broad-scale, coarse resolution (e.g., 30-m) versus fine-scale, fine-resolution (e.g., 10-m) land cover data due to differences in areal measurements of each land cover type.

Several researchers have extended the traditional methods of ECModeling by including other variables such as terrain shape, runoff pathway characteristics, and buffer likelihood into the modeling procedure. Few studies, however, have focused on

questions that arise when considering land cover scale and resolution in different modeling environments. Burian *et al.* (2002) compared several land cover datasets for application in urban environmental modeling. Their study found that in areas 24 km^2 in size, simulated nutrient and sediment loadings, based on broad-scale land cover (e.g., 1:250,000 and/or 30-m resolution), were 8% to 40% higher compared to results based on locally or regionally mapped land cover (e.g., < 10 m resolution). They suggest that in small, urban areas significant differences in runoff volume and pollutant load can be expected between models based on broad-scale, coarse-resolution and fine-scale, fine-resolution land cover.

Konarska *et al.* (2002) compared model results from 1-km and 30-m land cover in an assessment of the total value of ecological service for the conterminous United States. They used land cover to represent ecological value, which they described as the goods produced (e.g., timber, pharmaceuticals, and seafood) or the services provided by an ecosystem (e.g., air and water purification, stabilization of climate, and generation and renewal of soil and soil fertility). Konarska *et al.* (2002) found total ecological value, according to 30-m land cover, to be 200% higher than the value derived from 1-km land cover data. They note these differences are due to finer-resolution data (30 m) capturing more ecologically *valued* land cover types such as wetland areas.

Endreny *et al.* (2003) used three land cover datasets—Geographic Information Retrieval Analysis System (GIRAS), NLCD, and data derived from aerial color near-infrared digital orthophoto quarter quadrangles (DOQQ)—as inputs to test flow hydrograph sensitivity levels in the Croton watershed of southeastern New York produced from WinHPSF, a real-time hydrologic model bundled within BASINS. Their

study determined the degree to which different land cover datasets, which contain different measures of impervious surfaces and bare soil, control simulated flow level. In other words, are there differences in a specific flow peak(s), or does the general shape of the model-derived hydrograph change when swapping land cover data? Their results indicate that model sensitivity to different land cover datasets is significant for estimating specific peak flow discharges, but land cover data swapping does not significantly change the general shape of the flow hydrograph, which can be considered a broader-scale watershed characteristic.

These studies show significant differences between results produced from environmental modeling with broad- versus fine-scale land cover. While absolute pollutant loads or runoff volume estimates, for example, may differ significantly between land cover datasets, no existing research addresses the question: Are broad-scale land cover data (e.g., 30-m NLCD), incorporated within a broad-scale hydrologic model (e.g., ECM), appropriate for effectively screening county- or smaller-sized areas for excessive nutrient exports, prioritizing those areas, and making management decisions based on the prioritization?

Developing fine-scale, fine-resolution land cover data is costly in both time and money. As various broad-scale land cover data become more widely available and modeling is implemented in larger areas, the watershed manager is faced with important questions: Which land cover dataset to use? What spatial scale (e.g., watershed size) is appropriate for conducting ECModeling with 30-m data? Ultimately, the goal of my research is to provide insight into these issues and guide local watershed managers in future stream remediation projects. In this thesis, I implement an ECM that uses three

different land cover datasets (10-m, 30-m, and 1-km resolution) at three levels of spatial scale, which are represented by sub-watershed size, to address the following questions:

1. Can broad-scale, coarse-resolution land cover data capture enough detail to produce usable model results for stream remediation decisions?

2. At what spatial scale do model results produced from fine- and broad-scale land cover datasets become statistically different?

3. At what spatial scale does the prioritization of sub-watersheds for nutrient flux change between simulations that use different land cover data?

4. Within sub-watersheds, is excessive nutrient export more likely to originate in the riparian zone or farther from the stream?

5. Does the prioritization of areas within watersheds for nutrient flux reduction change between simulations using fine- and broad-scale data, such that model results suggest different management scenarios?

The study area for this project is Blount County and the Little River Watershed, Tennessee. In answering the above questions, I compare ECModeling results from three land cover datasets: (a) fine-scale (10-m) land cover data that are part of the Integrated Pollution Source Identification (IPSI) geographic database developed by the Tennessee Valley Authority (TVA); (b) broad-scale (30-m) National Land Cover Data (NLCD) developed by the Multi-Resolution Land Characterization (MRLC) consortium, a group of federally funded agencies; and (c) global-scale (1-km) Advanced Very High Resolution Radiometer Land Use/Land Cover (LULC-AVHRR), developed by the National Aeronautics and Space Administration (NASA).

In this research, I first use a multiple regression approach to develop TP and TN ECVs from in-stream measurements taken in the Little River watershed between January 1998 and November 2003. Next, I develop two ECMs within the Arc/Info© GRID©

module (ESRI 2001): (1) an unweighted ECM that uses traditional methods suggested by Reckhow *et al.* (1980), and (2) a weighted ECM that builds upon the work of Beven and Kirkby (1979), Beven (1995), and Endreny and Wood (2003). I calibrated both models with in-stream TP and TN concentrations collected from June to November 2003 in Ellejoy Creek and Nails Creek watersheds, which are Little River sub-watersheds. I ran the unweighted ECM at three different spatial mapping extents, which are represented by 4^{th}, 5^{th}, and 6^{th} order stream contributing areas. For clarity, I refer to each level of spatial mapping extent simply as *watershed extent*. I compare differences between unweighted ECM results based on varying levels of watershed extent using an ANOVA test and correlation matrix. I then use the weighted ECM, which considers topographic orientation and nutrient trapping ability, to illustrate nutrient flux differences within watersheds and between land cover simulations.

This thesis is organized as follows: Chapter II discusses the study area of Blount County and the Little River Watershed, and the importance of spatial scale in hydrologic modeling; Chapter III discusses data acquisition and preparation; Chapter IV presents methods and results from ECV calculation using multiple regression and details the development of weighted and unweighted ECMs; Chapter V presents the results from the ECM calibration, the unweighted ECM analysis, and the weighted ECM analysis. Finally, Chapter VI discusses research implications arising from the findings of this study, ECM limitations, and future research.

CHAPTER II
STUDY AREA AND LITERATURE SURVEY

This chapter discusses the study area used in this thesis, and surveys literature that addresses the relationship between land cover composition and water quality and the importance of spatial scale in hydrologic modeling.

The Study Area

The study area for this thesis is Blount County (BC), Tennessee and the Little River watershed (LRW), which extends into Sevier and Knox counties, Tennessee (Figure 1). Located in northeastern Tennessee, BCLRW covers approximately 1,744 km^2 and includes portions of two 8-digit USGS Hydrologic Unit Code (HUC) watersheds: Watts Bar Lake (06010201) and Lower Little Tennessee River (06010204) (Figure 2). The study area contains primarily forest land cover in the upland regions and intensive agriculture and urban areas in lowland regions.

BCLRW is located in the upper Tennessee River Valley, a northeast to southwest draining river basin that stretches from southwest Virginia to western Tennessee. Situated between the Blue Ridge Mountains and Cumberland Plateau, the study area includes portions of two major physiographic provinces: the Ridge and Valley in the west and the Blue Ridge Mountains in the east. Topography varies from gently rolling valleys to extremely steep slopes; elevations range from approximately 228 m in the valleys to 1,500 m in the mountains, creating a hydrologic environment where streams

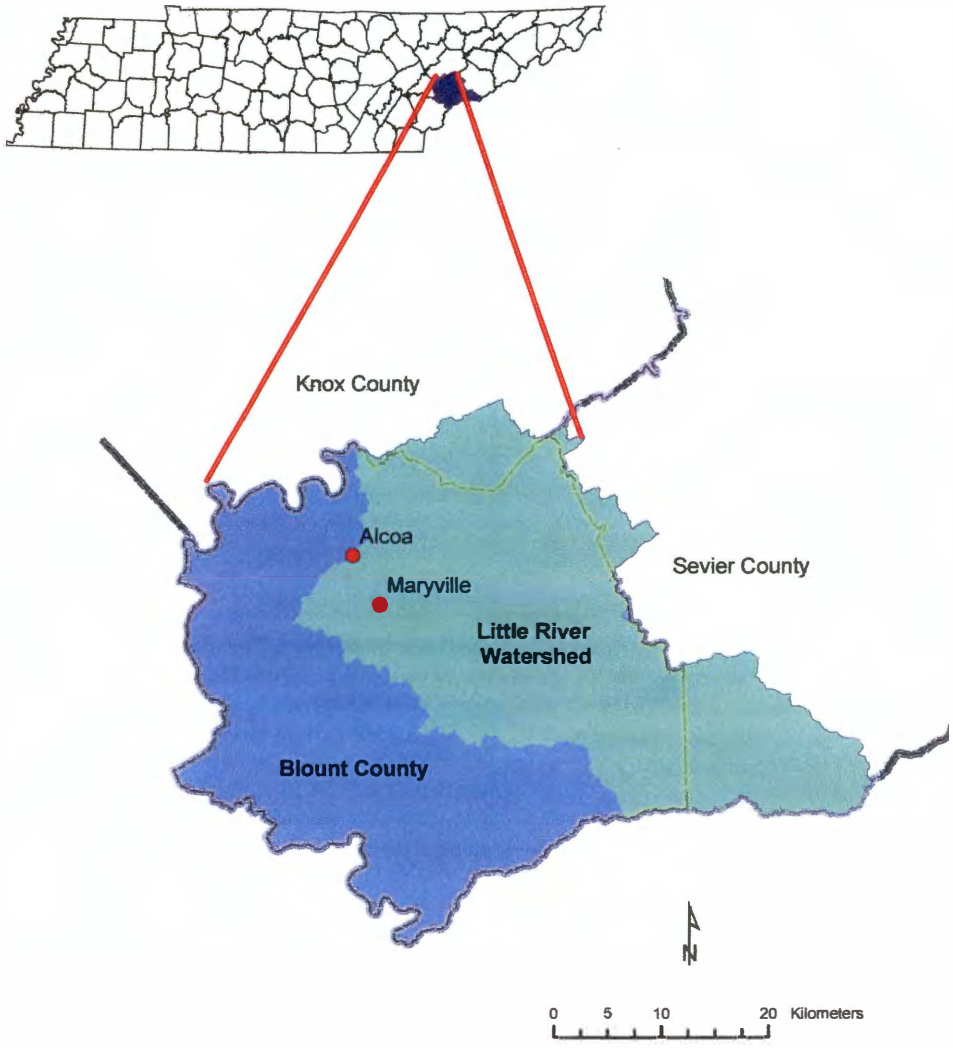


Figure 1: The study area. Blount County and the Little River watershed (BCLRW) of eastern Tennessee.

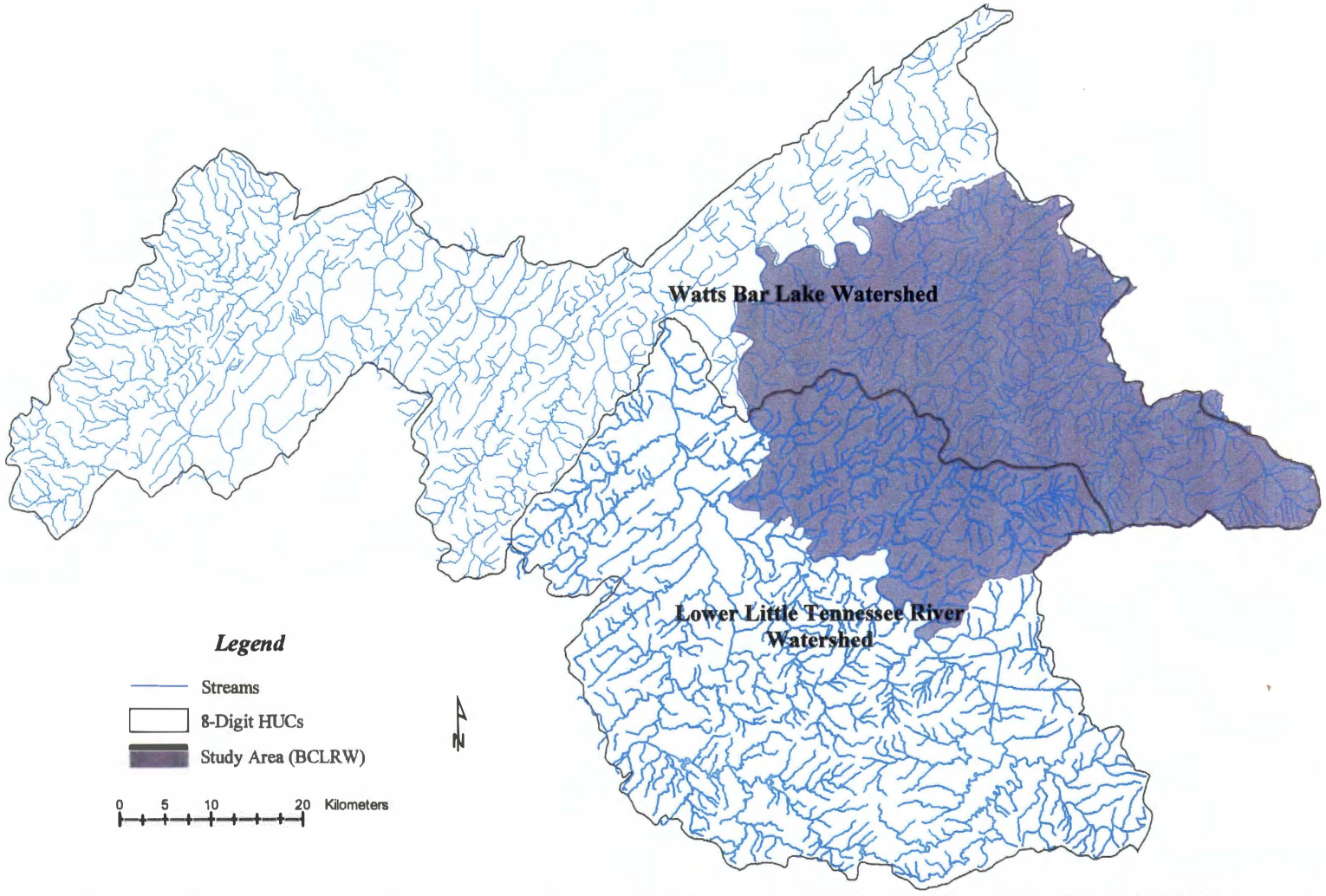


Figure 2: The study area and surrounding hydrologic features. BCLRW is located in the Watts Bar Lake (06010201) and Lower Little Tennessee River (06010204) USGS 8-digit watersheds.

follow a trellis pattern and flow through narrow valley floors or cut across steep ridges (Smith 2000).

The underlying geology includes Ordovician and Cambrian limestones, shales, dolomites, and Paleozoic sandstones (Rodgers 1953). Heavily forested mountain area soils are low in fertility, acidic, and light in color (Smith 2000), while valley soils—classified as Alfisols, Inceptisols, and Ultisols—are well drained, shallow to deep, and loamy to clayey (Springer and Elder 1980; Eric Henry, *personal communication*). Natural vegetation, primarily forest, contains a variety of hardwood and softwood species; however, various anthropogenic factors, such as logging operations, have converted portions of the mixed hardwood forest to predominately shallow-rooted, agricultural vegetation such as row crops and pasture grasses (Smith 2000; DeSelm 2001). Climatic conditions are characteristic of the eastern United States humid continental climate, with hot summers and short mild winters. Precipitation is greatest during the winter and spring months when annual rainfall averages roughly 112 to 140 cm. Annual temperature ranges are 50°C to 60°C, depending on topography (DeSelm 2001).

The Little River Watershed, which covers 28% of Watts Bar Lake Watershed and drains a total of roughly 979 km^2, includes approximately 27,435 ha of Great Smoky Mountain National Park forest in upland areas. Preserved tributary streams converge to form the upland portions of the Little River, which is an ecoregion reference stream, classified by the USEPA as a viable natural resource that can be used to establish water quality standards and for public recreation. However, water quality effects of intensive lowland agricultural practices and increases in urban growth have caused most Little

River tributaries, such as Pistol Creek, Ellejoy Creek, Nails Creek, Crooked Creek, Short Creek, Roddy Branch, and Russell Branch, to be listed on the 305(b) report of 2000 as impaired waters.

The portion of BCLWR that is not drained by the Little River watershed covers 21% of the Lower Little Tennessee River Watershed and includes 24,733 ha of Great Smoky Mountains National Park. Lowland sections of this region also include intensive urban development, and agricultural practices have caused most streams, such as Baker Creek and Ninemile Creek, to be listed as impaired on the Tennessee 305(b) report of 2000 (TVA 2003).

BCLRW includes the population centers of Maryville (~20,000) and Alcoa (~7,000). Total population in the study area during 2000 was roughly 105,823. Although most (63%) of BCLRW's population resides in urban areas, a high proportion (37%) lives in rural areas (U.S. Census Bureau 2000).

Blount County includes approximately 37,721 ha of agricultural land, which contain 2,380 farms that average roughly 36 ha in size. Total cropland covers roughly 2,701 ha; however, most farming operations are devoted to livestock (60%), which includes beef cattle, dairy cattle, hogs, and sheep. Beef cattle operations represent the largest proportion of livestock operations (96%), with a head count of 33,609 total cattle, while dairy cattle (2%), hog (1%), and sheep (1%) farms occupy smaller areas (USDA 1997).

As an area rich in water resources, outdoor recreation, wildlife and plant species, and farming, BCLRW is environmentally and economically important to the people of eastern Tennessee. Ongoing efforts by the Blount County government, United States

Department of Agricultural (USDA), Tennessee Department of Environmental Conservation (TDEC), Tennessee Valley Authority (TVA), the University of Tennessee (UT), and the Little River Water Quality Forum (LRWQF) share the goals of assessing and improving water quality for present and future use.

Literature Survey

Water quality remediation and the increasing impact of agricultural practices on surface waters makes BCLRW an ideal area for conducting water quality modeling analysis with geographic information science (GIS) and export coefficients. This section discusses the relationship between water quality and intense agricultural practices and reviews different theories behind broad-scale water quality modeling with export coefficients and GIS.

Land Use and Water Quality Problems

Empirical studies suggest a strong relationship between NPS pollution loading of surface waters and the intensity of human land use activity in upland and lowland areas (Likens and Bormann 1974; Henderson and Harris 1975; Dillon and Kirchner 1975; Haith 1976; Omernik 1976; Hill 1978; Konrad *et al.*1985; Gale *et al.* 1993; Heng and Nikolaidis 1998; Carrubba 2000; Nerbonne and Vondracek 2001; Wang *et al.* 2002).

In BCLRW, agricultural practices have been targeted as a primary land use contributing to water quality degradation (TVA 2003). Pollutants such as sediment, nitrogen, and phosphorus are transported through the area via runoff pathways to

standing and flowing surface waters. Forest cover extent and density are major factors regulating runoff rates in this region (TVA 2003; Eric Henry, *personal communication*). Dense forest cover provides deep-rooted vegetation that stabilizes soil, regulates infiltration rates, takes up moisture for photosynthesis, and filters subsurface and surface flow (Hill 1978; Mander *et al.* 1998). In BCLRW, most forested areas have been converted to shallow-rooted row crop and pasture lands, causing lower evapotranspiration levels, higher infiltration rates, higher runoff rates, less soil stability, less vegetative filtration and, ultimately, higher export of pollutants to surface waters.

In 1992, the USEPA targeted agricultural practices as the number one source of surface water pollution in the United States (Wang *et al.* 2002). Agriculture practices in upland areas can lead to the excess delivery of animal wastes, inorganic nutrients, pesticides, herbicides, and sediment to streams (Heng and Nikolaidis 1998; Nerbonne and Vondracek 2001; Wang *et al.* 2002). The reduction of riparian vegetation due to livestock grazing causes extensive stream bank instability, resulting in additional soil losses and destabilization of stream channels (Konrad *et al.*1985; Gale *et al.* 1993; Sliva and Williams 2001; Wang *et al.* 2002).

Sediment loading, the most common NPS pollutant in the United States, impairs approximately 50% of the nation's streams (Nerbonne and Vondracek 2001). Excessive delivery of sediment to surface waters via overland flow has detrimental effects on water quality, drinking water supplies, and stream habitat for fish and invertebrate species (Jones *et al.* 2001; Sliva and Williams 2001). Watersheds with high proportions of impervious surfaces from roads and urban areas greatly increase the frequency and magnitude of rainfall runoff and thus the risk of erosion and sediment loading into

surface waters (Harden 1992; Arnold and Gibbons 1996). Furthermore, agriculture on slopes greater than 3% can also cause erosion and excessive sediment loading (Wischmeier and Smith 1978; Jones *et al.* 2001), and will result in lower crop yields and lower pasture productivity due to infertile soils (Hill 1978). In this research, I was unable to locate sufficient sediment water quality data for sediment modeling. Therefore, the NPS modeling in this research assesses only nutrient export.

Nutrient loadings, such as nitrate-nitrogen (NO_3-N) and phosphorous, are growing concerns for watershed managers (Hill 1978; Reckhow *et al.* 1980). Excessive nutrient loading to surface water disrupts aquatic species interactions, disturbs the hydrologic cycle, and causes eutrophication. Moreover, nutrient loading can affect public drinking supplies, causing contamination and promoting hazardous public health conditions. Past researchers have shown a significant positive correlation between nitrogen concentration in surface waters and the area of agricultural land contributing flow to those waters (Likens and Bormann 1974; Haith 1976; Omernik 1976). In the United States, increasing fertilizer and manure applications have been targeted as primary causes of high nitrogen levels in surface waters (Hill 1978). Agricultural practices have also been linked to excessive total phosphorus exports to surface waters (Dillon and Kirchner 1975; Omernik 1976). Additionally, numerous empirical studies have found strong relationships between surface water phosphorus levels, human population, and urban development (Muir *et al.* 1973; Gburek and Folmar 1999).

Past research cites climate and soil type as major factors controlling nutrient fluxes to surface waters. Climate influences the distribution and decomposition of vegetation, the development of soil, and the distribution of fauna and microflora. Areas

within warm or temperate climates and zones of high rainfall have been associated with high levels of nutrient flux (Beaulac and Reckhow 1982). Likewise, soils with high infiltration rates, low cation content, and low erodibility (e.g., sandy/gravel soils) are ideal for reducing the nutrient flux via overland flow. Conversely, soils with high cation content, high erodibility, and low infiltration capacity (e.g., clay or silt loams) can promote high rates of nutrient export via overland flow (Beaulac and Reckhow 1982).

Henderson and Harris (1975) found that undisturbed, forested watersheds do not export high levels of nitrogen and are effective in minimizing nitrogen losses due to the natural recycling mechanisms of vegetative cover. Dense forest cover intercepts a significant amount of rainfall and decreases nutrient fluxes to surface waters (Dunne and Leopold 1978; Hill 1978). Coniferous forests have been observed to be more effective filters for nutrient fluxes compared to deciduous cover (Beaulac and Reckhow 1982). Gburek and Folmar (1999) found that first-order streams in upland agricultural areas have significantly higher concentrations of total nitrogen than those located in most forested areas. In addition, wetlands have been found to significantly decrease, through filtration and trapping, nitrogen and phosphorus delivered by surface waters (Yarbro *et al.* 1984). Reduction of forest cover and wetland area limits the available capacity of the land for hydrologic cycling of nitrogen and phosphorus and produces more concentrated nitrogen and phosphorus loads, which are exported more frequently to surface waters (Hill 1978).

Hill (1978) noted that although increasing agricultural activities have been related to high concentrations and exports of nutrients, landscape patterns—topography, drainage density, stream bank gradients, soil, and geology—are important factors that influence the rate at which nutrients are lost to surface waters. Therefore, the geographic scale of a

particular water quality analysis plays an important role when modeling nutrient constituents.

Geographic Scale in Water Quality Studies

Geographic scale, as Meentemeyer (1989) described, refers to the decrease or increase in spatial properties or in temporal properties of a certain phenomenon within a particular geographic region. Meentemeyer and Box (1987) categorized geographic scale into two categories: 1) spatial scale and 2) temporal scale.

Spatial scale can be expressed in absolute and relative terms. Absolute scale involves absolute measurements of distance, direction, shape and geometry. For example, watershed extent depends on the contributing area of a particular stream; as stream order increases the spatial extent and contributing area will increase. These measurements remain constant and can be expressed in absolute units, such as hectares or kilometers. Relative scale, on the other hand, retains these measurement properties; however, it conveys them based on one entity being relative to another (Meentemeyer and Box 1987). For example, consider nutrients being transported via overland flow down two hillslopes: hillslope X and hillslope Y. Nutrient travel time on hillslope X may be considered *slow* due to heavy vegetation growth, although hillslope X's length is shorter than hillslope Y.

Unlike spatial scale, temporal scale involves only a single dimension and direction. Ecological processes can progress slowly or rapidly depending on the type of processes and the context in which they occur (Meentemeyer and Box 1987; Meentemeyer 1989). Although temporal scale is an important concept in hydrologic

research, this study focuses on effects of spatial scale and does not consider the dimensions of time as they affect hydrologic processes.

Geographic scale is an important factor in modeling hydrologic processes. Explicitly defining a scale of analysis for research studies *a priori* has not been the practice of many researchers, including geographers. The scale of the analysis is often determined arbitrarily, especially when data availability, or the spatial extent of geospatial data, is limited (Meentemeyer 1989). Study areas in this research were, for example, chosen on the basis of data availability. The ability to determine an optimal watershed extent (e.g., 4^{th}, 5^{th}, and 6^{th} order sub-watersheds) for modeling annual pollutant loads (using export coefficients) could assist watershed managers in choosing which land cover data (e.g., 30 m or 10 m) are best for their modeling needs, and could save them the time and effort of testing and evaluating different datasets.

This study evaluates differences in spatial scale in water quality modeling by measuring absolute factors of watershed extent and data resolution to determine the spatial extent at which coarse-resolution and fine-resolution data begin to produce similar model results. From the global scale to the local scale, different land cover and elevation data are available for use in ecological modeling applications. Differences in terminology regarding scale and resolution are important to consider when choosing different scales *a priori* because the spatial extent of the data may not always be related to the resolution of the data. For example, in a raster GIS environment, one may conduct a global water quality analysis with a land cover dataset that extends to all areas of the earth (broad scale) but has a resolution of 10 m (fine resolution); hence, the scale of the analysis is broad while the resolution of the data is fine. Incorporating both spatial extent

and resolution into their definition of geographic scale, Allen *et al.* (1987) noted that extent refers to the largest of distinctions, and resolution (or grain) refers to the smallest of distinctions that can be made in an observation set. In this thesis, I will refer to *broad-scale* data as having a large spatial extent (global or conterminous U.S.) and a coarse pixel resolution (1 km or 30 m), while *fine-scale* data will be represented by a smaller spatial extent (state- or county-sized area) and a fine pixel resolution (10 m).

Hydrologic Modeling and Geographic Scale

Broad-scale ecological models have been criticized for not considering various chemical, organic, and physical processes in modeling calibration (Meentemeyer and Box 1987; Meentemeyer 1989; Johnes 1996; Endreny and Wood 2003). In hydrological modeling, plant uptake rates, infiltration rates, hourly precipitation, evapotranspiration rates, and rates of other biotic processes are all used as variables for determining pollutant concentrations and loadings to surface waters. Hourly time-step models use extensive data (e.g., hourly rainfall, 10-year water quality monitoring data, and an extensive soil survey) to provide detailed analysis for making inferences about current water quality trends and future scenarios, and these models are validated with high levels of confidence (Arnold *et al.* 1998; Di Luzio *et al.* 2002; Tong and Chen 2002).

Hierarchy theory (Allen and Starr 1982) explains that lower level ecological variables (e.g., plant uptake rates, infiltration rates, hourly precipitation, etc.) can be modeled at broader scales by extrapolating and generalizing the individual (at lower levels) to the entire group (at higher levels) (Allen *et al.* 1987). Coarse scales are farther removed from basic processes, so, although these processes still exist, results from basic

processes may not convey usable information in the model. Therefore, by choosing a limited set of variables that vary spatially, one can concentrate on their geography and compensate for the problem of scale changes (Meentemeyer and Box 1987). For example, when modeling annual loads of nitrogen per hectare in a small watershed (i.e., a first-order stream contributing area), detailed variables of plant uptake, vegetation type, soil infiltration, overland flow pathway location, and runoff rates must be used to effectively predict loading amounts. As study area extent increases (to the entire watershed and surrounding watersheds), more broadly defined variables such as land use, slope, and terrain shape become the most effective predictors of nitrogen loading. Finally, at the global scale, precipitation and runoff rates are the most effective predictors of nitrogen loading (Meentemeyer and Box 1987). Thus, when moving from fine to broad scales, detailed information and basic processes are sacrificed for increasing spatial extent. At the same time, landscape patterns become more apparent and explain more about a particular phenomenon at broad than at fine scales (Allen *et al.* 1987; Meentemeyer 1989).

Detailed hydrological models have traditionally been applied to small watersheds where fine-scale variables are identified and can be modeled in real time (Johnes 1996). In larger areas that include multiple watersheds, these models become very complex and difficult to calibrate because of extensive data requirements (Soranno *et al.* 1996; Johnes 1996; Sliva and Williams 2001; Endreny *et al.* 2003; Endreny and Wood 2003). Therefore, the use of detailed models that consider site-specific variables (e.g., hourly precipitation and plant uptake rates) at broad scales, where landscape patterns are more apparent, is very cumbersome and time consuming.

Hierarchy theory has prompted environmental management to focus on broader variables for ecosystem management. Geographers and other researchers have taken advantage of this paradigm shift by basing more research on patterns of phenomena across the landscape. For example, the ecosystem approach to species protection has produced applications in habitat conservation planning, where ecosystems rather than individual species are conserved and protected (Noss *et al.* 1997). Similarly, the watershed approach to water quality management has focused on the entire watershed rather than specific point sources of pollution (e.g., the USEPA's Watershed Initiative of the 1990s). The advancement and popularity of GIS have facilitated this broad-scale paradigm shift, allowing fast and efficient manipulation and analysis of larger areas for which data file size exceeds manual computation ability.

The Impact of Geographic Information Science (GIS) on Hydrologic Modeling

Hydrologic modeling includes a wide variety of non-GIS, computer-based models that rely on different theoretical assumptions and mathematical algorithms (Tong and Chen 2002). These models include such efforts as the Sacramento Soil Moisture Accounting Model (Burnash *et al.*1973), Soil and Water Assessment Tool (SWAT) (Arnold *et al.* 1998), Soil and Water Integrated Model (SWIM) (Krysanova and Luik 1989), HYDROTREND (Syvitski *et al.* 1988), Hydrologic Simulation Program-FORTRAN (Johanson *et al.* 1984), Groundwater Loading Effects of Agricultural Management Systems (GLEAMS) (Leonard *et al.* 1987), Simulator for Water Resources in Rural Basins (SWRRB) (Arnold *et al.*1990), Areal Non-point Source Watershed

Environmental Response Simulation (ANSWERS) (Beasley *et al.* 1980), and AGricultural Non-Point Source (AGNPS) (Young *et al.* 1989).

Over the past 30 years, researchers have used these non-GIS, computer-based water quality models in numerous urban and rural applications; however, the models were developed for smaller, data-rich areas, and were not all able to handle larger dataset processing and geospatial visualization that are inherent to GIS modeling. As the scope of ecological conservation efforts broadened, the USEPA and other government and private agencies began to encapsulate GIS functionality and theory into their hydrologic modeling efforts. The most notable GIS/hydrologic modeling effort came with the USEPA's release of BASINS.

BASINS Overview

During the mid-1990s, the USEPA Office of Water began development and distribution of the Better Assessment Science Integrating Point and Nonpoint Sources (BASINS) software system that coupled 30 years of hydrologic modeling with powerful GIS processing and the familiar ArcView© interface (Wittemore *et al.* 2000; Di Luzio *et al.* 2002; Miller *et al.* 2002). Di Luzio *et al.* (2002) describe the USEPA's development of BASINS as setting out to achieve the following goals: (1) facilitate examination of environmental information, (2) support analysis of environmental systems, (3) provide a framework for examining management alternatives, and (4) embrace simple and highly evolved models that allow for assessment of point source and NPS pollution at both broad and fine scales. Freely distributed over the World Wide Web (*www.epa.gov/ost/basins*), BASINS attempts to meet these goals by providing a versatile

toolset that can be applied to a wide variety of modeling situations in different human and/or natural environments.

BASINS operates as a subsystem within the ESRI ArcView 3.x GIS architecture. It provides a collection of environmental data, along with database management tools and hydrologic models that use powerful GIS analysis and visualization. Hydrologic models distributed with BASINS include SWAT, QUAL2E, the Hydrological Simulation Program – Windows (WinHPSF), and PLOAD. BASINS provides a seamless, graphically explicit interface where customized tools and models are grouped as ArcView extensions, enabling users to assess areas quantitatively and qualitatively by pointing and clicking (Arnold *et al.* 1998; USEPA 2001a; Di Luizo *et al.* 2002). The system is categorized into four arenas of operation and functionality: geographic databases, GIS tool applications, hydrologic models, and graphical output analysis and report writing (Whittemore *et al.* 2000; USEPA 2001a; Di Luzio *et al.* 2002).

SWAT is a complex, daily time-step model developed by the United States Department of Agriculture (USDA) that aims to assess water management practices by simulating sediment loading and agricultural chemical production. SWAT allows users to study the long-term physical processes of water movement, sediment movement, crop growth, and nutrient cycling by considering various impacts of land use practices, hydrometerology, vegetation, and topography (Arnold *et al.* 1998; USEPA 2001a).

QUAL2E is a simple, steady-state, one-dimensional model for simulating the transport of water quality constituents in streams under a given flow condition. QUAL2E requires a combination of user-specified point source data, reach data, and non-point-source data for simulation (USEPA 2001a).

WinHPSF is a complex, lumped parameter, hourly time-step model used to predict runoff and in-stream water quality constituent concentrations through the simulation of NPS pollution transport at a variety of temporal scales (Carrubba 2000; USEPA 2001). WinHPSF functionality derives from the HPSF-FORTRAN model used by water quality modelers for over 40 years, which is considered the most complete NPS pollutant-loading model available (Laroche *et al.* 1996; Carrubba 2000). Developed by AQUA TERRA Consulting, WinHSPF emulates all functionality of the older FORTRAN version in a Windows© environment. Because WinHSPF considers annual, monthly, daily, and hourly modeling, calibration requires extensive acquisition of data, such as hourly meteorological data, stream networks, channel geometry, and land use (USEPA 2001a). Although WinHSFP may be applied to a variety of study sites and projects (Carrubba 2000), data availability may dictate the applicability of the model.

PLOAD is a simplified, broad-scale model that prioritizes critical watersheds by calculating lumped annualized pollutant loading and identifying pollutant-related problem areas. Developed by CH2M Hill Consulting, PLOAD provides a graphically explicit, user-friendly GIS interface for export coefficient modeling (discussed in the next section) with minimal data requirements (e.g., land cover, export coefficient values, and watershed boundaries) to produce lumped annual watershed loadings. The model can be applied to a wide range of water quality projects in various landscapes, and it has been extensively used by water quality investigators from both federal agencies and private consulting firms in building total maximum daily load (TMDL) reports for section 303(d) of the Clean Water Act (USEPA 2001b).

The Export Coefficient Model

The export coefficient model (ECM) uses export coefficient values (ECV) to predict the export of annual pollutant loads from land use source areas to surface waters under conditions of uncertainty. Ideally, NPS pollution areas are identified and evaluated using in-stream measurements from the entire hydrologic network; however, the extensive amount of time and personnel needed to accomplish such a daunting task necessitates methods for extrapolating estimates of pollutant loading from incomplete/sparse data (McFarland and Hauck 2001). Recommended as an alternative to in-stream measurements (Reckhow *et al.* 1980; Beaulac and Reckhow 1982; Frink 1991; McFarland and Hauck 2001), ECVs estimate the rates at which pollutants are lost to surface waters per unit area of land use types annually, and they can be extrapolated to broad scales. Empirical studies (e.g., Lin 1972; Loehr 1974; Uttormark *et al.*1974) have observed pollutant exports from small watersheds over five- to ten-year periods and have provided ranges of ECVs (*see* Reckhow *et al.* 1980) that can be calibrated—based on local conditions of soil, rainfall, and runoff rates—and extrapolated to larger areas.

The ECM uses a linear equation to sum annual exports of pollution by land cover type as:

$$L_N = \sum_{c=1}^{N} \left(E_{pc} * A_c \right) \qquad \text{(Eq. 1)}$$

where L_N represents the total basin pollutant load (kg/yr), E_{pc} is a pollutant-loading rate for land cover type c (kg/ha/year), and A_c is the area of land cover type c (ha) (Reckhow *et al.* 1980). Unlike the more complex models discussed earlier, the ECM does not require extensive hourly meteorological data or sophisticated biogeophysical equations;

rather, fine-scale detail is sacrificed for simplicity and readily available data that can generalize broader-scale watershed processes and detect spatial variability across the landscape (Endreny and Wood 2003). Ultimately, ECModeling conserves valuable time, effort, and money by providing a management team the ability to scope large areas *a priori*, target critical pollutant contribution (or risk) areas (Maas *et al.* 1988; Gale *et al.* 1993), and prioritize them accordingly. Once critical contributing areas have been identified and prioritized, more extensive and detailed analyses may then be implemented to determine which management action will be most economically and environmentally productive. GIS, combined with an ECM, enables watershed managers to broaden the spatial scale with more ease, functionality, and robustness. For example, Wickham and Wade (2002) applied ECModeling with GIS to 1,000 watersheds in Maryland for estimating risk areas for nutrient export. Broadening the spatial scale to the state level, they were able to depict spatial variability of annual nutrient loading and land cover distribution between watersheds across a state-sized landscape, finding a strong relationship between areas high in agriculture or urban cover and high nutrient exports.

Early development of ECMs relied on spreadsheet analyses of land cover metrics and precluded the possibility for analyzing spatial variability and landscape patterns (Endreny and Wood 2003). This approach has since been built upon and modified, incorporating more ecological variables, correcting erroneous assumptions, and further broadening the spatial scale. For example, traditional ECMs, such as Equation 1, portray each land use type as homogenous across the landscape, and assume that similar land use types export the same amount of load and that 100% of that load will reach surface waters, not considering factors of terrain and vegetation that may accentuate or attenuate

pollutant loadings along flow paths (Soranno *et al.* 1996; Endreny and Wood 2003). Furthermore, researchers have shown that nutrients often reach surface waters attached to sediment particles and may be deposited or transformed before they reach surface waters (Novotny and Chesters 1989; Soranno *et al.* 1996). In a raster-modeling environment, homogenous landscapes allow no interaction between pixel loads and their upslope contributing and downslope dispersal area (Endreny and Wood 2003), therefore missing any nutrient transformation or distance-decay that may occur.

Researchers have developed several GIS-based ECMs that modify the traditional methods and take into account the ecological variables listed above with less uncertainty. For example, Mattikalli and Richards (1996) used a GIS-ECM to conduct a time-series analysis of ECV change in relation to land use changes over a multiyear period. Soranno *et al.* (1996) developed a method that uses phosphorus (P) flux coefficients with traditional ECVs as a function of overland flow pathway lengths. For every unit of travel along the flow path, P-fluxes will attenuate P loadings and not assume 100% of P export will reach surface waters. Johnes and Heathwaite (1997) developed a distance-decay component that treated riparian corridors as critical areas for filtering nutrient loads to surface waters. They assigned larger land use loads for areas within 50 m from the stream; however the values remained static (as they were chosen *a priori*) and did not dynamically change with the variation in terrain shape and vegetation buffers. Endreny and Wood (2003) developed a method for weighting ECVs based on terrain and vegetative buffer characteristics. Unlike the method provided by Johnes and Heathwaite (1997), they dynamically weighted ECVs as overland flow pathways interact with different terrain types and vegetative buffers, thus portraying pollutant loadings as

heterogenous in relation to different land use types. These advances and new approaches allow spatially explicit models that consider the effect of landscape features on nutrient export.

The above examples provide watershed managers with more flexibility and functionality for ECModeling; nevertheless, the modifications to traditional ECMs all retain a common goal for future replication—simplicity. Successful implementation of these modified ECMs allows the watershed manager or researcher to reduce uncertainly in scoping different remediation areas by providing methods for considering other important biophysical factors (e.g., nutrient distance decay) and aiming model application at fine or broad scales while maintaining a simple model.

GIS provides a computing environment in which overland flow pathways, terrain shape indices, slope, and land cover can be processed quickly and inexpensively. Land cover is the primary component in any ECM, and the availability of accurate land cover datasets is a critical issue in ECModeling. Also, the different scales of available land cover datasets play an important role in ECModeling. As a watershed manager, certain concerns arise: Should I choose finer- or broader-scale land cover? At what watershed extent should I choose broad-scale land cover over fine-scale or vice versa for ECModeling purposes? When modeling areas at risk for high nutrient export within sub-watersheds, will model results using broad-scale data suggest that different management practices need to be implemented compared to model results from fine-scale data?

These questions stem from the growing availability of GIS and land cover data, and the uncertainly surrounding issues of geographic scale. Because ECModeling is typically used in rural watersheds due to the high amount of uncertainty associated with

urban ECVs (Beaulac and Reckhow 1982; Frink 1991), BCLRW provides an excellent location for conducting modified and traditional ECModeling to answer these questions.

CHAPTER III
METHODS: OBJECTIVES AND DATA PREPARATION

Project Scope and Objectives

In this research, I test the hypothesis that an export coefficient model (ECM) based on broad-scale land cover data can capture enough detail to produce results comparable to those from an ECM based on fine-scale data at the county-mapping scale. Again, I identify broad-scale datasets as having a global or conterminous U.S. extent with a 1-km or 30-m resolution, while fine-scale datasets have a county-wide extent with a 10-m resolution. Additionally, I answer the questions: At what watershed extent do ECM results produced from fine- and broad-scale land cover datasets become statistically different? At what watershed extent does the prioritization of sub-watersheds for nutrient flux change between simulations using broad- and fine-scale land cover data? Within sub-watersheds, is excessive nutrient export more likely to originate in the riparian zone or farther from the stream? Does the prioritization of areas within sub-watersheds for nutrient flux reduction change between simulations using fine- and broad-scale datasets, such that model results suggest different management scenarios?

Specific objectives for addressing these questions include:

1. To develop nutrient export coefficient values (EVCs) of total phosphorus (TP) and total nitrogen (TN) from in-stream measurements observed in BCLRW between 1998 and 2003 using a multiple regression technique.

2. To develop two ECMs within Arc/Info© GRID© that model (a) lumped annual nutrient loads by 4th, 5th, and 6th order stream contributing areas

and (b) topographically weighted nutrient loads within contributing areas.

3. To calibrate the ECM model against in-stream measurements taken in the Ellejoy Creek and Nails Creek watersheds.

4. To implement an ensemble of ECM simulations that model 4th, 5th, and 6th order sub-watershed nutrient loads using IPSI, NLCD, and LULC-AVHRR.

5. To statistically compare model results from the three land cover datasets at different watershed scales.

6. To employ a second ECM that uses runoff likelihood and nutrient trapping potential to weight ECVs, allowing the researcher to analyze export variability within each sub-watershed.

GIS and Water Quality Data

Data for this thesis have been obtained from federal and state government agencies and in-stream field surveys conducted by myself and graduate students from the Biosystems Engineering and Environmental Science (BEES) department at the University of Tennessee (UT). Geospatial data, which include land cover and digital elevation models (DEM), were acquired from the Untied States Geological Survey (USGS), National Aeronautics and Space Administration (NASA), the United States Environmental Protection Agency (USEPA), the Multi-Resolution Land Characterization (MRLC) Consortium, and the Tennessee Valley Authority (TVA). The Tennessee Department of Environmental Conservation (TDEC) provided in-stream TP and TN water quality measurements taken during 1998 and 1999. Primary data collection of TP and TN started in June 2003 and continued monthly until November 2003.

Land Cover Data

Broad-scale land cover data are represented by 1-km resolution USGS-NASA Land Cover/Land Use (LCLU) and 30-m resolution National Land Cover Data (NLCD), while fine-scale data are represented by land cover derived from sub-meter, low-level aerial photography distributed as part of a multi-layer geographic database produced by TVA and referred to as Integrated Pollutant Source Identification (IPSI).

Land Use/Land Cover (LULC) data were derived from Advanced Very High Resolution Radiometer (AVHRR) satellite imagery collected during April 1992 through March 1993. LULC-AVHRR is freely distributed by the USGS-NASA Land Processes Distributed Active Archive Center's (*http://edcdaac.usgs.gov*) Global Land Cover Characterization (GLCC) program, which characterizes the global landscape at a 1-km spatial resolution for use in broad-scale environmental modeling and assessment studies, such as global climate change and species habitat assessment (USGS-NASA 2003). Applying 1-km data to ECModeling at the county mapping scale (e.g., BCLRW) is not practical for accurate modeling. However, incorporating LULC-AVHRR in this study will help determine whether general patterns of water quality variability are maintained as scale of the analysis expands from 4^{th} to 6^{th} order watersheds and from 10-m to 1-km resolution data.

Derived from the Anderson Level I classification scheme (Anderson *et al.* 1976), LULC-AVHRR uses a 24-class scheme (Table A.1) that was first released in 1997 (version 1.0) and supplemented with a modified version 2.0 in 2000. Informal data quality assessments have been performed on LULC-AVHRR's version 1.0, in which sets of randomly chosen pixels were referenced to Landsat-5 and SPOT satellite imagery,

yielding accuracy levels between 54.9% and 78.7% (Scepan 1999; USGS and NASA 2003). Although no current accuracy assessments have been conducted for LULC-AVHRR version 2.0, I have chosen to use this dataset in my analysis because it represents the most up-to-date version of 1-km land cover data available.

National Land Cover Data (NLCD) are derived from Landsat-5 Thematic Mapper (TM) satellite imagery of the conterminous United States circa 1992 (Loveland and Shaw 1996; USEPA 2003b). Developed by the MRLC consortium, a group of federal agencies designated specifically for landscape characterization, NLCD uses a modified Anderson classification scheme (Anderson *et al.* 1976) of 21 classes (Table A.1) to depict land cover across the landscape at a spatial resolution of 30-m (Vogelmann *et al.* 2001; Konarska *et al.* 2002). NLCD is freely distributed by the MRLC Consortium and USGS at the USGS' seamless data distribution website (*http//seamless.usgs.gov*).

NLCD is a supervised classification that relies on human selection of training grounds, with different individuals working on each state. Training grounds for particular land cover classes also vary by state, introducing some classification error. Accuracy assessments were conducted for the ten USEPA regions such that samples of each region's land cover were referenced to aerial photography and raw TM imagery. Pixels of unknown classification within the sample were compared to Landsat TM composite imagery and photo-interpreted 1:40,000 scale National Aerial Photography Program (NAPP) images (Yang *et al.* 2001). Error matrices of this analysis have been developed by the USEPA and are available from USEPA. Overall, NLCD provides a good representation of land cover, with the eastern United States yielding accuracy levels of 59.9% for Anderson Level II and 80.5% for Anderson Level I (Yang *et al.* 2001). It is

especially appropriate for regional studies, although small amounts of classification error exist in the data (e.g., between row crops and pasture) (Vogelmann *et al.* 1998; Smith *et al.* 2002).

TVA's ISPI database is developed from low-level, high-resolution, color-infrared aerial photographs (< 30-cm resolution) acquired during the leaf-off season in February 2000. GIS software and photo interpretation methods were used to analyze the aerial photographs, building accompanying geospatial data layers that identify a 55-class land use/land cover layer (Table A.1), hydrological network, stream bank erosion sites, livestock operations, and other potential sources of nonpoint pollution (i.e., quarry operations, junk pile sites). The IPSI land cover dataset was digitized at a 1:12,000 mapping scale, for which the minimum mapping unit is roughly one hectare (TVA 2003). While IPSI includes multiple geospatial datasets, this research uses only the land cover dataset; for clarity, I will refer to the IPSI land cover dataset simply as *IPSI*. IPSI is distributed to watershed group clients as part of TVA's environmental program to assess different watersheds within and outside the TVA river system and provide clients assistance in watershed remediation and stream restoration (TVA 2002; TVA 2003). IPSI, however, only covers watershed- or county-sized areas, is site specific based on client needs, and is only available for client and TVA personnel usage.

Land Cover Reclassification

In order to compare datasets, I reclassified the land cover datasets to a common six-class scheme (Table 1; Figure 3). I developed this broadly defined class scheme based on the relevancy of each land cover type in traditional ECM approaches, and the availability of literature-reported ECVs. For example, Beaulac and Reckhow (1982) and

Table 1: Reclassified land cover composition.

	IPSI		*NLCD*		*LULC-AVHRR*	
Land Cover	**ha**	**%**	**ha**	**%**	**ha**	**%**
Urban	19,644	11.3	7,595	4.4	2,568	1.5
Forest	112,520	63.1	129,681	74.2	135,083	77.1
Pasture	35,369	20.3	28,683	16.4	14,840	8.5
Cropland	3,281	1.9	6,120	3.5	21,975	12.5
Barren Land	1,077	0.6	389	0.2	0	0.0
Open Water	2,594	1.5	2,013	1.2	761	0.4
Totals	174,486	100	174,479	100	175,228	100

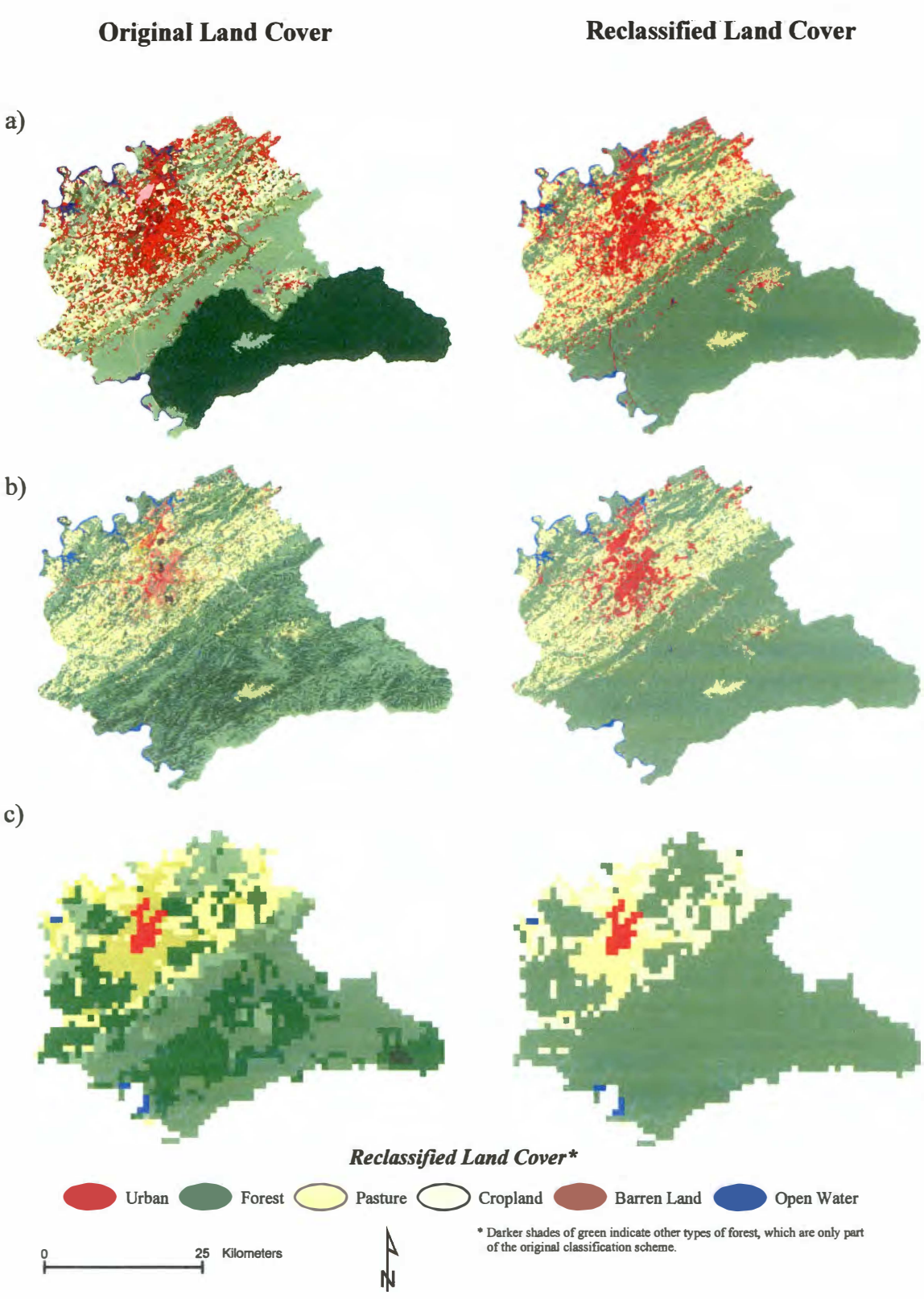


Figure 3: Land cover reclassification. (a) IPSI, (b) NLCD, and (c) LULC-AVHRR reclassification.

Frink *et al.* (1991) noted that a great deal of uncertainty exists when considering ECVs in an urban landscape. Modeling specific urban land covers (e.g., residential, commercial, and transportation) with the ECM can promote unrealistic estimates of pollutant loading due to the complexity and interactions of human-made entities, such as storm drains and sewage networks (McFarland and Hauck 2001). Furthermore, the ECM is intended for rural landscape applications (Reckhow *et al.* 1980) where agriculture and other less complex land covers can be isolated as NPS pollutant contributors with greater confidence. In this research, I modeled urban areas as one land cover type without a further breakdown of land cover subcategories. I aggregated agricultural land into *Pasture* and *Cropland*, two broadly defined land uses, because of their differences in NPS pollutant fluxes (Beaulac and Reckhow 1982). For example, differences in fertilizer application type and quantity between tobacco crops and pasture grasses will lead to different amounts of nutrient export.

Itemizing the IPSI, NLCD, and LULC-AVHRR land cover types into this six-class scheme was based on broadly defined class definitions of the original data (if available), and the impact that each land cover type may have on fluxes of nutrient loadings to surface waters. NLCD and IPSI are classified in a hierarchical manner so that detailed descriptions of land cover types exist within more broadly defined categories (Table A.1). Figure 3 illustrates the change in land cover composition from detailed land cover classes to the generalized six-class scheme, while Table A.2 provides a detailed reclassification overview; my basis for itemizing classifications is discussed further below.

Urban reclassification for NLCD and LULC-AVHRR included all residential (low and high density), commercial/transportation and industrial land uses, along with residential development and urban grasses (e.g., parks and golf courses). The IPSI reclassification included the same land use types and all those included in IPSI's broadly defined categories (Table A.2). *Forest* reclassification combined all forested NLCD and LULC-AVHRR land cover types of deciduous, coniferous, and mixed forest. Park and Great Smoky Mountains National Park (GSMNP) land cover from IPSI were also grouped within this category. GSMNP and park land cover types were developed with the assumption that all GSMNP areas—excluding Cades Cove, a grassland area—are complete forest cover. Because IPSI is developed specifically for locating NPS pollution, forest land cover was generalized during development into one class and not separated into individual forest types (TVA 2003). I categorized all wetland land cover identified by IPSI and NLCD into the *Forest* reclassification because, like forested areas, they reduce nutrient loads to surface waters (Yarbro *et al.* 1984; Preston and Bedford 1988; Wickham and Wade 2002). LULC-AVHRR does not capture these areas within the study area.

Pasture reclassification included all agricultural land that functions as livestock grazing land. Mixed pasture/woodland land use classes identified by IPSI and LULC-AVHRR were included in *Pasture* due to their presence as livestock areas. Although IPSI classified Cades Cove as grassland, NLCD identified it as pasture. I grouped this area into the *Pasture* class due to its function as a forage area for larger, terrestrial wildlife species. LULC-AVHRR classifications of grassland and savanna, which define areas of natural and/or prairie grasses, were also reclassified to *Pasture*. Natural savanna

grasses are typically found in midwestern prairie landscapes and are not indigenous to eastern Tennessee.

Cropland reclassification included all cultivated lands. I included all row-cropping land uses from the three land cover datasets as well as the IPSI classifications of orchards, vineyards, and nurseries in this reclassified category. Although the nutrient generation from row and cover crops may differ, I could not reclassify row and crops into their own class because the original land cover classification only identifies a single category for cropland and does not identify individual crop types.

Barren Land reclassification included all barren, clear-cut, and transitional land. IPSI's disturbed areas, landfills, mining, quarries, borrow, and forest clear-cut land covers were included in this category. Likewise, NLCD land cover of bare rock/soil, quarry operations, and transitional land were included in this group. Transitional land is defined as areas changing (with < 25% vegetative cover) from one land cover to another because of a certain land use activity such as residential development, forest fire, or other vegetative clearing activities (USEPA 2003b).

Elevation Data

The USGS freely distributes seamless 30- and 10-m digital elevation models (DEM), which are part of the National Elevation Dataset (NED) program and cover most United States regions *(http://seamless.usgs.gov)*. Thirty- and 10-m NED are corrected versions of the older DEMs typically derived from existing USGS topographic maps and stereo photogrammetry (Garbrecht and Martz 2001). The NED program was implemented to spatially correct previously developed DEMs that exhibit human-caused

(e.g., data collection and rounding) and systematic errors. Systematic error results from mosaicking smaller (7.5-minute quadrates) DEMs and changing mapping projections. NED is distributed as a seamless dataset that incorporates one common projection, eliminating many of the systematic errors associated with older DEMs. The 30-m NED is available for the conterminous United States, while 10-m NED datasets are available for only selected, state-sized areas, which include Tennessee.

DEMs are an important asset to hydrologic modeling applications. DEMs are raster-based geospatial layers in which elevation values are stored in a matrix of cells such that each cell contains only one elevation value and rows and columns within the matrix represent locations on the earth. The simplicity in aggregation of data within the raster DEM promotes quick and effective computation ability, allowing modeling and evaluation of large areas in a short amount of time (Garbrecht and Martz 2001). Well-developed research has incorporated DEMs into a variety of hydrologic modeling efforts, and, over the years, the possibilities of modeling hydrologic systems with DEMs have spawned new methods and techniques for modeling broad-scale hydrologic processes such as flow path extraction (O'Callaghan and Mark 1984; Quinn *et al.* 1991; Tarboton 1997), runoff processes (Beven 1995; Endreny and Wood 2001), drainage area delineation (Abt *et al.* 1995), and flood simulation (Colby *et al.* 2000).

In this research, 30-m NED represents broad-scale elevation data, while 10-m NED represents fine-scale elevation data. Global DEMs of 1-km resolution are available from the USGS-NASA Land Processes Distributed Active Archive Center (*http://edcdaac.usgs.gov/main.asp*); however, I excluded this dataset from the weighted ECM computation because 1-km data, simply put, are not practical for modeling nutrient

export within 4th, 5th, or 6th order watersheds. The raster modeling approach I have chosen requires each set of land cover and elevation data (30-m and 10-m) to maintain the same spatial projection and resolution. The land cover datasets are distributed in a variety of different mapping coordinate systems and projections; therefore, I transformed all geospatial data, including NED, to the State Plane Coordinate System with a Lambert Conformal Conic projection. IPSI land cover is distributed as a vector geospatial layer as it has been digitized from aerial photographs. In maintaining common spatial resolutions between land cover and DEMs, I converted IPSI land cover to a 10-m raster data format in order to represent the *fine-scale* land cover.

Water Quality Data

Stream quality data for this thesis incorporate both primary data collected by myself and other UT graduate students, and secondary data acquired from TDEC. In-stream water quality measurements were used for the BCLRW-ECM calibration and ECV development. Primary data collection was part of a collaboration between UT-BEES, TVA, and TDEC to develop a Total Maximum Daily Load (TMDL) report, as required by Section 303(d) of the US Clean Water Act (USEPA 2003c), for the Little River tributaries of Ellejoy Creek and Nails Creek.

Secondary data, collected by TDEC, included stream water quality from June 1998 to October 1998 for the Little River watershed. These data were from 14 sampling sites located along the Little River where tributary reaches converge with the main steam (Figure 4). TDEC complemented 1998 data with a three-month—April, August, and December 1999—sampling survey, collecting from two sampling sites (Figure 4) located

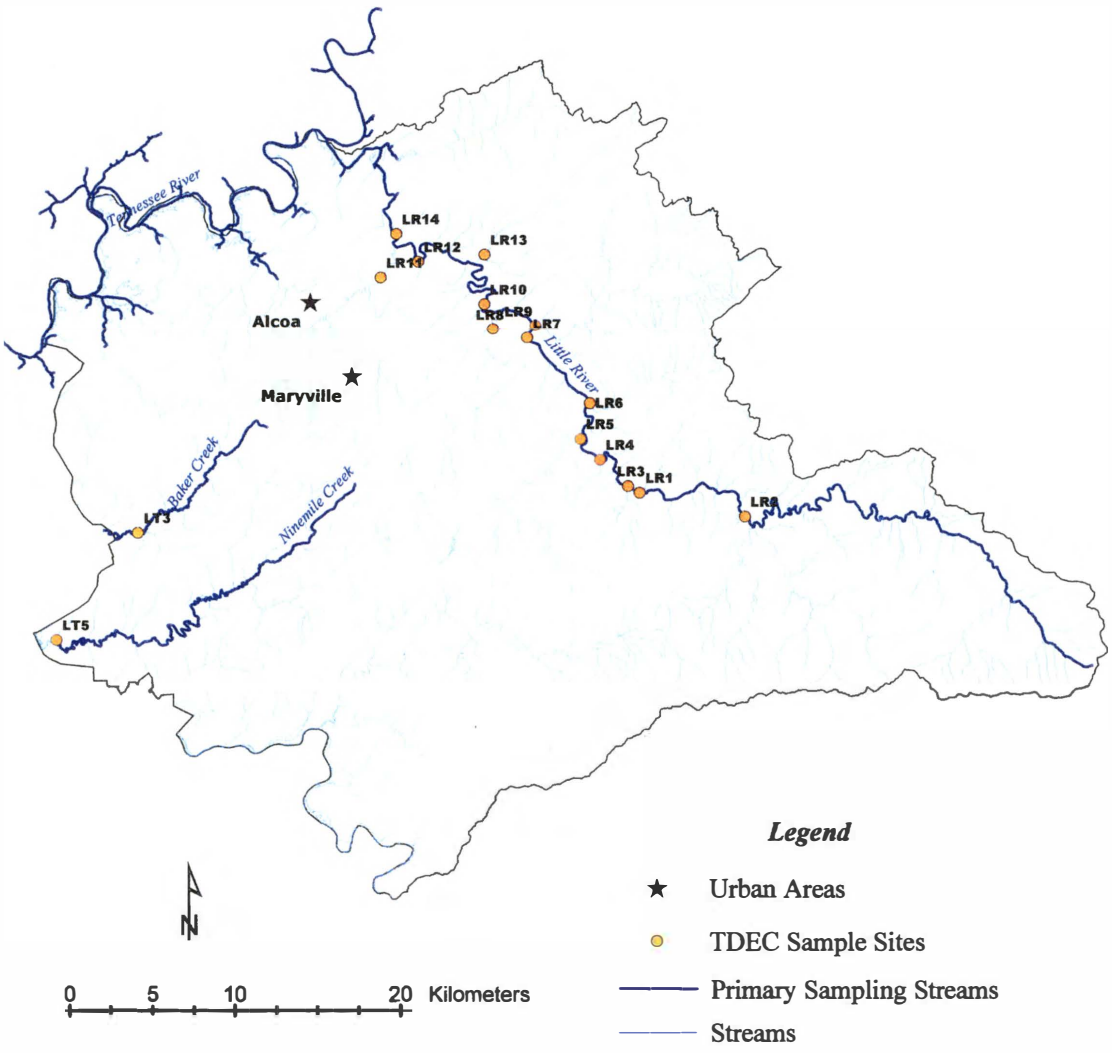


Figure 4: TDEC sampling site locations.

in southern Blount County. Both 1998 and 1999 data included phosphate and nitrite-nitrate species which were measured in grab samples taken during base flow conditions. Data were analyzed in Tennessee State Health Department laboratories that maintained TDEC and USEPA Office of Water Resource Control (WRC) quality control standards.

Primary stream quality data were collected monthly from June 2003 through November 2003. We sampled 12 sites along Ellejoy Creek and Nails Creek, which are tributaries of the Little River (Figure 5). Following sampling procedures used by TDEC in 1998 and 1999 and USEPA WRC lab standards, grab samples were analyzed by BEES laboratories.

I computed TP and TN nutrient counts from both TDEC and BEES samples by using the sum of total kjeldahl phosphorus (TKP) and total phosphate (PO_4) measurements to represent TP, and the sum of total kjeldahl nitrogen (TKN), total nitrate (NO_3), and total ammonia (NH_4-TN) to represent TN. These individual nitrogen and phosphorus species are susceptible to seasonal variations in concentration levels; thus, the ECModeling approach uses *total* representations of individual phosphorus and nitrogen species, allowing more reliable indicators of variations in nutrient loading annually (Yarbro *et al.* 1984; Johnes 1996; Johnes and Heathwaite 1997).

We determined stream flow at each site with a Swoffer 3000 portable flow meter that measured flow velocity rates (m/sec) with a 30-sec count. To compute flow discharge rates (m^3/sec), we collected flow velocity rates (m/sec) at 1-m intervals across the channel and noted the depth at each interval. Water depths were averaged and multiplied by the total channel width to give stream channel area. We then averaged flow velocities at each 1-m interval width and multiplied those products by the channel area to

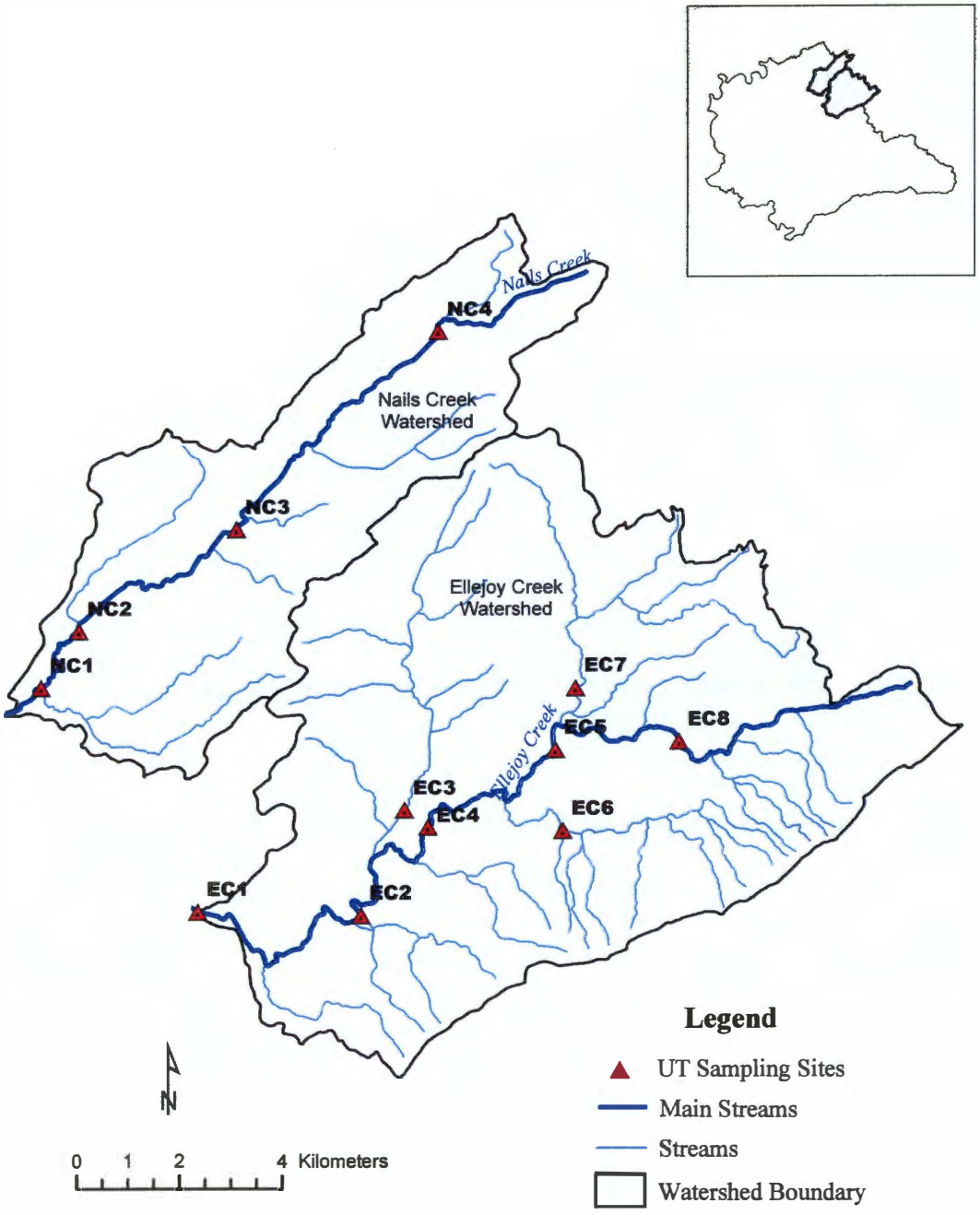


Figure 5: Ellejoy Creek and Nails Creek sampling sites.

give a discharge rate (Watson and Burnett 1995). Stream flow rates from 1998 and 1999 had been obtained by TDEC in a similar manner. Although many methods exist for calculating stream discharge, we used TDEC's method to keep continuity between primary and secondary data collection methods.

Data used in this research are not continuous over the five-year sampling period (1998 to 2003). No sampling was conducted within BCLRW during the 2000-2002 period, which may cause misrepresentations of stream chemistry in BCLRW. BCLRW does not contain any continuously monitored streams (e.g., USGS Gauge Station streams); hence, water quality sampling in this area has been limited and relies primarily on TDEC sampling efforts. Additionally, water quality sampling was part of an ongoing project to develop TMDL reports for Ellejoy and Nails creeks; therefore, sampling sites were selected by TDEC personnel with the purpose of providing a basic representation of water quality conditions along Ellejoy and Nails Creek. While a representation of the entire study area would be more practical for this thesis, the limited amount of existing data and limited time prevented me from conducting a more extensive water quality survey.

Sub-Watershed Delineation

Each sub-watershed layer (Figure 6) was computed from the 10-m DEM using hydrologic modeling tools available within GRID©. The 10-m DEM represents the finest representation of elevation available for the area, as watershed boundaries created from this dataset are more detailed than those from the 30-m or 1-km data. I used a five-step watershed delineation process that (1) calculates flow direction, (2) calculates flow

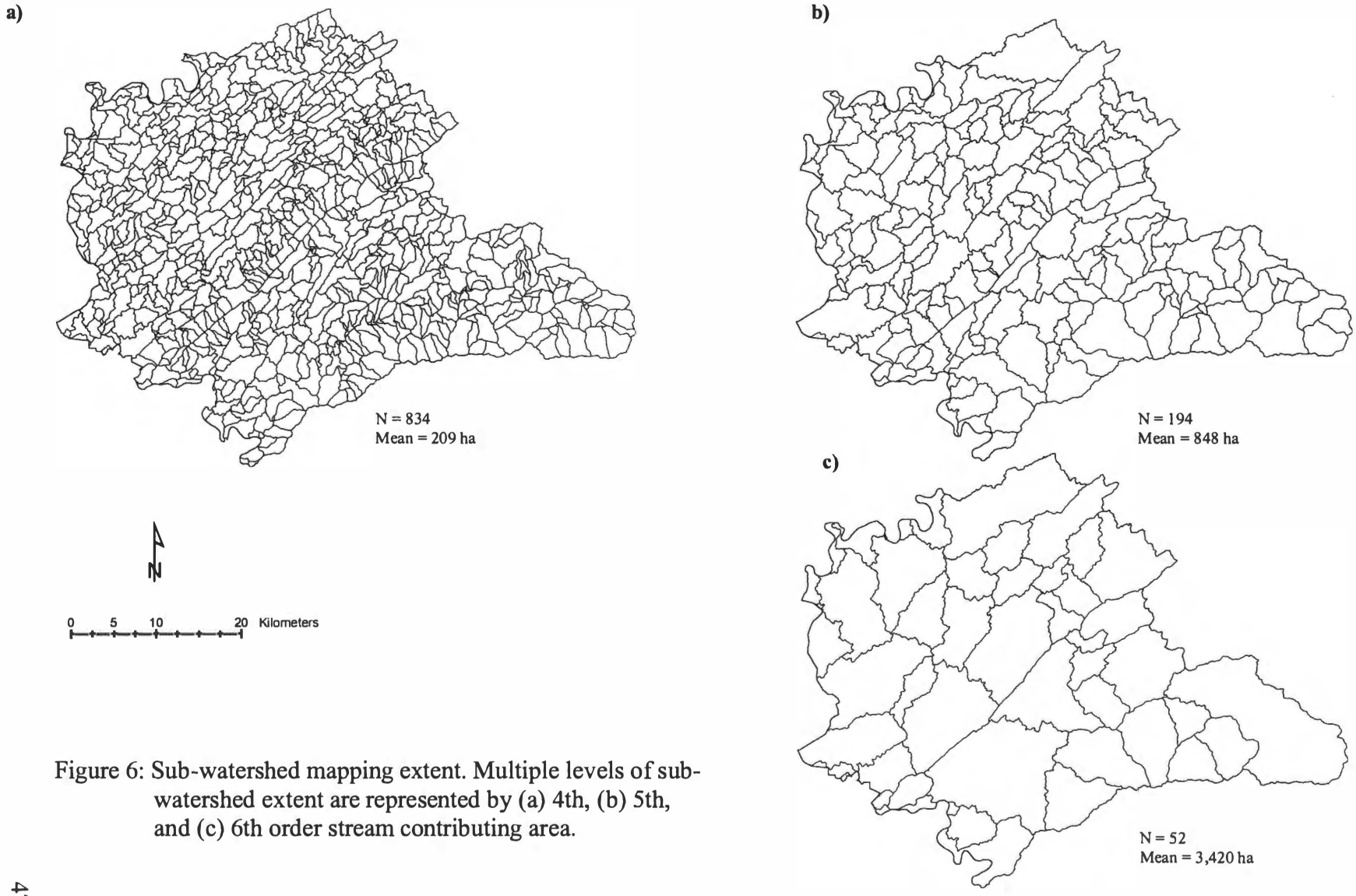


Figure 6: Sub-watershed mapping extent. Multiple levels of sub-watershed extent are represented by (a) 4th, (b) 5th, and (c) 6th order stream contributing area.

accumulation, (3) extracts flow paths, (4) determines stream order, and (5) determines drainage areas for each stream of specified order. The flow accumulation algorithm with GRID© uses the Deterministic 8-node (D-8) method (O'Callaghan and Mark 1984), whereby only the steepest angle of descent between eight neighboring pixels is extracted on a pixel-by-pixel basis.

The D-8 method works well in areas where terrain is rugged, and flow usually follows a single descent path because of the extreme differences in one elevation pixel to the next. However, flat, gently rolling terrain may be problematic for the D-8 method because pixel-by-pixel elevation differences are less apparent, creating multiple flow paths; runoff has multiple pathways to travel rather than one distinct descent. BCLRW consists of mostly rugged terrain; however, bottomland areas follow a more gently rolling topography. While alternative flow path extraction algorithms that perform better in flat terrain exist—the Multiple Flow (Quinn *et al.* 1991) or DEMON (Costa-Cabral and Burges 1994)—only the D-8 method was used in this research. Flow paths are identified by the number of pixels accumulated into one another. The output flow path layer assigns an accumulated pixel count to each pixel's attribute value. Pixel values with higher counts identify those pixels that are likely to be a stream channel or drainage path.

In this research, I identify streams by extracting pixels from the 10-m DEM that accumulated 500 or more upland pixels. Assuming that NED 10-m DEMs are the most accurate representation of elevation, I use only this layer for defining sub-watershed boundaries. The pixel accumulation layer was derived from a 10-m DEM free of depressions. DEM depressions are systematic errors that arise during the DEM development from erroneous (human) data collection or, in most cases, the changing of

precision (e.g., rounding from floating-point to integer values) (Garbrecht and Martz 2001). Depressions in the DEM interrupt overland flow path extraction and therefore must be filled. While topographic depressions exist in the landscape and may serve as runoff (Dunne and Leopold 1978) and/or nutrient storage, it is uncharacteristic for topographic depressions in the eastern United States, even in karst regions, to be equal to pixel-sized areas (e.g., 100 m^2) (Mark 1984). While NED attempts to minimize systematic errors, removing depressions will further insure correct hydrologic extraction. I used a subsequent stream-ordering algorithm to calculate stream order, which computes order based on the Strahler method (*See* ESRI 2004), and, finally, sub-watershed boundaries. GIS layers illustrated in Figure 6 identify resulting 4^{th}, 5^{th}, and 6^{th} order stream contributing area boundaries that serve as the sub-watersheds within BCLRW. Fourth order sub-watersheds average 209 hectares (N = 834), 5^{th} order sub-watersheds average 848 hectares (N = 194), and 6^{th} order sub-watersheds average 3,420 hectares (N = 52). These three GIS layers represent watershed mapping extents in the ECModeling processes discussed in Chapter IV.

BCLRW includes both political (Blount County) and natural boundaries (Little River watershed). I clipped sub-watersheds that extend beyond the Blount County political boundary, leaving only portions of those sub-watersheds. Simply excluding the entire area of bordering sub-watersheds usually resulted in a significant loss in total study area. Once sub-watershed boundaries were defined, I calculated ECVs from in-stream measurements and/or values reported in empirical studies in the literature.

CHAPTER IV
METHODS: THE EXPORT MODEL APPROACH

The export coefficient model (ECM) is a simple water quality model that uses commonly available data, such as land cover, elevation data, and export coefficient values (ECV) to model broad-scale watershed processes (Reckhow *et al.* 1980; Frink 1991; McFarland and Hauck 2001). Using readily available land cover data and ECVs, which are annual estimations of pollutant loading per land cover area unit, ECModeling assumes that for similar climatic regimes a given land cover will export a known amount of nutrients. Under this assumption, it is possible to estimate a watershed's total nutrient load entering surface waters (Winter and Duthie 2000). This research uses two variations of ECModeling; an unweighted ECM, and a weighted ECM. The unweighted ECM uses land cover measurements and ECVs to sum nutrient export by sub-watershed and allow for an examination of variability between watersheds. The weighted ECM approach uses runoff likelihood and vegetative trapping ability to weight ECVs to the landscape, which allows for an examination of export variability within each sub-watershed.

Built within a GIS framework, either ECM allows the researcher to evaluate broad-scale areas for water quality remediation *a priori* by visualizing risk areas and prioritizing them accordingly (Johnes *et al.* 1996; Endreny and Wood 2003). I have developed both ECMs in Arc/Info© GRID© and calibrated the BCLRW-ECM against in-stream readings taken within Ellejoy Creek and Nails Creek watersheds. I used unweighted and weighted ECMs in two separate analyses. Weighted ECM results were used to determine where high nutrient export levels are most frequently occurring within

watersheds, and whether management needs (e.g., riparian restoration) change between land cover simulations.

I used results from the unweighted ECM to compare total watershed nutrient summations and answer the questions: At what watershed extent (4^{th}, 5^{th}, or 6^{th} order contributing areas) do model results between three land cover datasets become statistically identical? At what watershed extent does the prioritization of sub-watersheds for remediation of excessive nutrient flux change between simulations using different land cover datasets?

The remaining sections of this chapter discuss calibration of each ECM, and their implementation in the GIS framework. In addition, the chapter discusses a preliminary statistical analysis in which I attempt to calculate nutrient ECVs of total phosphorus (TP) and total nitrogen (TN) from in-stream water quality measurements. In this preliminary analysis, I review the background, methods, and results of ECV calculation.

Export Coefficient Value Calculation

Background and Methods

Based upon the work of Hodge and Armstrong (1993) and McFarland and Hauck (2001), I use a multiple regression technique for calculating export coefficient values (ECV) from in-stream nutrient measurements. Drainage areas above each water quality sampling site within BCLRW contain a mix of land cover types and vary in size (Table A.3). Ideally, developing ECVs involves several years of field plot observation to isolate pollutant export from individual land uses (Reckhow *et al.* 1980; McFarland and Hauck

2001). Published ECVs have been derived from empirical investigations whereby researchers conducted three- to ten-year experiments on agricultural, forested, and urban land uses from several different geographic regions (Beaulac and Reckhow 1982), including the southeastern United States (i.e., Alabama, Georgia, and North Carolina). While field plot observations may be the most intuitive approach for estimating ECVs, watersheds (small and large) include varying land uses; and, as the geographic scale increases to county- or state-sized areas, monitoring single land use watersheds for developing ECVs becomes unrealistic. Alternatively, the multiple regression approach isolates different nutrient-source land uses by associating in-stream constituent concentrations (mg/L) with surrounding land cover composition such that concentrations are portrayed as annual exports per land use area by land use type (kg/ha/year).

The multiple regression technique employed by McFarland and Hauck (2001) assumes a linear relationship between land cover composition within the drainage area above each sampling site and in-stream constituent concentrations. However, this method does not account for spatial location of land uses within the drainage area, which can be problematic in other study areas, such as BCLRW. For example, in drainage areas where a dairy farming operation is located in the riparian zone immediately upstream from an in-stream measurement and forest occupies the remaining drainage area, forest would be assigned a high total nitrogen (TN) ECV (because it occupies a high proportion of the total drainage area), obscuring the reality that the riparian dairy operation is the main TN exporter. Therefore, I modified this regression model to only include land cover within 200 m of the stream, rather than land cover from the entire drainage area.

The multiple regression model follows a three-step process. First, I calculated the drainage area above each sampling site, developed a 200-m buffer around all streams within the drainage area, and tabulated the proportion of land cover composition within the buffer (Table 2). Drainage area delineation was similar to the ordered watershed delineation, except calculations originated from each sampling site's XY coordinates rather than ordered streams. Because IPSI is the most detailed and up-to-date (*ca* 2000) land cover representation available for the study area, I used only this dataset for depicting land cover within drainage areas. Land cover proportions extracted from the buffered areas were used as independent variables. I chose a buffer width of 200 m based on research conducted by the USEPA (2002) in the Clinch and Powell Valley Watershed, Virginia, which is located within the same physiographic providence as BCLRW. USEPA (2002) found a strong correlation between riparian land cover and overall stream habitat where riparian zones extend 200 m across the streams, but weak correlations where riparian widths were > 200 m.

Second, I annualized concentrations of TP and TN by combining flow volumes and in-stream constituent concentrations. TP and TN concentrations (mg/L) were converted to kilograms per cubic meter (kg/m^3), multiplied by flow volumes (m^3/second), and portrayed annually (kg/year) to represent a total annual pollutant flux. Annual TP and TN (kg/year) loads were normalized by the area within each riparian buffer to give an estimate of nutrient load per area unit (kg/ha/year). Table 3 summarizes these calculations as average flow volumes and nutrient fluxes for the riparian zone of each sampling site's riparian zone. TDEC, for unknown reasons, did not include flow data for

Table 2: Riparian land cover composition associated with drainage areas above each sampling site.

Site	*Urban* (%)	*Forest* (%)	*Pasture* (%)	*Cropland* (%)	*Barren Land* (%)	*Total Area* (ha)
EC1	4.7	52.7	36.9	4.2	0.3	2,531
EC2	4.2	51.2	38.9	4.5	0.3	2,171
EC3	6.4	18.7	69.7	2.8	1.2	412
EC4	3.7	60.6	32.1	2.9	0.0	1,468
EC5	4.0	54.1	40.6	1.0	0.0	936
EC6	3.3	82.8	13.8	0.0	0.1	370
EC7	4.0	33.8	61.7	0.0	0.1	350
EC8	5.2	79.3	15.5	0.0	0.0	373
LR1	1.4	93.9	4.3	0.0	0.0	6,781
LR2	0.0	100.0	0.0	0.0	0.0	5,671
LR3	1.5	92.7	5.3	0.0	0.1	7,167
LR4	2.0	91.7	5.7	0.1	0.1	7,939
LR5	3.3	86.0	9.3	0.0	0.0	1,912
LR6	1.7	88.9	9.2	0.0	0.0	871
LR7	2.9	88.7	7.1	0.3	0.1	11,296
LR8	9.9	45.8	41.8	1.8	0.3	1,646
LR9	4.7	52.7	37.0	4.2	0.3	2,529
LR10	4.2	76.5	16.7	1.2	0.3	15,889
LR12	5.2	71.5	20.2	1.6	0.4	17,600
LT1	10.4	29.6	52.6	7.0	0.2	632
LT2	5.3	72.1	21.6	0.1	0.1	1,247
NC1	17.1	25.2	53.3	3.6	0.5	704
NC2	18.0	25.8	52.0	3.5	0.4	669
NC3	24.3	25.8	48.5	0.1	0.8	427
NC4	41.6	22.7	35.5	0.1	0.0	131

Table 3: Annualized riparian nutrient fluxes associated with drainage areas above each sampling site.

	Flow Volume		*TP*		*TN*	
Site	**m^3/yr**	**m^3/ha/yr**	**kg/yr**	**kg/ha/hr**	**kg/yr**	**kg/ha/yr**
EC1	18,222,656	7,201	14,855	5.87	56,387	22.28
EC2	13,769,362	6,343	10,970	5.05	40,462	18.64
EC3	2,494,678	6,055	1,993	4.84	8,911	21.63
EC4	6,462,565	4,401	5,825	3.97	15,750	10.73
EC5	5,885,575	6,289	5,136	5.49	17,486	18.68
EC6	1,586,064	4,282	1,694	4.57	2,644	7.14
EC7	1,821,897	5,211	1,231	3.52	5,592	15.99
EC8	1,166,989	3,127	981	2.63	1,764	4.73
LR1	6,076,861	896	33	0.00	2,650	0.39
LR2	8,494,537	1,498	139	0.02	1,291	0.23
LR3	2,474,188	345	129	0.02	1,044	0.15
LR4	12,542,246	1,580	263	0.03	9,382	1.18
LR5	18,265,903	9,551	621	0.32	10,558	5.52
LR6	10,571,372	12,139	296	0.34	9,155	10.51
LR7	18,230,583	1,614	547	0.05	14,694	1.30
LR8	1,582,350	962	32	0.02	665	0.40
LR9	7,897,624	3,123	142	0.06	2,575	1.02
LR10	71,638,439	4,509	90	0.01	8,955	0.56
LR12	94,349,405	5,361	4,859	0.28	29,720	1.69
LT1	12,538,714	19,830	88	0.14	4,012	6.35
LT2	14,949,325	11,988	149	0.12	12,333	9.89
NC1	10,285,076	14,611	1,282	1.82	17,995	25.56
NC2	10,915,509	16,310	11,902	17.78	19,864	29.68
NC3	3,174,031	7,438	390	0.91	10,768	25.23
NC4	1,574,901	12,016	171	1.31	4,097	31.26

LR11, LR13, and LR14 measurements; therefore, these sampling sites were omitted from the analysis.

Third, I developed a multiple regression model such that loadings per unit area (kg/ha/yr) at each sampling site were the dependent variable, while proportions of land use in the stream buffers above each sampling site were the independent variables. The regression coefficients generated from this analysis may then be used as ECVs in the ECM.

Results and Discussion of Export Coefficient Value Calculation

Overall regression results indicate that the independent land cover categories do not explain a large proportion of the variability in TP and TN annual loads ($R^2 = 0.10$ where $\alpha = 0.05$). Table 4 illustrates coefficient estimates for the five land cover classes, the associated standard error, and significance level. None of the TP and TN coefficient values for the land cover variables were found to be statistically significant. Moreover, negative TN coefficients produced from the barren land variable are considered unacceptable as an export coefficient because previous research supports the expectation of some positive loading from all land cover (Reckhow *et al.* 1980; Beaulac and Reckhow 1982; Frink 1991; McFarland and Hauck 2001; Winter *et al.* 2002). The McFarland and Hauck (2001) method used land cover proportions from an entire drainage area above each sampling site, rather than only those found in the 200-m riparian zone. They found the multiple regression models for TP and TN to be highly significant ($p = 0.0001$ and $R^2 = 0.95$ where $\alpha = 0.05$). I conducted an analysis using land cover from the entire BCLRW sampling site drainage areas, but still found no

Table 4: Multiple regression model coefficient estimates for nutrient loadings as a function of land cover percent in BCLRW.

	TN (kg/ha/yr)		*TP (kg/ha/yr)*	
Land Cover	**Parameter Estimate**	**p-Value**	**Parameter Estimate**	**p-Value**
Urban	1.64 ± 10.05	0.87	0.50 ± 0.83	0.55
Forest	0.69 ± 10.10	0.95	0.49 ± 0.85	0.56
Pasture	1.06 ± 10.15	0.92	0.50 ± 0.84	0.55
Cropland	0.79 ± 11.11	0.94	0.94 ± 0.94	0.32
Barren Land	-1.12 ± 23.88	0.96	1.03 ± 1.92	0.59

statistically significant coefficient values. Below, I identify three primary reasons for the lack of significant ECVs from multiple regression that uses land cover from the entire sampling drainage area or from the 200-m riparian zone.

First, a high level of multicollinearity exists between the independent land cover variables—particularly between forest and pasture. Most drainage areas within BCLRW are primarily composed of forest and pasture land; thus, as one increases the other decreases, creating negative correlations. To limit this, McFarland and Hauck (2001) simply combined land covers and omitted those land covers that characterized only a small proportion of the total drainage area. However, land cover within BCLRW has already been reclassified (*see* the GIS and Water Quality Data Section) and any further reclassification would be unreasonable. For example, combining pasture and forest is unreasonable for predicting annual TN exports because empirical studies have shown dramatic differences in TN exported from pasture versus forest land (*See* Chapter II).

Second, in-stream water quality data collected from BCLRW include only three sampling years (1998, 1999, and 2003), and continuous sampling within each sampling year does not exceed a six-month period. Data in the McFarland and Hauck (2001) study were collected bi-weekly and spanned a continuous 4-year period. Moreover, in BCLRW, all sampling was conducted during base (or low) flow conditions and two to three days after storm events. A more extensive and continuous BCLRW water quality survey that included storm events would be more representative of stream dynamics and might improve regression model results. However, the timeframe of this study prevented me from conducting a more extensive survey, and the data provided by TDEC were the only available.

Third, the multiple regression method (using land cover either from the entire sampling drainage area or from the riparian zones) assumes that land cover within the contributing area of each sample contributes 100% of the load flowing through that site. This assumption is problematic in that it does not consider additional nutrients that already exist in the stream from upland stream reaches that are beyond the sampling site's contributing area or decay that may occur as the nutrient flows through the drainage network.

The multiple regression model employed in BCLRW was unsuccessful for determining ECVs in BCLRW. Therefore, I calibrated the ECM with literature-reported values. Literature-reported values are widely available in a number of USEPA reports and environmental articles. They vary considerably depending on temporal scale and geographic region (Beaulac and Reckhow 1982) and thus must be calibrated to the study area.

Export Coefficient Model Calibration

The ECModeling approach, discussed further in the next section, requires one ECV for each input land cover class; hence, model results will be dependent on the input ECV. Nutrient ECVs cited in the hydrologic literature are highly variable; a number of interrelated factors contribute toward differences in nutrient loads, including climate, soil, and local land use management. Differences in ECVs may also arise from both measurement and/or estimation error (Reckhow *et al.* 1980; Beaulac and Reckhow 1982). To represent the uncertainty associated with literature-reported ECVs, I conducted a

sensitivity analysis using ECVs observed in similar climatic regimes as BCLRW. BCLRW is characterized by a temperate climate, with high rainfall, and primarily clay and silt loam soils with low infiltration rates (TVA 2003; Eric Henry, *personal communication*). Table A.4 illustrates the wide range of ECVs reported for the southeastern United States. All ECVs presented in Table A.4 were observed in southeastern regions, where climatic conditions are similar to BCLRW. Using the TP and TN distributions in Table A.4, I computed minimum, lower, median, upper, and maximum quartile ECVs for each land cover class (Table 5) (Winter *et al.* 2000; Wickham and Wade 2002; Endreny and Wood 2003).

Each quartile ECV (of TP and TN) was modeled individually and compared to water quality data collected from sampling sites EC1 and NC1 (Figure 5). Because BCLRW is not entirely defined by natural watershed boundaries, I was unable to calculate a cumulative nutrient flux for the entire study area. Furthermore, Little River Watershed sampling locations selected by TDEC in 1998 (Figure 4) did not include a site located at the river mouth, which would capture loading from the entire drainage area. Therefore, I have concentrated model calibration on Ellejoy Creek and Nails Creek, which are smaller sub-watersheds (Figure 5). These two sites are at pour points and capture water quality for the entire Ellejoy and Nails Creek drainage area. I computed annual nutrient fluxes (kg/yr) at sites EC1 and NC1 by combining in-stream nutrient concentrations (mg/L) with flow measurements (m^3/sec) (*See* the previous section—Export Coefficient Calculation—for more details). Five samples were taken at both EC1 and NC1 between June and November 2003. I repeated the annual flux calculation for each sample reading. Then, I averaged annual loads from NC1 and EC1 separately and

Table 5: Quartile aggregation of literature reported TP and TN ECVs by land cover.

	TP (kg/ha/yr)					*TN (kg/ha/yr)*				
Land Cover	**Min.**	**25%**	**50%**	**75%**	**Max.**	**Min.**	**25%**	**50%**	**75%**	**Max.**
Urban	0.43	1.90	2.25	4.34	5.35	1.56	7.19	10.88	13.32	28.00
Forest	0.01	0.20	0.39	1.23	2.00	0.03	0.13	0.24	2.19	3.12
Pasture	0.14	0.16	0.56	1.35	3.80	3.46	6.28	9.23	10.99	13.00
Cropland	0.40	1.14	2.41	3.70	17.64	3.04	4.05	14.98	19.30	46.50
Barren Land	0.05	0.15	0.25	0.39	0.52	0.50	1.25	2.00	4.00	6.00

summed their quotients. The summation represents the total nutrient load for both Ellejoy and Nails Creek watersheds portrayed as an annual flux (kg/yr).

In order to compare differences in model results from different land cover datasets, a common set of ECVs must be selected and used in both models. The sensitivity analysis allowed me to assess overall change of model prediction by quartile simulation and choose one set of ECVs. Each simulation was calibrated against the data collected at EC1 and NC1, and the ECV quartile which produced the best results compared to observed loading was selected. While lumped summation of total nutrient load produced from weighted and unweighted ECMs should be similar, I implemented the sensitivity analysis for these models separately. Assuming that IPSI is the most accurate land cover dataset, I limited model calibration to this dataset only. Results of the sensitivity analysis are presented and discussed in Chapter V.

The Unweighted Export Coefficient Model

The traditional ECM (*see* Equation 1) method considers area and land cover type for assigning one lumped summation of nutrient export to each sub-watershed, which is a simple approach that allows the researcher to analyze pollutant export variability *between* watersheds and prioritize them accordingly. The broad-scale nature of the unweighted model is especially useful in regional studies that, for example, examine the degree of nutrient variability between 1,000 watersheds within a state boundary or between 8-digit HUCs across the Mid-Atlantic (Jones *et al.* 1997; Wickham *et al.* 2002; Wickham and Wade 2002). However, when examining nutrient risk variability between sub-watersheds

within a county mapping region, uncertainties in land cover scale arise. In this research, the unweighted ECM provides a method for examining the level of uncertainty between land cover datasets in nutrient-loading simulations within a county-sized mapping region.

I implemented an ensemble of unweighted ECM simulations that swapped 10-m (fine scale), 30-m (broad scale), and 1-km (broad-scale) land cover datasets. The simulations were employed at the 4^{th}, 5^{th}, and 6^{th} order watershed extent for both TP and TN. I compiled nutrient model results produced from the three land cover datasets at multiple watershed extents and statistically tested, using a one-way ANOVA (SPSS 2001), for differences between result-group means. Using the mean, a one-way ANOVA tests for difference within and between groups and assumes normality within each dataset. Model results from each land cover simulation were negatively skewed; therefore, I transformed (natural logarithm) each result-group distribution *a priori* and removed outliers—null and zero values (Figures A.1 and A.2). The natural logarithm transformation will compute null values where original values are zero and negative values where original values are less than one. Including the negative values will distort the transformed distribution.

In addition to the ANOVA analysis, I aggregated nutrient export by watershed into four classes (or rankings) of prioritization and constructed a correlation matrix that examines changes in the prioritization of watersheds for nutrient export between IPSI- and NLCD-based simulations. The correlation analysis graphically maps exactly which and how many watersheds changed prioritization between simulations, allowing for a better understanding of differences between ECModeling with broad- and fine-scale data.

The Weighted Export Coefficient Model

Traditional ECModeling methods assume TP and TN exports are homogenously distributed across the landscape such that each similar land cover type exports the same nutrient load and 100% of that load reaches surface waters. The traditional ECM evaluates land cover composition within a watershed, assigns a nutrient ECV to those land covers (e.g., 2.3 kg/ha/year), and summarizes the total nutrient export for the entire watershed. Lumped summation of nutrient export by watershed does not allow the researcher to analyze spatial variability and prioritize risk areas within the watershed. In raster GIS, this shortfall is emphasized as traditional methods consider each pixel as a pollution source and do not consider the interaction between the other pixels' land cover type and topographic orientation, which either attenuate or accentuate loading levels (Endreny and Wood 2003).

When modeling broad scales (e.g., county- or state-sized areas), higher order variables, such as topography and land use begin to control pollutant fluxes and should be included in hydrologic modeling efforts (Meentemeyer 1989) while keeping modeling techniques simple (Soranno *et al.* 1996; Johnes *et al.* 1996; Sliva and Williams 2001; Endreny and Wood 2003). The ability to examine heterogeneously distributed nutrient exports in raster GIS allows the researcher a more detailed modeling technique (e.g., ranking 100-m^2 or 900-m^2 areas, rather than entire watersheds), while maintaining the simplicity and timeliness of traditional ECModeling at the county mapping level. The combination of traditional ECM methods and work by Beven and Kirkby (1979), Beven (1995), and Endreny and Wood (2003) provide a raster-based ECModeling approach that

computes topographic (TI) and buffering (BI) indices which dynamically weight ECVs to these higher order landscape variables and allow the researcher to identify spatial variability of nutrient export within the watershed.

The Topographic Index (TI)

The raster-based TI model identifies watershed areas that have a high potential of saturation after a significant rainfall or snowmelt event and thus a high likelihood for producing runoff. The model uses an index of wetness based on topography to illustrate the variability in hydrologic response from different areas within the watershed by determining the relationship between a pixel's upslope contributing area, per contour length, and slope. The TI is expressed as:

$$TI_i = \ln\left(\frac{a_i}{\tan B_i}\right) \qquad \text{(Eq. 2)}$$

where a is the land pixel i's upslope contributing area per contour length, which assumed to be equal to pixel size (e.g., 10 or 30 m), and B is land pixel i's slope angle (Beven and Kirkby 1979; Beven 1995; Endreny *et al.* 2000; Endreny and Wood 2003). The TI is applicable to humid areas, much like eastern Tennessee, where water table levels presumably follow the same pattern as the topography, and is based on the concept that runoff is produced as watershed soils become saturated and storage capacity reached (Dunne and Leopold 1979). Thus, those areas having a high potential of saturation are highly likely to produce runoff. Subsequent research investigated the spatial distribution and temporal history of water table levels in the eastern United States and found that the

TI is a reasonable measure for estimating water table elevation and saturation potential in humid areas of Pennsylvania (Torch *et al.* 1993; Hornberger and Boyer 1995).

Using elevation data from the DEMs, I generated a TI (with 10-m and 30-m DEMs) for BCLRW within Arc/Info© GRID©, generating a raster GIS layer that illustrates high to low values of pixel saturation potential and runoff likelihood. Primary GRID© functions used include `SLOPE`, `FLOW DIRECTION`, and `FLOW ACCUMULATION`. The flow accumulation algorithm identifies drainage networks by calculating flow direction and pixel accumulation on a cell-by-cell basis. It should be noted that values associated with the output layer from a flow accumulation routine are generic. Flow paths are identified by the number of pixels accumulated into one another. However, a weight layer can be used in lieu of simple pixel accumulation. For example, a raster layer that identifies levels of rainfall lost to runoff per pixel can be included in the GRID© drainage network computations as a weight layer such that the output pixel value identifies surface water volumes rather than simple pixel counts (ESRI 2004). In this research, I use a contour length layer, which has values equal to the DEM's resolution (10 or 30 m) as a weight layer in order to calculate the length of upslope contributing areas.

Using a four-step process I constructed TIs from 10- and 30-m DEMs. Figure 7 shows a graphic illustration of the GRID© computations and data utilized for TI generation, while the discussion below details each computational step.

Step 1 – Preparation of Raster Layers

Topographic depressions (or sinks) in the DEM (NED) were filled such that each pixel was not completely surrounded by pixels of higher elevation values. Again,

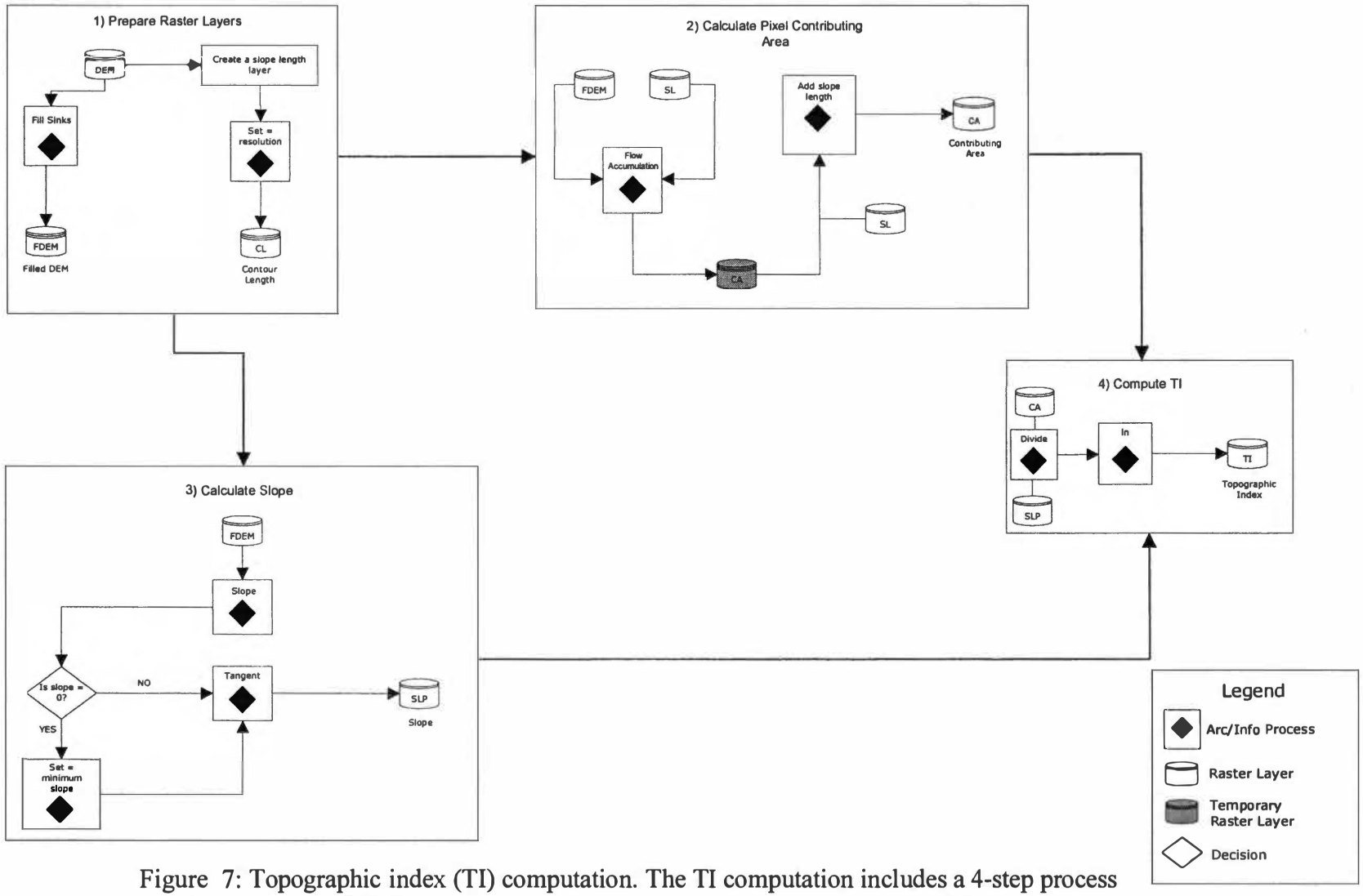


Figure 7: Topographic index (TI) computation. The TI computation includes a 4-step process within Arc/Info GRID. Each raster layer is evaulated and processed on a cell-by-cell basis.

depressions in the DEM interfere with flow path extraction and must be filled, which will be used to determine the lengths of upslope contributing areas.

Step 2 – Upslope Contributing Area Calculation

I extracted a drainage network from the filled DEM using the flow direction and accumulation algorithms. To identify slope length pixel-by-pixel, I created a contour length layer, set each pixel's value equal to the pixel's resolution, and used it as a weight layer in the flow accumulation computation. The output layer identified accumulated slope length across the entire study area; hence, each pixel's upslope contributing area, and the numerator (a) in Equation 2.

Step 3 – Slope Calculation

I calculated each pixel's maximum rate of elevation change to its neighbor as degrees and computed the tangent of that quotient, which provided the denominator (tan B) in Equation 2. In preparation for Step 4, I converted all zero slope values equal to the minimum slope value observed in BCLRW, which will avoid division by zero.

Step 4 – TI Calculation

Finally, I divided the contributing area and slope layers generated in Steps 2 and 3, and calculated the natural logarithm of the quotient to normalize the layer value distribution. Higher TI values identify those areas where saturation potential and runoff likelihood are high (Figure 8a).

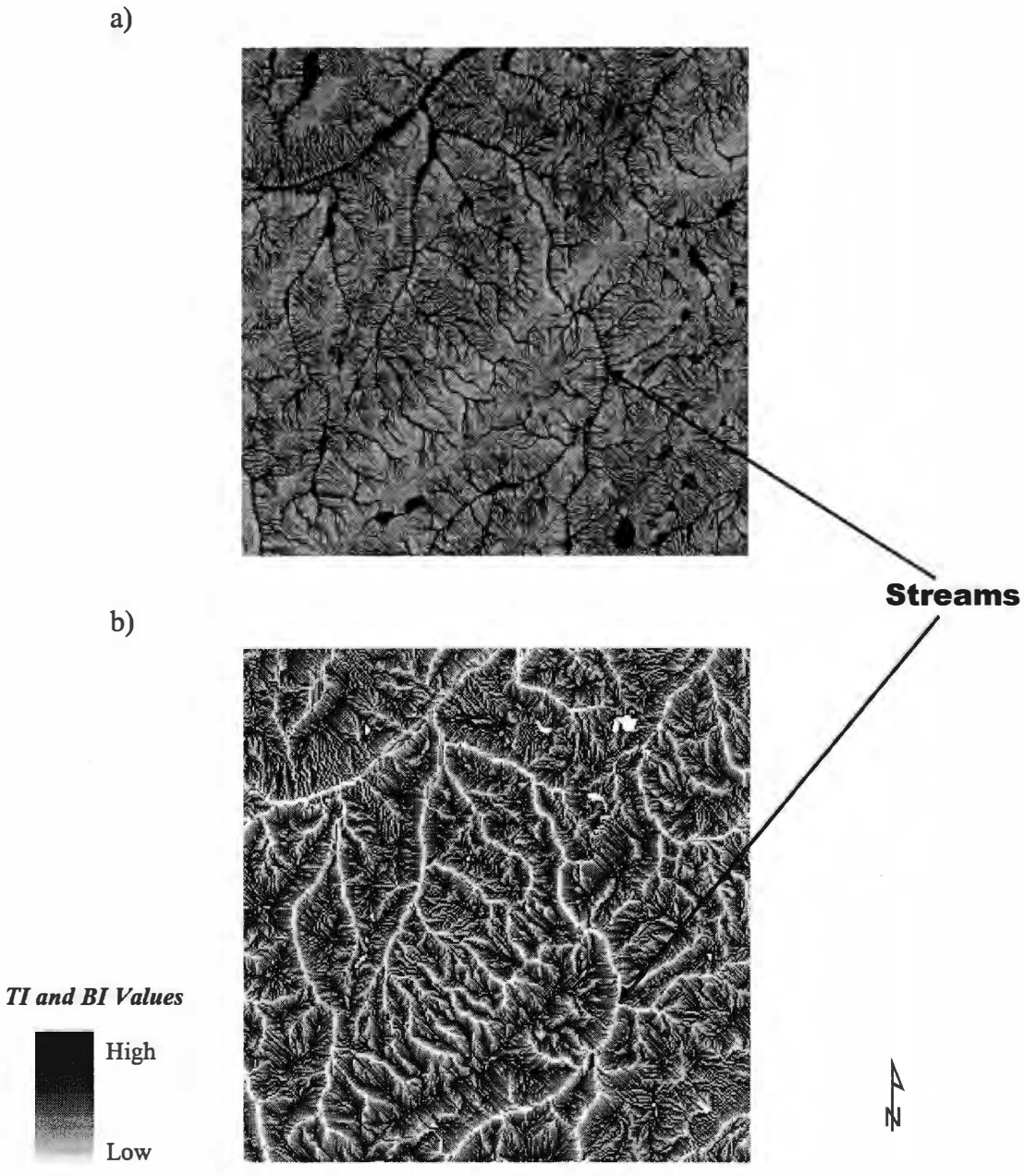


Figure 8: Topographic and buffer indices map. Mapped accross a 3 x 3 km area, the topographic index (a) identifies saturation and runoff likelihood, while the buffer index (b) identifies nutrient retention potential. Higher values in both cases indicate areas high in runoff likelihood or nutrient retention.

The Buffer Index (BI)

The BI was built upon the work of Endreny and Wood (2003) and uses a raster land cover layer and DEM for predicting each watershed pixel's potential for nutrient filtration by calculating pixel dispersal areas and relative nutrient trapping ability. The BI identifies overland flow dispersal areas and estimates relative values for each pixel's buffering likelihood using a DEM analysis that determines if each pixel's runoff actually enters a vegetative buffer. The BI is computed as:

$$BI_i = \ln\left(\frac{\sum_{DA=1}^{N} T_{DAi}}{\tan B_{DAi}}\right) \qquad \text{(Eq. 3)}$$

where $\sum T_{DAi}$ represents the dispersal area's total trapping efficiency and B_{DAi} represents the dispersal area's average slope. The BI computation combines DEM computed flow accumulation and slope with pre-determined values of nutrient trapping ability assigned to each land cover class. I computed Equation 3 for both 10-m and 30-m datasets (DEMs and land cover) in a six-step process within GRID© using much of the same algorithms used for the TI model with the exception of some additional processing steps. Figure 9 illustrates a graphic model of the processing steps used for the BI model's development.

Step 1 – Preparation Raster Layers

In preparing the land cover layers, I calculated a trapping layer of nutrient-reduction rates set to a fraction that represents buffering capacity and release based on the land cover dataset. For example, if a forest pixel traps 80% of TP carried by runoff, the output trapping layer will depict that pixel value as 20% (or 0.2) of that load being

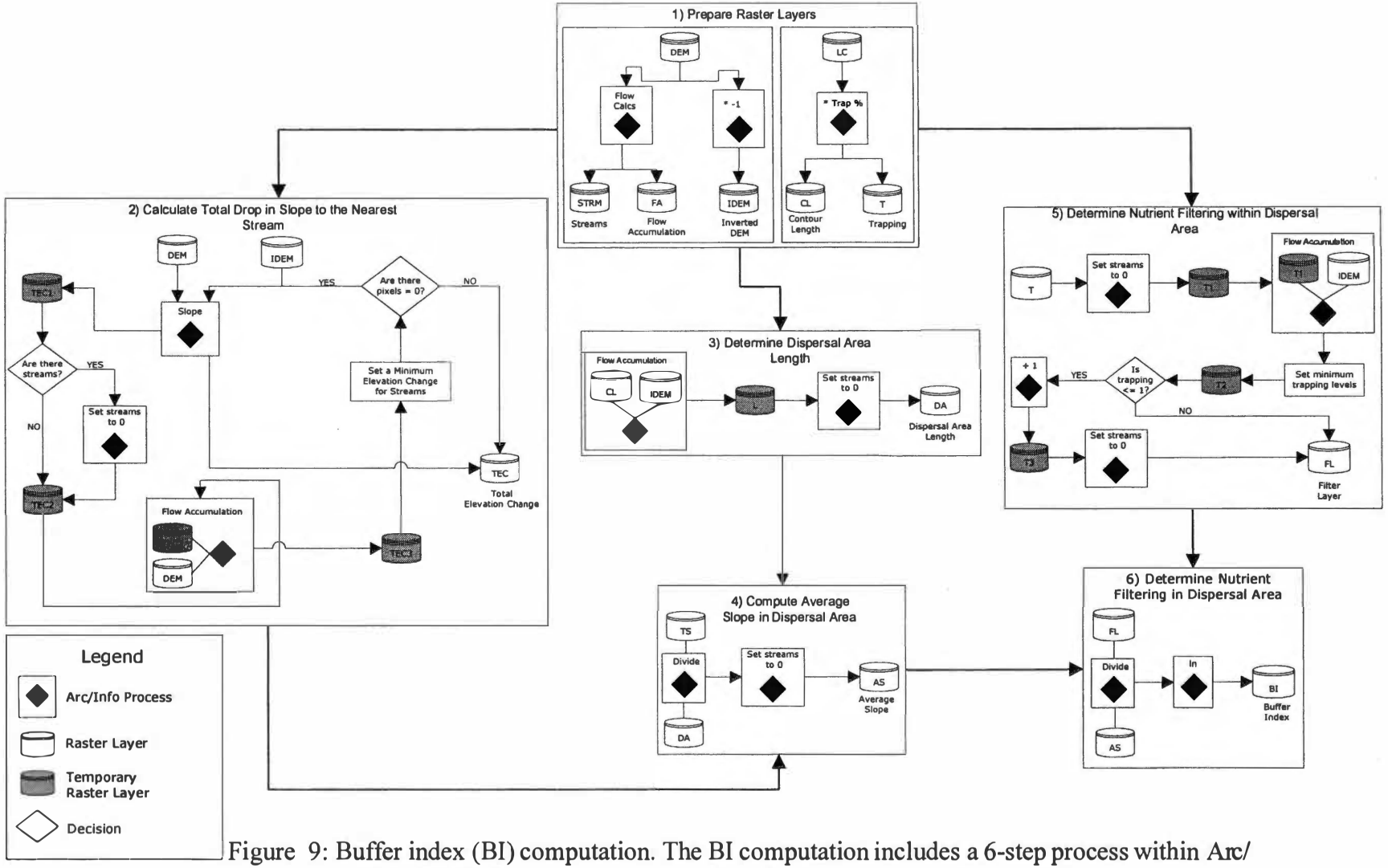


Figure 9: Buffer index (BI) computation. The BI computation includes a 6-step process within Arc/Info GRID. Each pixel is evaluated and calculated on a cell-by-cell basis.

released. Other researchers report a 40% to 90% reduction in TP by forested field plots 5 to 30 m in length (Uusi-Kamppa *et al.* 1997). Likewise, observed trapping rates for TN were estimated to be 60% to 97% in native grassland and forested plots 30 m in length (Lee *et al.* 2003). The raster approach to modeling land cover identifies one value for each pixel that is 10 or 30 m in length; hence each 30-m pixel of forest, for example, must represent a 900 m^2 forested area (or trapping plot). Therefore, I base the selection of trapping percentages (Table 6) on plot size (or resolution of the input data). Finer-resolution data (e.g., IPSI) were assigned lower trapping values, while broader-resolution data (e.g., NLCD) were assigned the higher values. I was unable to acquire any additional research that provided more support to the observations made by Uusi-Kamppa *et al.* (1997) and Lee *et al.* (2003). Additional literature would make it possible to examine variability in nutrient retention values between different climatic and physiographic regimes. Also, additional literature-reported nutrient retention values could have been included in the sensitivity analysis, which would help to calibrate the BI with nutrient retention characteristic of BCLRW.

The grass plots observed by Uusi-Kampp *et al.* (1997) and Lee *et al.* (2003) included native grass and switchgrass species. All grassland within BCLRW is classified by IPSI and NLCD as pasture. Of the pasture I observed during water quality surveys, all appeared to be active grazing land. Un-grazed/un-maintained pasture patches, which may function like native grass and switchgrass species in reducing nutrient loads, are uncharacteristic of BCLRW because of the limited land suitable for agricultural practices available to farmers (Eric Henry, *personal communication*).

Table 6: Nutrient retention values by land cover class.

	IPSI		*NLCD*	
	TP	**TN**	**TP**	**TN**
Urban	1%	1%	3%	3%
Forest	40%	40%	95%	95%
Pasture	5%	5%	15%	15%
Cropland	1%	1%	3%	3%
Barren Land	5%	5%	15%	15%

Assuming that a minimal amount of nutrient retention occurs in pasture, I conservatively assigned minimal retention values (1% and 3%) to TP and TN in pasture. Likewise, urban areas and barren land may contain patches of filtering vegetation (such as forest within a golf course); however, the scale of the three land cover datasets is too coarse to depict such a detailed classification, and urban areas consist of more complex runoff systems (e.g., sewer systems) that will divert runoff away from any retention opportunities and complicate the retention process. Therefore, I have assumed that forest—woody vegetation, shrub lands, and wetlands—is the only significant filtering land cover within the six-class scheme. Urban, cropland, and barren land cover were also assigned minimal retention values because no existing literature provides evidence that they significantly contribute to the retention of TP and TN transported via runoff.

In preparing the filled DEM for dispersal area delineation, I created a stream layer and an inverted DEM. The stream layer was calculated from the flow direction and accumulation algorithms and was manipulated such that all high-accumulation pixels (> 500) were set to zero. Streams are the destination for nutrients transported via overland flow; therefore, the final BI layer must identify all streams as zero or null. To be consistent with the streams used in sub-watershed delineation, I used only streams extracted from the 10-m DEM in both 10- and 30-m BI analysis.

The inverted DEM was calculated by multiplying filled DEM values by -1, which portrayed all ridges as low-lying valleys and valley bottoms as ridge tops. This layer is crucial for identifying a pixel's dispersal area, and the total length of that dispersal area. The flow direction and accumulation routines determine the direction and accumulation of flow from higher to lower elevation, hence each pixel's upslope-contributing area.

The inverted DEM enables the same calculations to be made except in reverse, thus determining pixel dispersal areas.

Step 2 – Calculate Total Drop in Slope from Pixel to Nearest Stream

I used the slope algorithm to generate a maximum change (or drop) in slope layer such that all stream-pixel values are set to zero. I then calculated flow accumulation using the filled DEM and slope layer as a weight layer, which generated a layer identifying the total (or accumulated) drop in slope from every terrain pixel to the nearest stream. Stream pixels within this layer were then set to the minimum-slope value, which is in preparation for avoiding division by zero in Step 4.

Step 3 – Determine Pixel Dispersal Area Length.

In this step, I used a contour-length layer as a weight layer and inverted DEM within the flow accumulation algorithm to calculate each pixel's total dispersal-area length (or run) from each terrain pixel to the nearest stream. The contour-length layer assumes that contour length at each raster-pixel location is equal to the resolution (or length) of each pixel. As in the computation in Step 2, incorporating a weight layer of contour length allows the flow accumulation routine to assign each pixel a value indicating accumulated length from that pixel to the nearest stream. To avoid division by zero in Step 4, stream-pixel values within the resulting layer were set to one.

Step 4 – Compute Average Slope in Dispersal Area

The denominator in the Equation 3 was obtained by dividing the two flow accumulation layers obtained from Steps 2 and 3—the total change in elevation, and the dispersal-area length. The streams in the subsequent layer were set to zero by identifying their spatial location in relation to the streams created in Step 1. In other words, all

stream pixels in the denominator layer that share the same spatial location as the stream layer were set to a value of zero, while all other pixels maintained their value.

Step 5 – Determine Nutrient Filtration within Dispersal Area

The trapping layer computed in Step 1 was further processed for deriving the total nutrient reduction within each pixel's dispersal area. A zero stream layer and trapping layer overlay identified all stream pixels within the trapping layer. The trapping layer was then included in a flow accumulation (using the inverted DEM) routine as a weight layer to identify an accumulated amount of trapping within each pixel dispersal zone. Again, this step excluded all streams, which were assigned a trapping value of zero.

Step 6 – Determine Nutrient Filtration in Dispersal Area

Finally, I generated the BI layer by computing the natural logarithm of the total nutrient filtering (numerator) and the average-slope-in-dispersal-area (denominator) quotient. The natural logarithm is computed in order to collapse the spread of the BI distribution. Higher raster values identify the pixels with a higher likelihood of nutrient filtration (Figure 8b). Typically, ridge tops within forest cover have high-BI values because of their large dispersal area. Overland flow associated with larger dispersal areas and forest cover has a longer traveling time to reach streams and thus has more opportunities to become trapped.

Normalization of Topographic and Buffer Indices

The BI and TI were used to map hydrologically sensitive areas in BCLWR. Because the weighted ECM models nutrient variability within sub-watersheds, TI and BI datasets must first be normalized such that each sub-watershed's cumulative nutrient load

is equal to that of its weighted nutrient load (Endreny and Wood 2003). The normalization is computed as: (Eq. 4)

$$NTI_i = \frac{TI_i}{\Phi TI}$$

$$NBI_i = \frac{\Phi BI}{BI_i}$$

where Φ indicates the median BI or TI value. The median was used rather than the mean because TI and BI (both 10-m and 30-m) consisted of skewed value distributions. This weighting scheme requires a median value from each watershed used in the analysis, which allows for normalized TI and BI values to override one another once placed in the final ECM equation. However, the normalized TI and BI distribution must be somewhat similar for the weighting scheme to work correctly (Endreny and Wood 2003).

Normalized 10- and 30-m BI distributions for BCLRW included both negative and positive values. This is problematic because a negative BI value will result in negative nutrient exports and all watershed pixels, in this research, are assumed to be associated with a positive export. The negative BI numbers are calculated during natural logarithm computation. High retention values assigned to the forest land cover result in low nutrient release rates. During natural logarithm calculations, lower values (e.g., < 1.0) are computed as negative. I compensate for this problem by shifting the BI distribution so that all BI values are positive and similar to the TI distribution. Again, the weighting scheme identifies relative (pixel-by-pixel) nutrient export, allowing the researcher to prioritize nutrient areas and not to report accurate export amounts. Furthermore, negative nutrient export values could be considered as hydrologic sinks;

however, in this research, I assume that sinks ≥900 m^2 are unlikely to occur in eastern United States regions (Mark 1988). While sinks of 100 m^2 have the potential to exist in areas similar to BCLRW, I did not include them in the analyses because of the broad scale nature of ECModeling.

Weighted Export Coefficient Model Application

The weighted ECM analysis will evaluate each watershed pixel's terrain orientation, downslope trapping ability, and land cover for determining relative nutrient export pixel-by-pixel, generating a single raster GIS layer. The resulting NTI and NBI values were used in Equation 1 as:

$$L_N = \sum_{i=1}^{N} \left[\left(E_i * NTI_i * NBI_i \right) * A_i \right] \qquad \text{(Eq. 5)}$$

where L is the summarized load for watershed N, E is the ECV for watershed pixel i, NTI and NBI are the normalized topographic and buffer indices for watershed pixel i, and A is the area of watershed pixel i. The area of each watershed pixel remained consistent (100- and 900- m^2). While the cumulative load calculations in Equation 1 and Equation 5 are similar, I chose to implement two separate ECMs in this research to save computer-processing time. TI and BI generation for large areas with multiple datasets (e.g., 10-m and 30-m raster layers) at multiple watershed extents (e.g., 4^{th}, 5^{th}, and 6^{th} order watersheds) can be time-consuming. Analyzing cumulative loadings for the entire study area with Equation 1 versus Equation 5 minimizes processing time.

Unlike the unweighted ECM, the GIS layer produced from the weighted ECM allows the researcher to visualize where high nutrient exports are originating within the

watershed (e.g., in the riparian zone or on concave hillslopes) and then begin to consider different management scenarios (e.g., riparian reforestation, pasture improvement, etc.) for mediating the area (Figure 10). Once a particular best management practice (BMP) has been identified, a management team can then verify the decision with field surveys. By swapping land cover datasets during weighted ECM simulations, I can determine (1) if broader-scale-based (e.g., NLCD and 30-m NED) results are appropriate for making the same decisions regarding potential BMP scenarios, and (2) whether usable loading information can be extracted from critical areas—such riparian zone loading—compared to results using finer-scale data (e.g., IPSI and 10-m NED).

I implement the weighted ECM in only three sub-watersheds that exhibit low, moderate, and high nutrient loading with IPSI and NLCD, which were identified by the unweighted ECM analysis. LULC-AVHRR was excluded from this analysis because the large pixel resolution (1-km) is not practical for prioritizing risk areas within sub-watersheds. Using IPSI and NLCD, I was able to visualize the areas where nutrient flux was originating (i.e., in the riparian or non-riparian zone) and consider different BMP scenarios. I based riparian buffer widths on stream order. First- and second-order streams were assigned buffer widths of 50 m; whereas, third-, forth-, and fifth- order streams received buffer widths of 100 m. It was necessary to decrease the riparian-zone widths from the width suggested by USEPA (2002) because within smaller sub-watersheds a 200-m buffer will occupy most of the total area. The sub-watershed extent (e.g., 4^{th} or 5^{th} order sub-watersheds) for this analysis was based on results from the unweighted ECM analysis. In Chapter IV, I further discuss these three sub-watersheds and results from calibration, unweighted, and weighted ECM analyses.

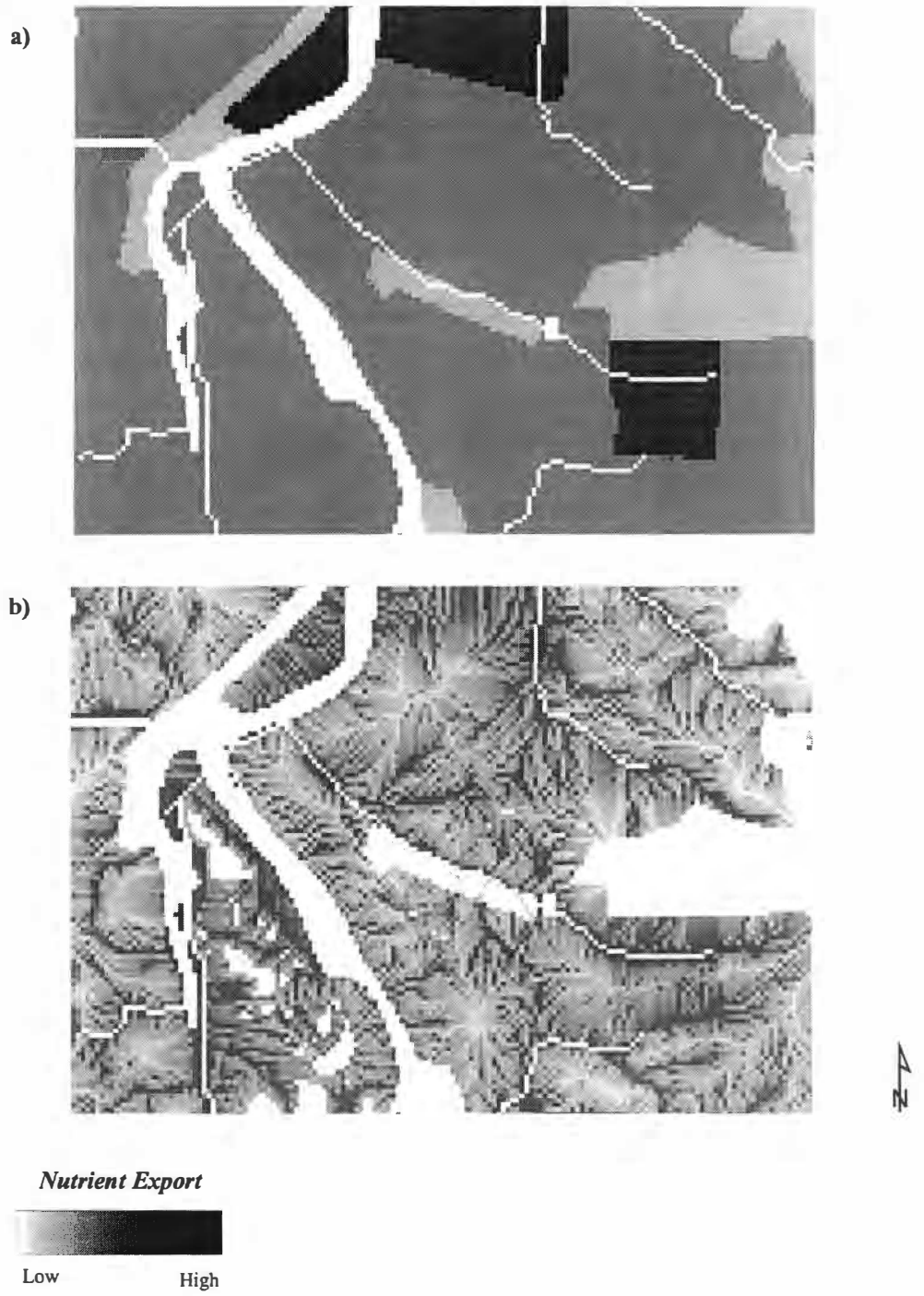


Figure 10: Unweighted vs. weighted ECM nutrient export map. Mapped within a 1 km^2 section of BCLRW, the (a) unweighted ECM only accounts for land cover type; whereas, the (b) weighted ECM accounts for topographic orientation and nutrient retention.

CHAPTER V
RESULTS

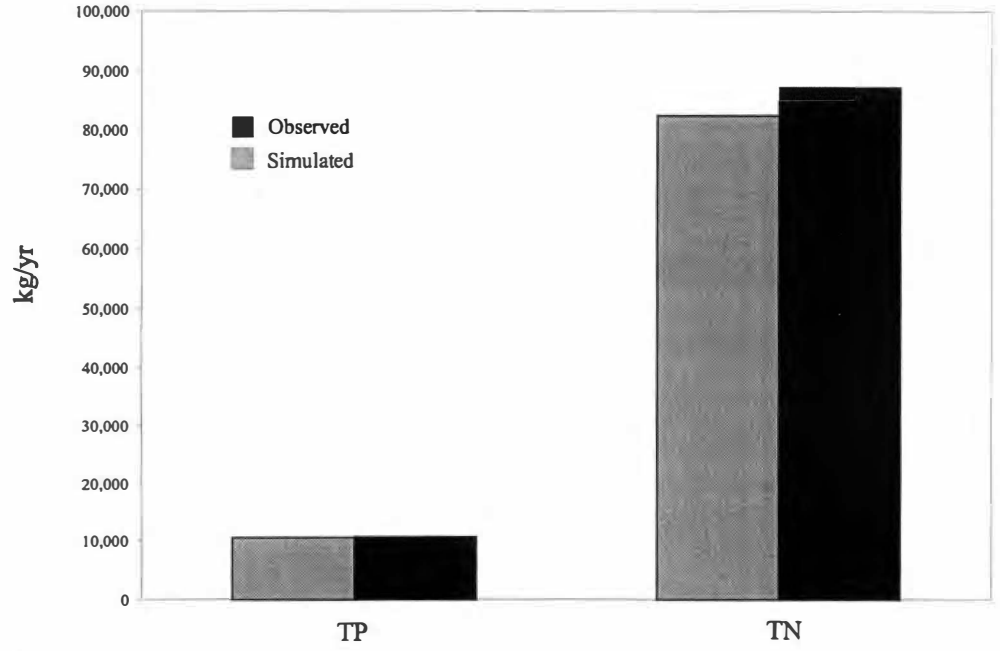
This chapter presents three sets of results from: (1) Export Coefficient Model (ECM) calibration analysis, (2) unweighted ECM statistical analysis, and (3) weighted ECM analysis.

Calibration Analysis: Export Coefficient Value Selection

The calibration analysis included both unweighted and weighted ECMs. In both cases, the set of median total phosphorus (TP) and total nitrogen (TN) export coefficient values (ECV) from Table 5 yielded comparable results to observed loads in Ellejoy Creek (EC1) and Nails Creek (NC1) watersheds (Figure 11; Table A.5). Using median ECVs, I found the unweighted ECM results to be within 5% of observed loads, and weighted ECM results to be within ±12% of observed loads. Table A.5 illustrates absolute loading values produced from all ECV quartile simulations. Figure 11 indicates that both unweighted and weighted ECM simulations, using the median set of ECVs, slightly underestimated observed nutrient loads. While slightly increasing ECVs would compensate for this underestimation, I felt the variation between observed and simulated loadings was minimal and chose to use only the median set of ECVs in the BCLRW-ECMs.

In this analysis, I used only the IPSI land cover because this research assumes that IPSI (*ca.* 2000) is the most accurate representation of land cover in BCLRW. A

a)



b)

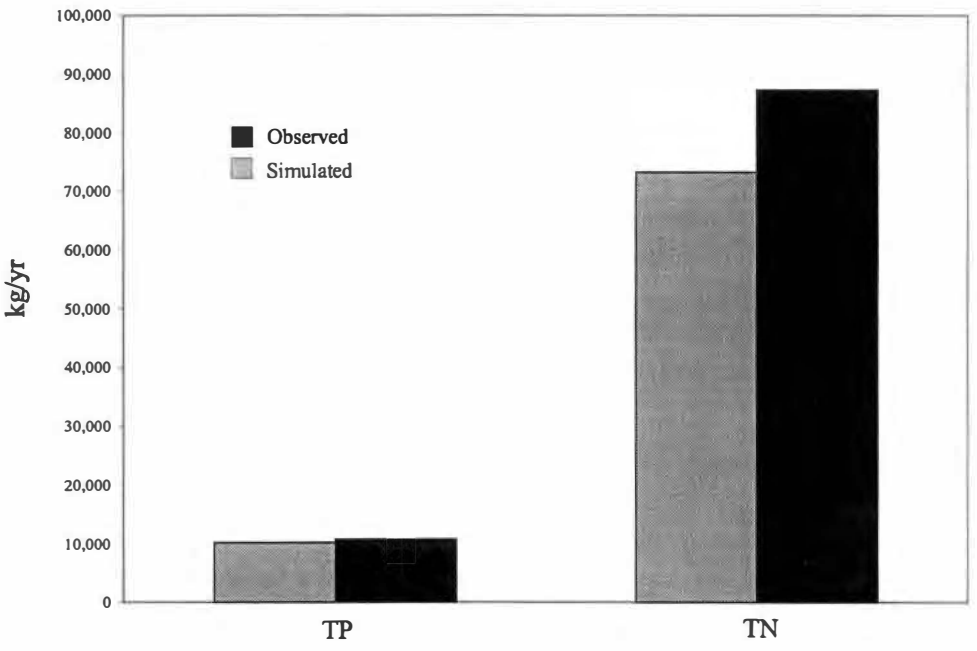


Figure 11: ECM calibration results. Difference between observed loadings and loadings calculated in the (a) unweighted ECM using median ECVs were -0.9% (TP) and -5.0% (TN). Likewise, difference between observed loads and loads produced by the (b) weighted ECM were -0.5% (TP) and -12.0% (TN).

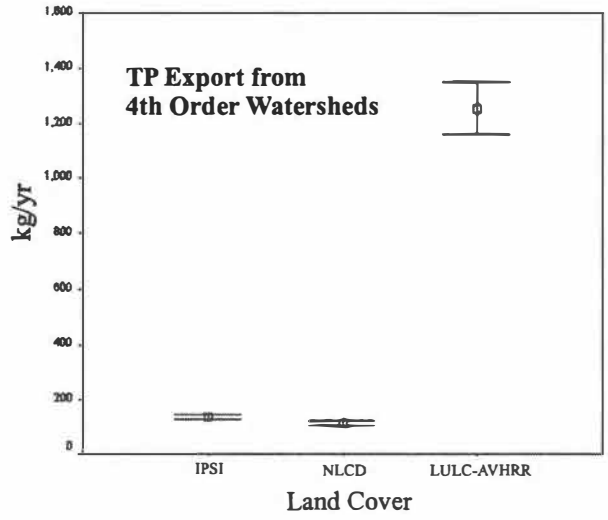
preliminary calibration analysis using NLCD also suggests the median ECVs yield results closest to the observed loads.

The Unweighted Export Coefficient Model Analysis

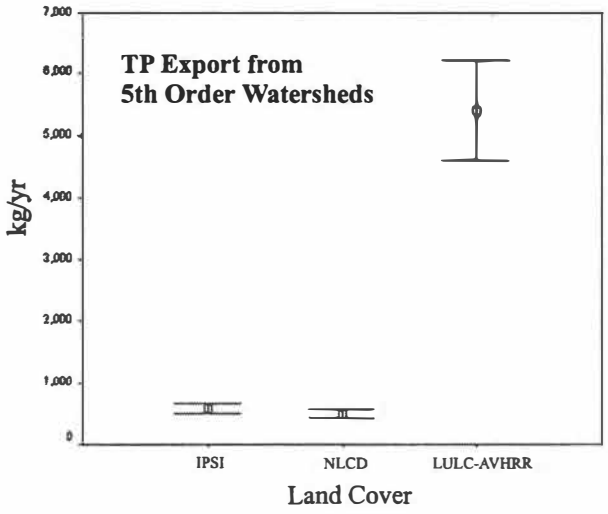
ANOVA results indicate a significant difference ($p = 0.0001$ $\alpha = 0.05$) between IPSI-, NLCD-, and LULC-AVHRR-based simulation results when modeling TP and TN at the 4th, 5th, or 6th order watershed mapping extent. Figures 12 and 13 illustrate that, while the difference between land cover simulation groups decreases as spatial extent is broadened, difference in nutrient loading as simulated within land cover groups increases with the change in watershed extent. This phenomenon is related to spatial data aggregation, and the modifiable aerial unit problem (MAUP) (Jelinski and Wu 1996). Statistically significant differences between the three groups, however, are obviously due to extreme variation between the LULC-AVHRR-based results and the IPSI- and NLCD-based results. This suggests that general landscape patterns of nutrient export are statistically lost between 10-m or 30-m and 1-km data.

Therefore, I conducted a second ANOVA analysis in which LULC-AVHRR-based results were excluded. Using only IPSI- and NLCD-based results, the ANOVA test indicates that result groups are statistically significantly different *only* at the 4th order watershed extent (Table 7). Differences between TP and TN model results produced from IPSI and NLCD at the 5th and 6th order mapping extent *are not* statistically significant, which implies the 5th order mapping extent is the threshold mapping scale at which differences in broad- and fine-scale (e.g., IPSI and NLCD) model results are not

a)



b)



c)

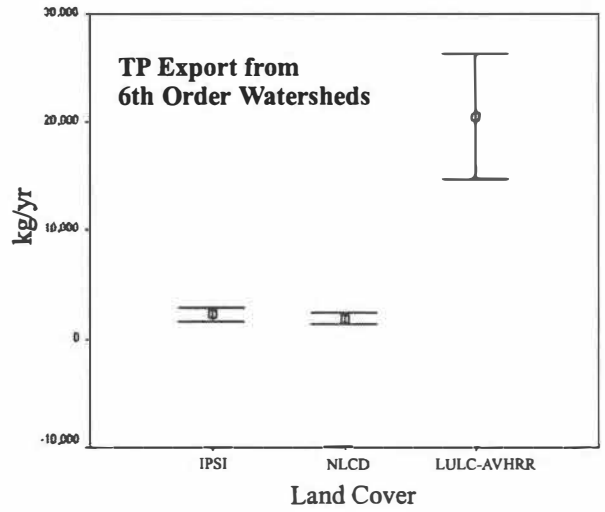
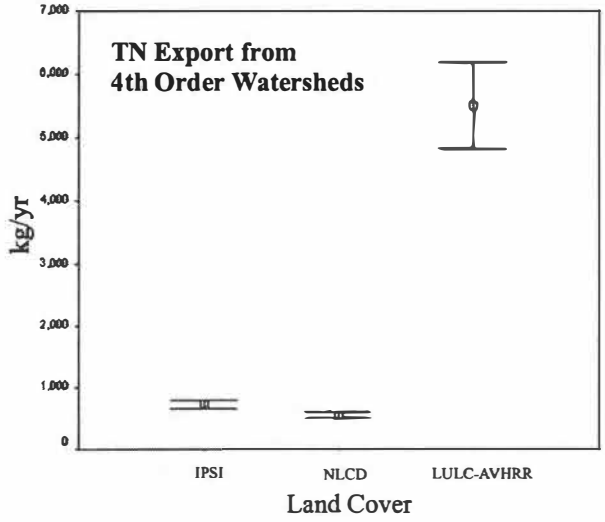
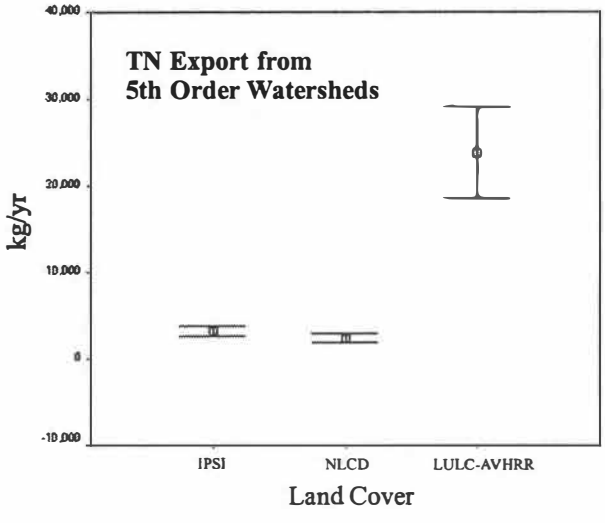


Figure 12: Difference within and between land cover-based TP simulation results.

a)



b)



c)

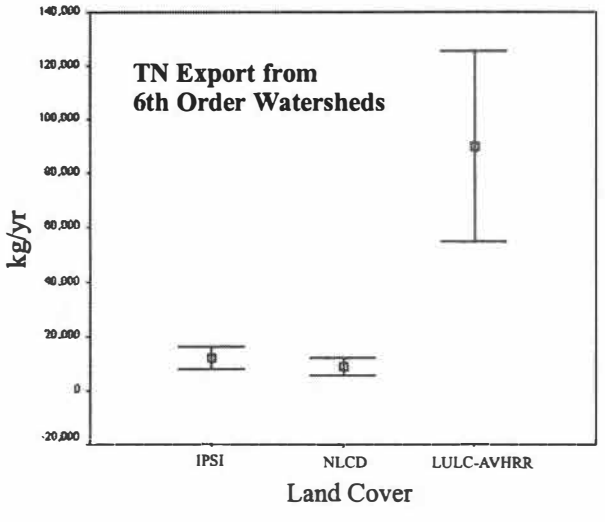


Figure 13: Difference within and between land cover-based TN simulation results.

Table 7: Statistical differences in unweighted ECM results between IPSI- and NLCD-based simulations.

	TP p-Values	*TN p-Values*
4th Order	0.001*	0.0001*
5th Order	0.082	0.25
6th Order	0.574	0.331

* Denotes statistically significant differences between groups with 95% confidence.

apparent. Because ANOVA assumes normality within and equal variance between each dataset (SPSS 2001), I transformed each ECM-result dataset using the natural logarithm (Figures A.1 and A.2) and tested for homogeneity of variance using the Levene statistic. The homogeneity of variance test indicated that all data distributions consisted of statistically equal variances ($\alpha = 0.05$).

Although modeling TP and TN at the 4th order watershed extent produces results from NLCD that are statistically different than results from IPSI, it is important to consider the difference in the prioritization of watersheds for nutrient flux that occurred between model simulations using NLCD and IPSI. Figures 14 to 19 illustrate differences in the prioritization of watersheds between 4th, 5th, and 6th order watersheds. I categorized total watershed nutrient export into four classes, which were developed from natural breaks in the modeled TP- and TN-result distributions (Figures A.2 and A.3; Table A.6). TP and TN value distributions produced from ECM simulations vary considerably between land cover datasets.

Patterns of nutrient flux are a function of land cover locations. Classification schemes, such as quantiles or equal intervals, assign an equal number of watersheds to each grouping. While this may be ideal for comparing multiple datasets, it causes undesirable representations of nutrient flux by associating, for example, a high rank to forested watersheds that have lower exports. This would contradict empirical evidence that has shown strong negative correlations between forested cover and nutrient flux (*See* Chapter II). On the other hand, the natural breaks classification scheme assigns breaks to small groups that are inherent to each dataset (ESRI 2004). Because BCLRW 4th, 5th, and 6th order watersheds vary considerably in size, I normalized the cumulative loads per

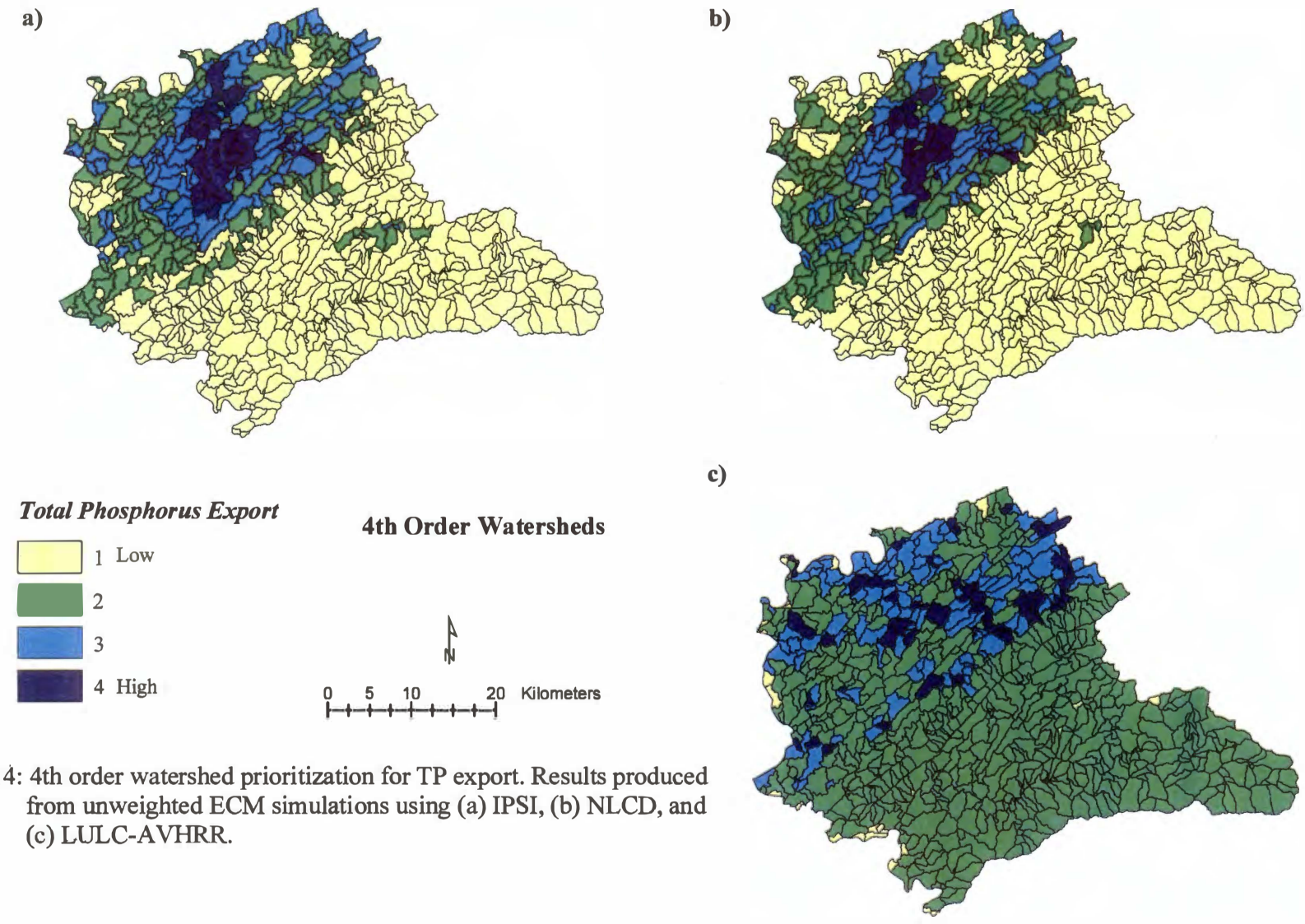


Figure 14: 4th order watershed prioritization for TP export. Results produced from unweighted ECM simulations using (a) IPSI, (b) NLCD, and (c) LULC-AVHRR.

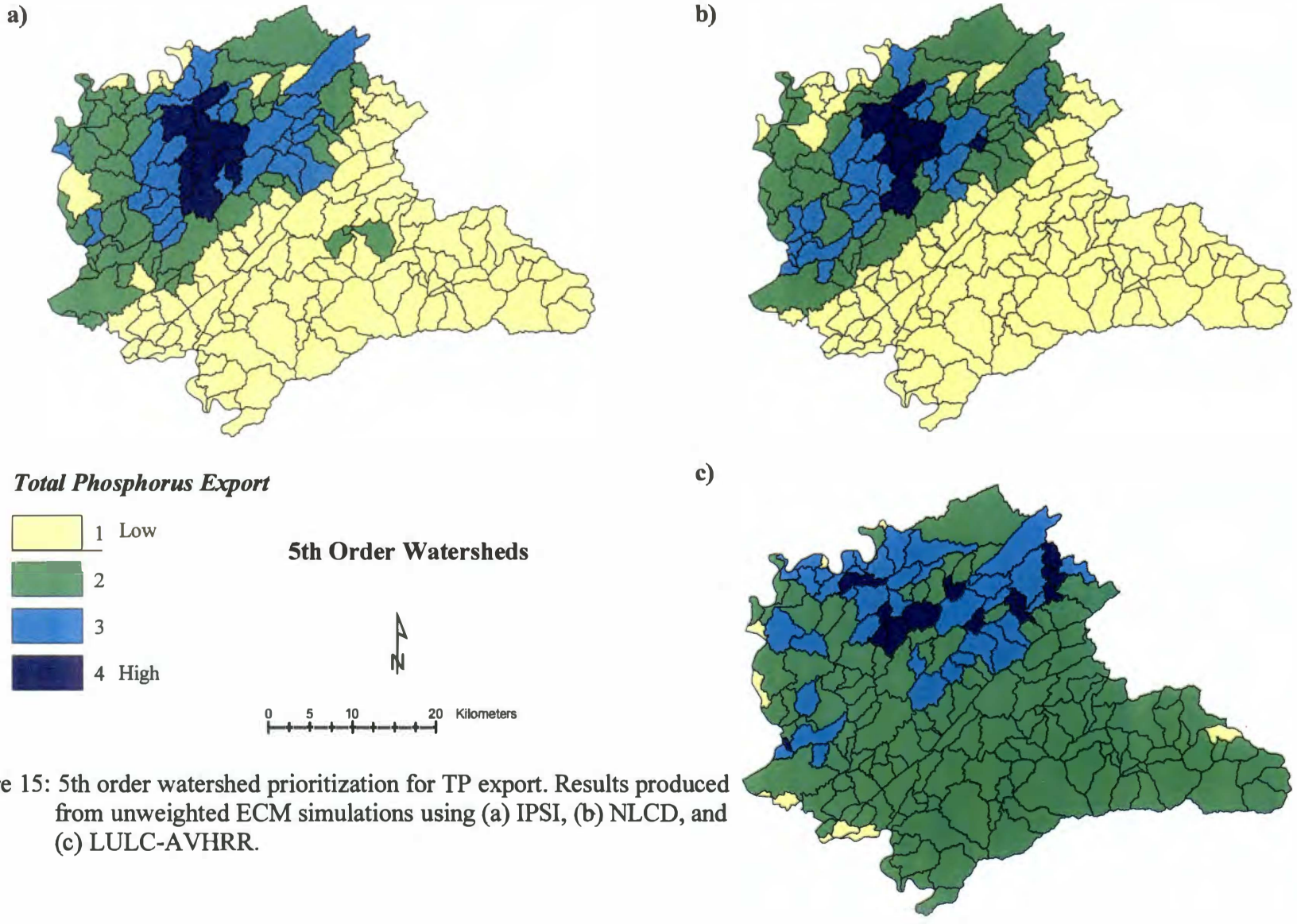


Figure 15: 5th order watershed prioritization for TP export. Results produced from unweighted ECM simulations using (a) IPSI, (b) NLCD, and (c) LULC-AVHRR.

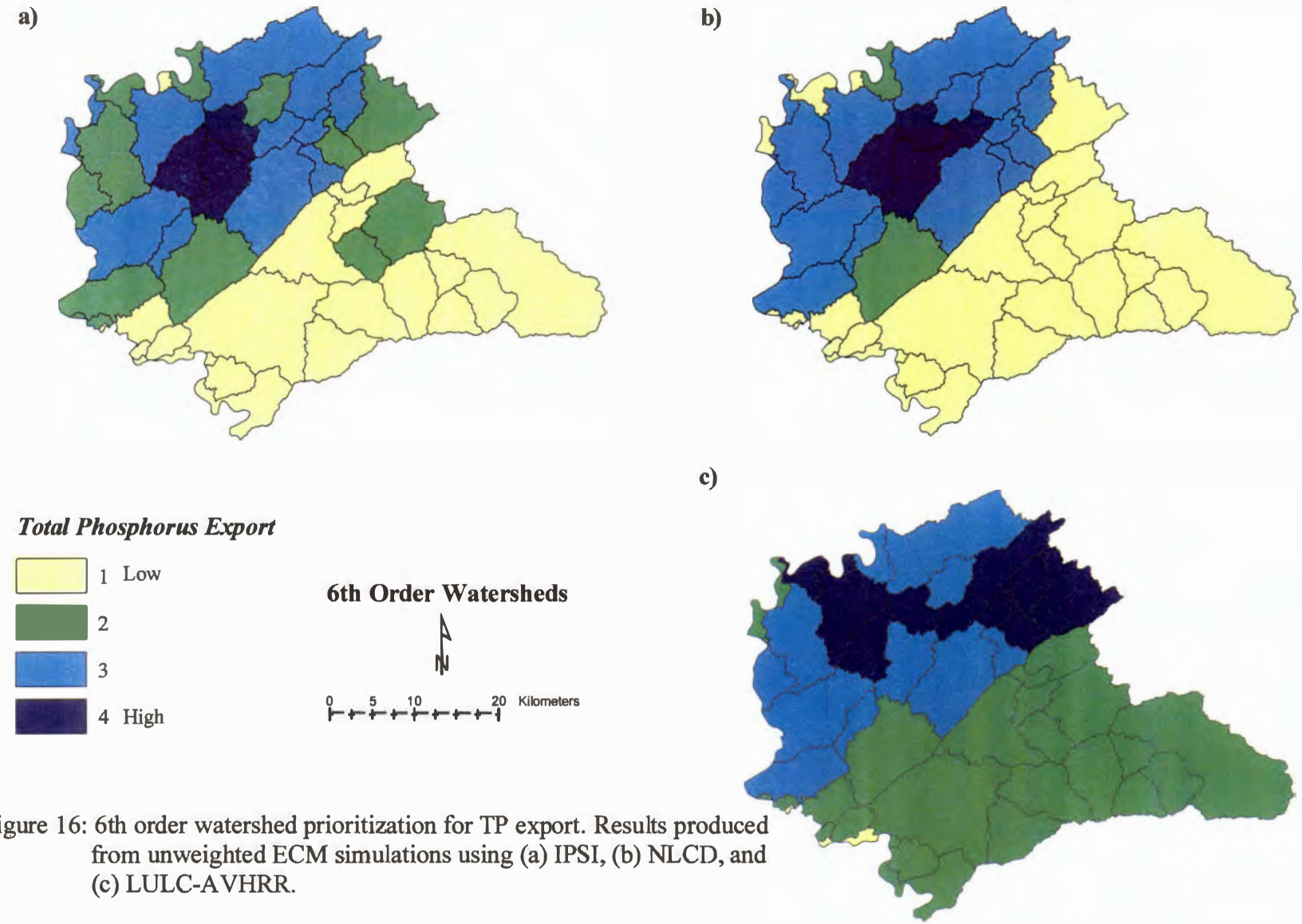


Figure 16: 6th order watershed prioritization for TP export. Results produced from unweighted ECM simulations using (a) IPSI, (b) NLCD, and (c) LULC-AVHRR.

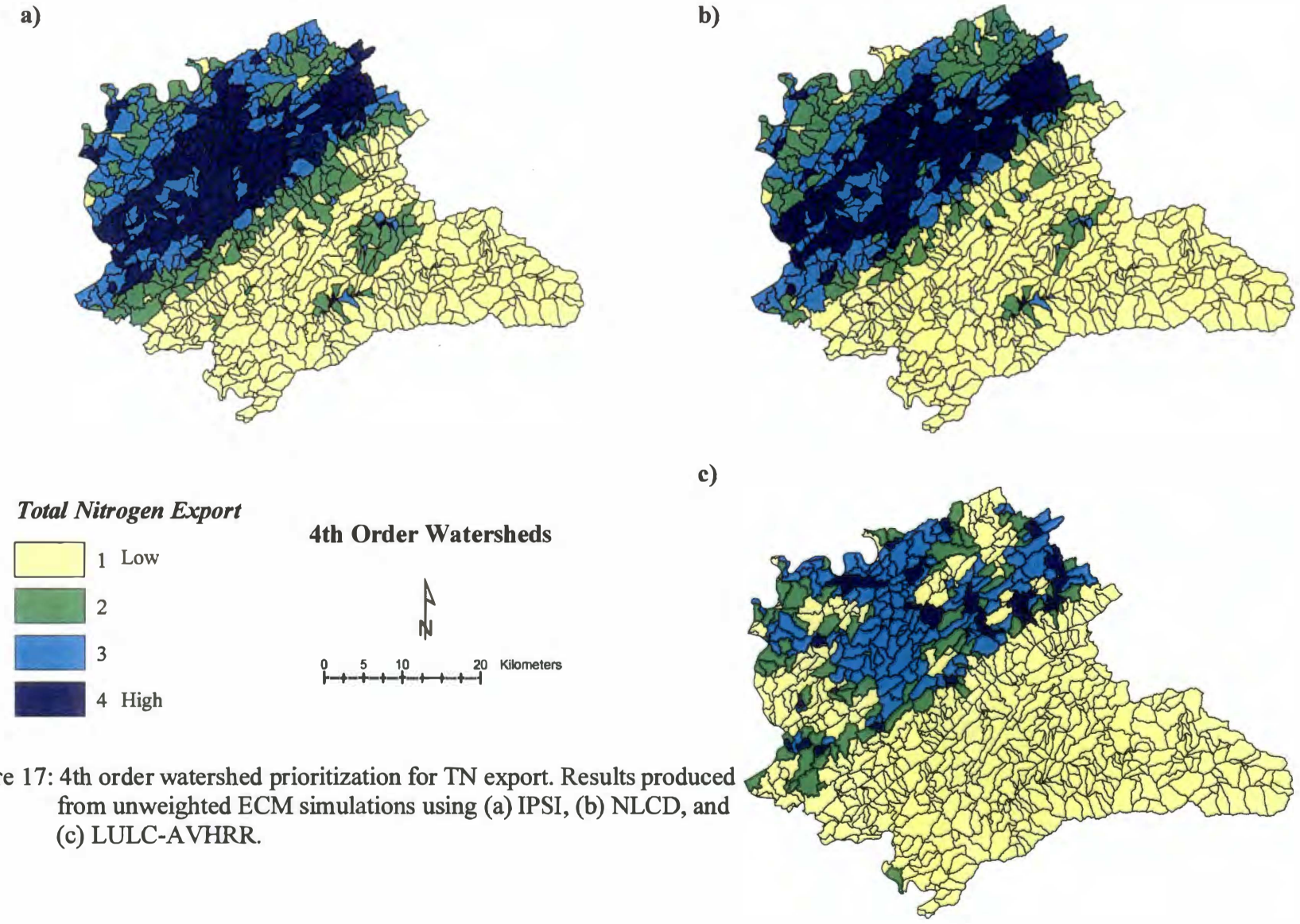


Figure 17: 4th order watershed prioritization for TN export. Results produced from unweighted ECM simulations using (a) IPSI, (b) NLCD, and (c) LULC-AVHRR.

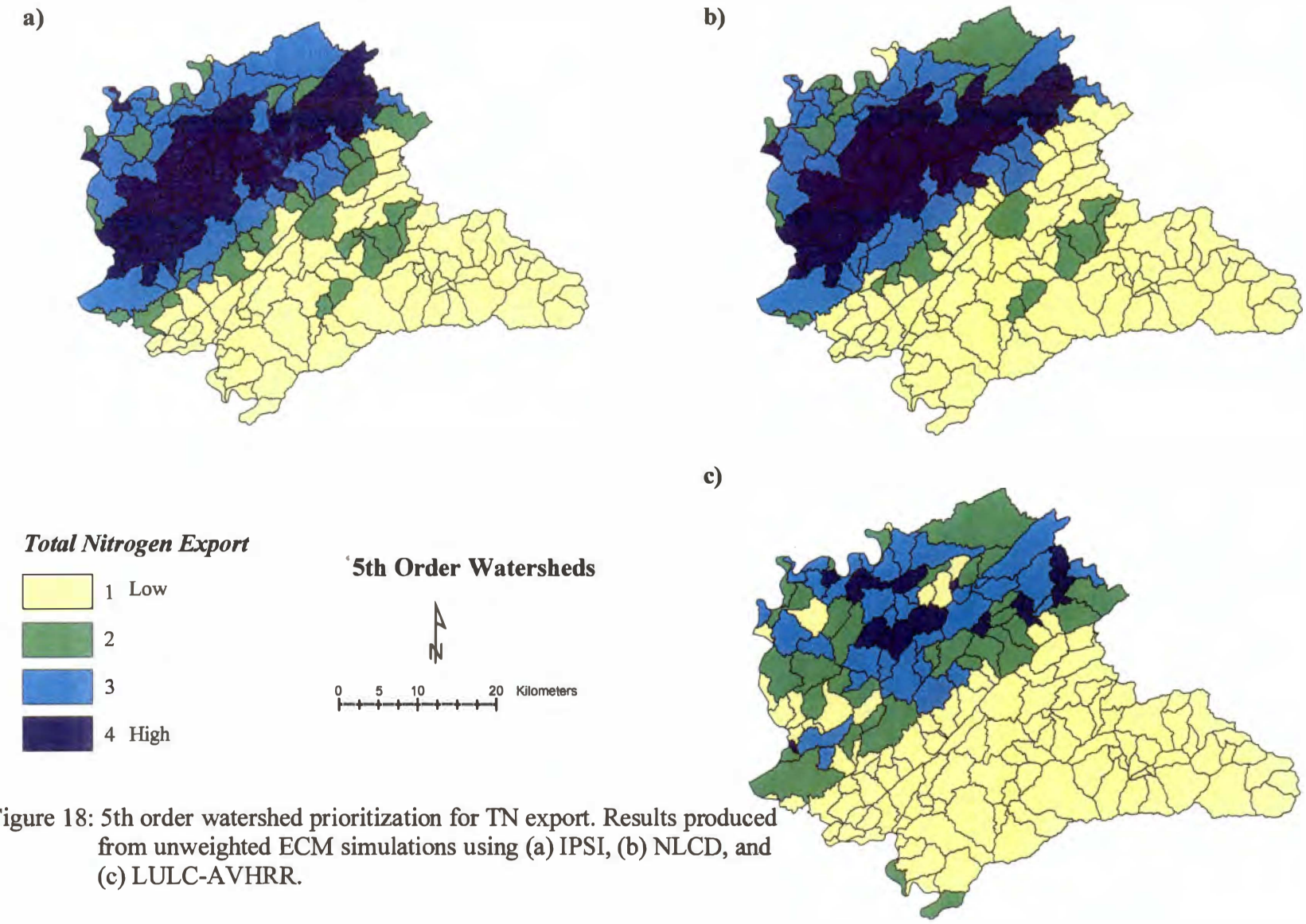


Figure 18: 5th order watershed prioritization for TN export. Results produced from unweighted ECM simulations using (a) IPSI, (b) NLCD, and (c) LULC-AVHRR.

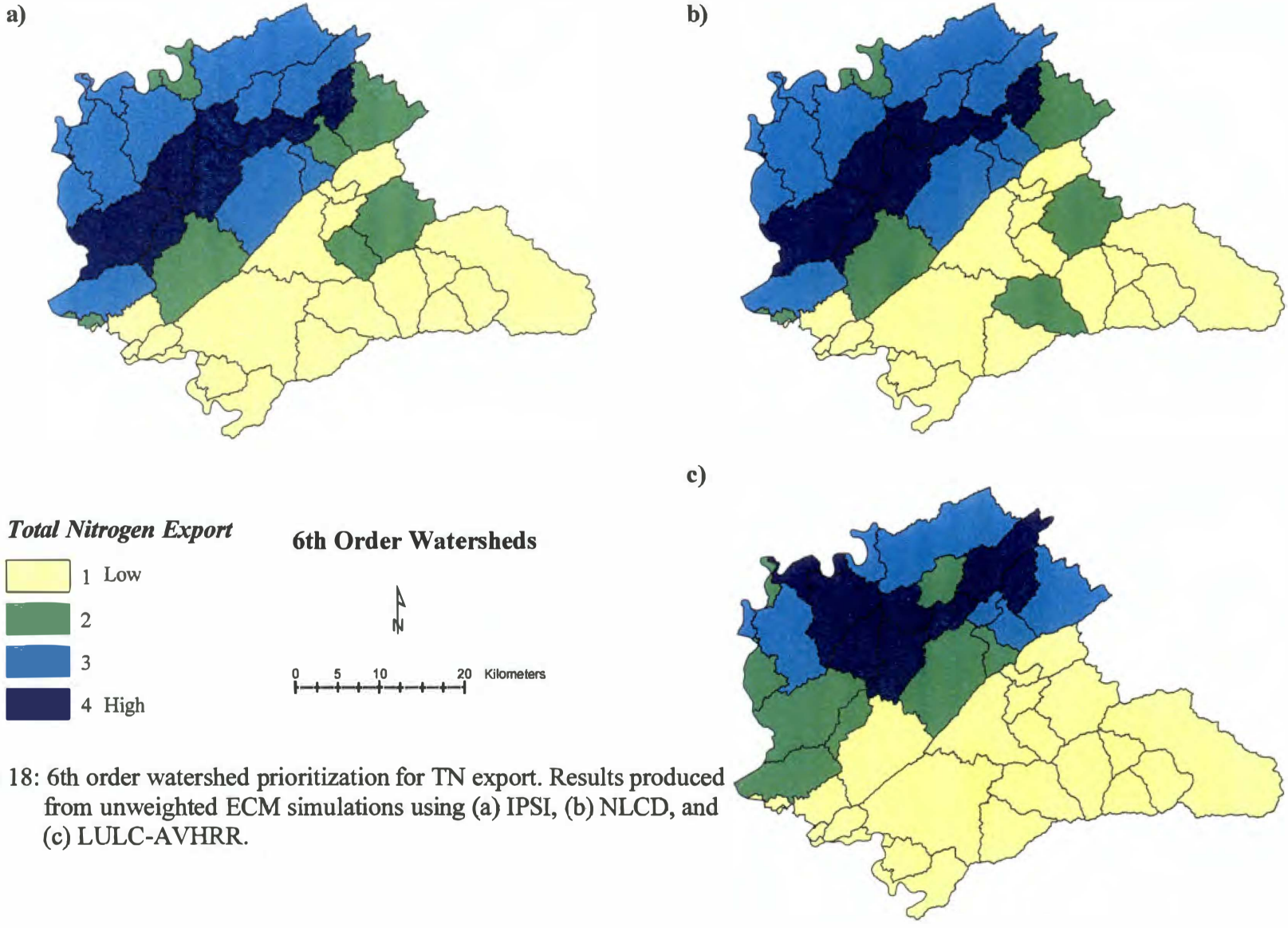


Figure 18: 6th order watershed prioritization for TN export. Results produced from unweighted ECM simulations using (a) IPSI, (b) NLCD, and (c) LULC-AVHRR.

watershed (kg/yr) by watershed area (kg/ha/yr). The four-class aggregation can be viewed as four degrees of prioritization.

Overall, TP and TN simulations reveal that while the nutrient fluxes of 4th order watersheds statistically differ between all three land cover dataset simulations, maps that prioritize watersheds for nutrient flux illustrate minimal differences between IPSI- and NLCD-based simulations. As watershed extent broadens to 5th and 6th order watersheds, differences in watershed prioritization between IPSI- and NLCD-based simulations become less apparent. Although the prioritization of watersheds for TN in LULC-AVHRR-based simulations differs from those based on IPSI and NLCD (Figures 17c to 19c), general patterns of TN loading across the landscape are not lost. However, the prioritization of watersheds for TP derived from LULC-AVHRR-based simulations (Figures 14c to 16c) does lose general patterns of nutrient loading; therefore, I excluded LULC-AVHRR from the correlation analysis and included only IPSI- and NLCD-based results, which are strongly correlated ($R^2 = 0.95$) (Figures 20 and 21).

Figures 22 and 23 illustrate the relationship between results from the IPSI- and NLCD-based simulations by mapping watersheds that showed different prioritizations nutrient flux. The color-coding scheme shows the degree of difference between land cover dataset simulations. Greatest change (red) represents a two- or three-category switch between IPSI- and NLCD-based model results, moderate change (beige) represents a one-category switch, and green represents no switch. For example, if a simulation using IPSI prioritizes a given watershed in the first category and the simulation using NLCD prioritizes that watershed in the fourth category, the correlation result is a three-category switch and a high degree of change. Overall, at the 4th, 5th, and

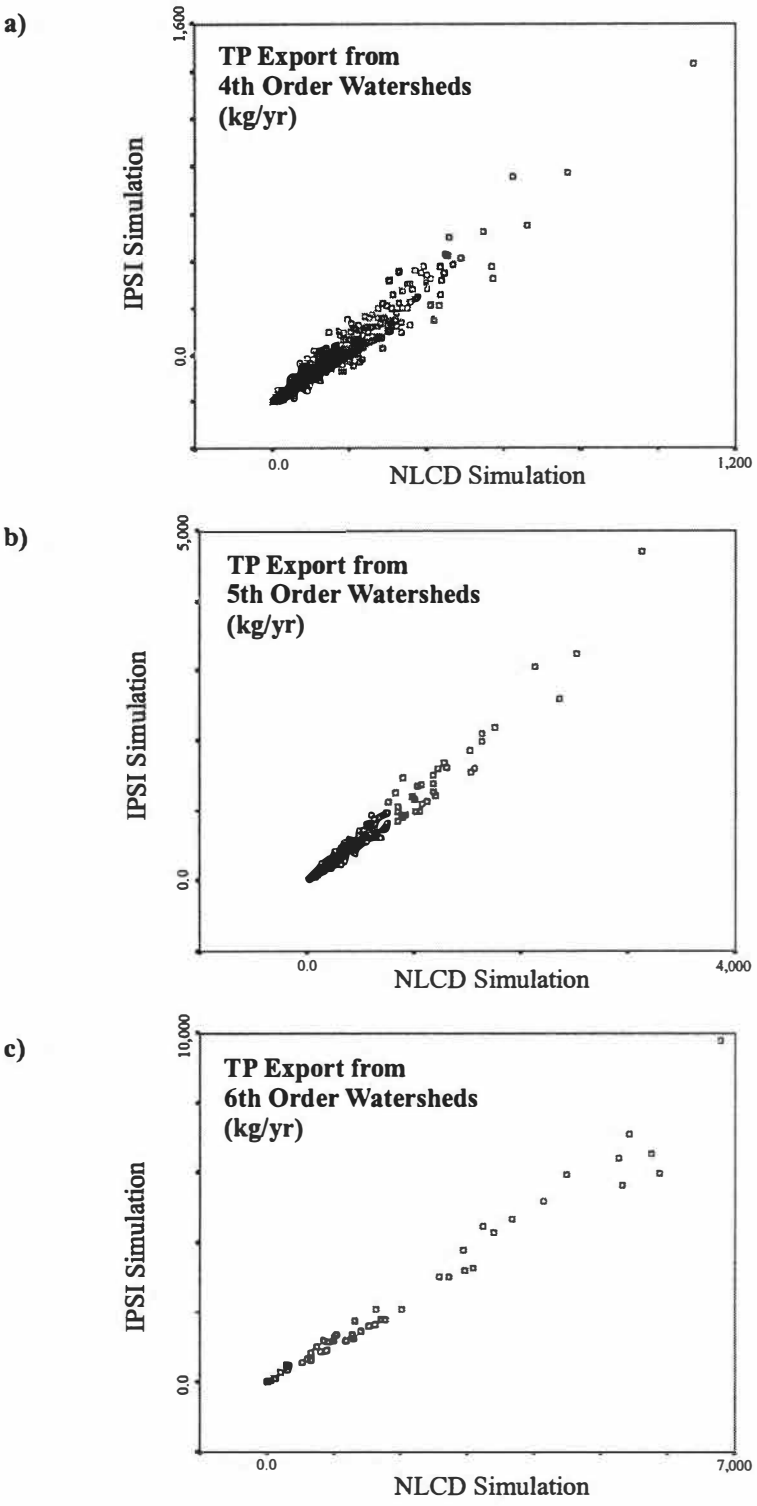


Figure 20: Correlation between IPSI- and NLCD-based TP simulations. Model results were from unweighted ECM simulations at the (a) 4th, (b) 5th, and (c) 6th order watershed extent.

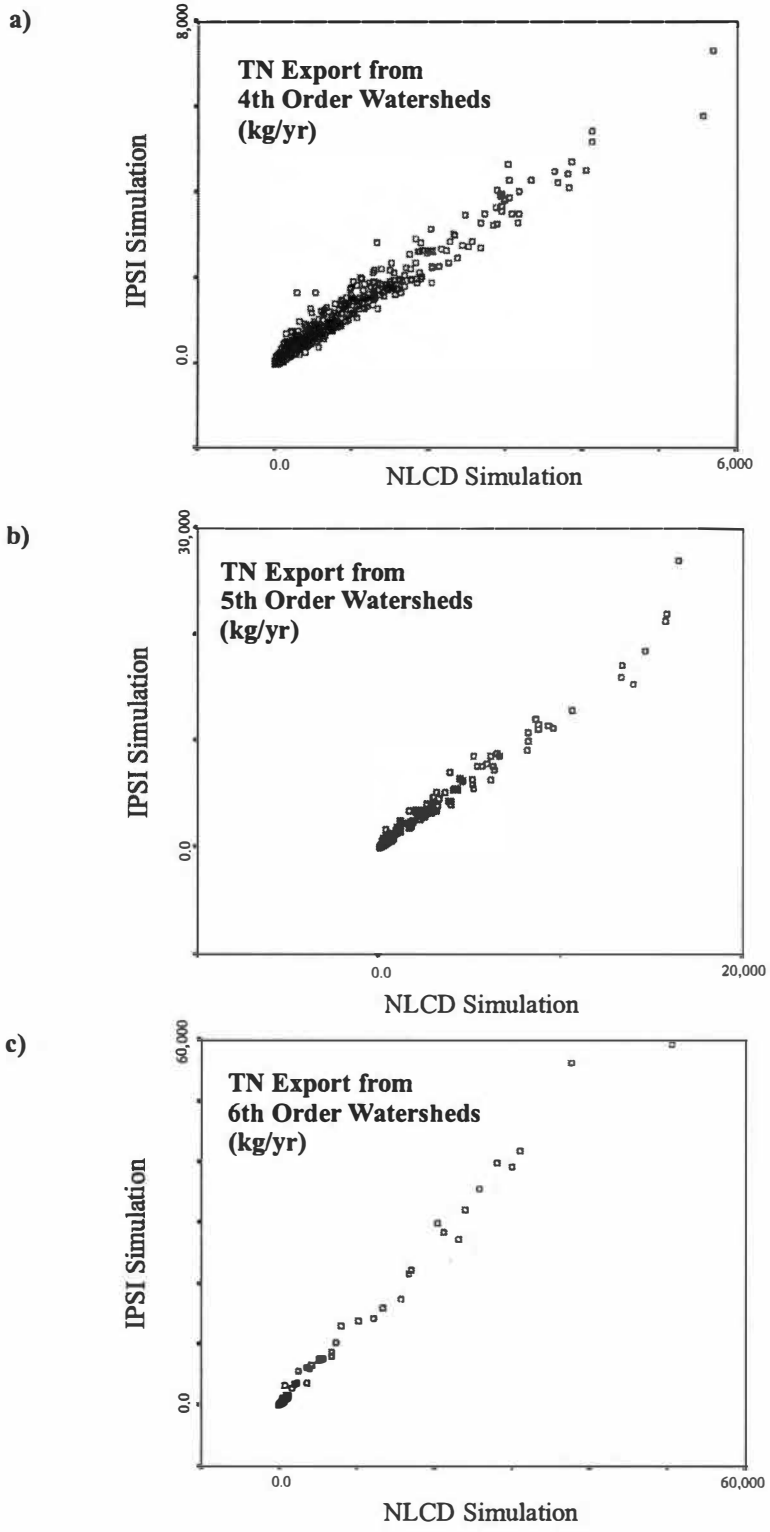


Figure 21: Correlation between IPSI- and NLCD-based TN simulations. Model results were from unweighted ECM simulations at the (a) 4th, (b) 5th, and (c) 6th order watershed extent.

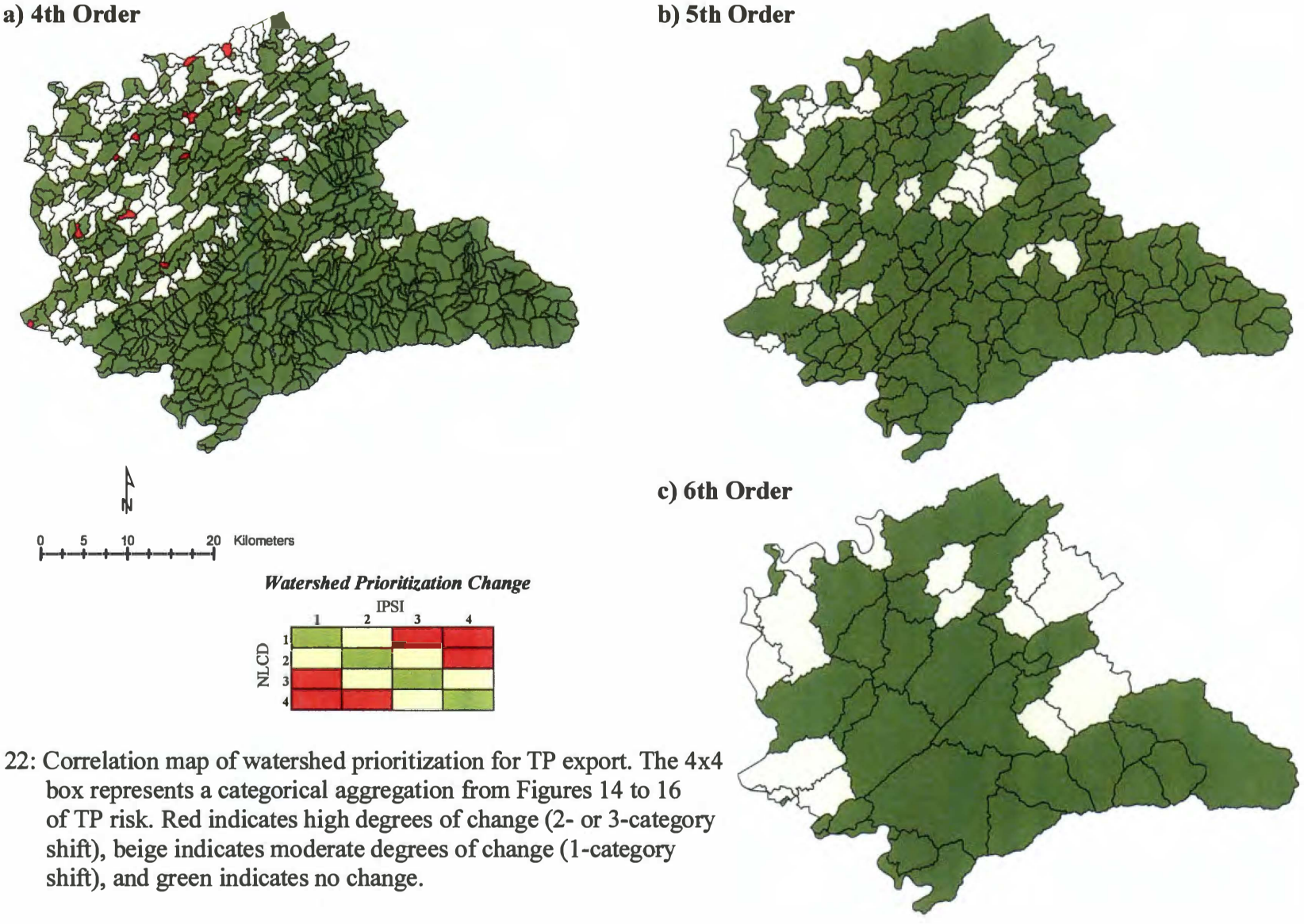


Figure 22: Correlation map of watershed prioritization for TP export. The 4x4 box represents a categorical aggregation from Figures 14 to 16 of TP risk. Red indicates high degrees of change (2- or 3-category shift), beige indicates moderate degrees of change (1-category shift), and green indicates no change.

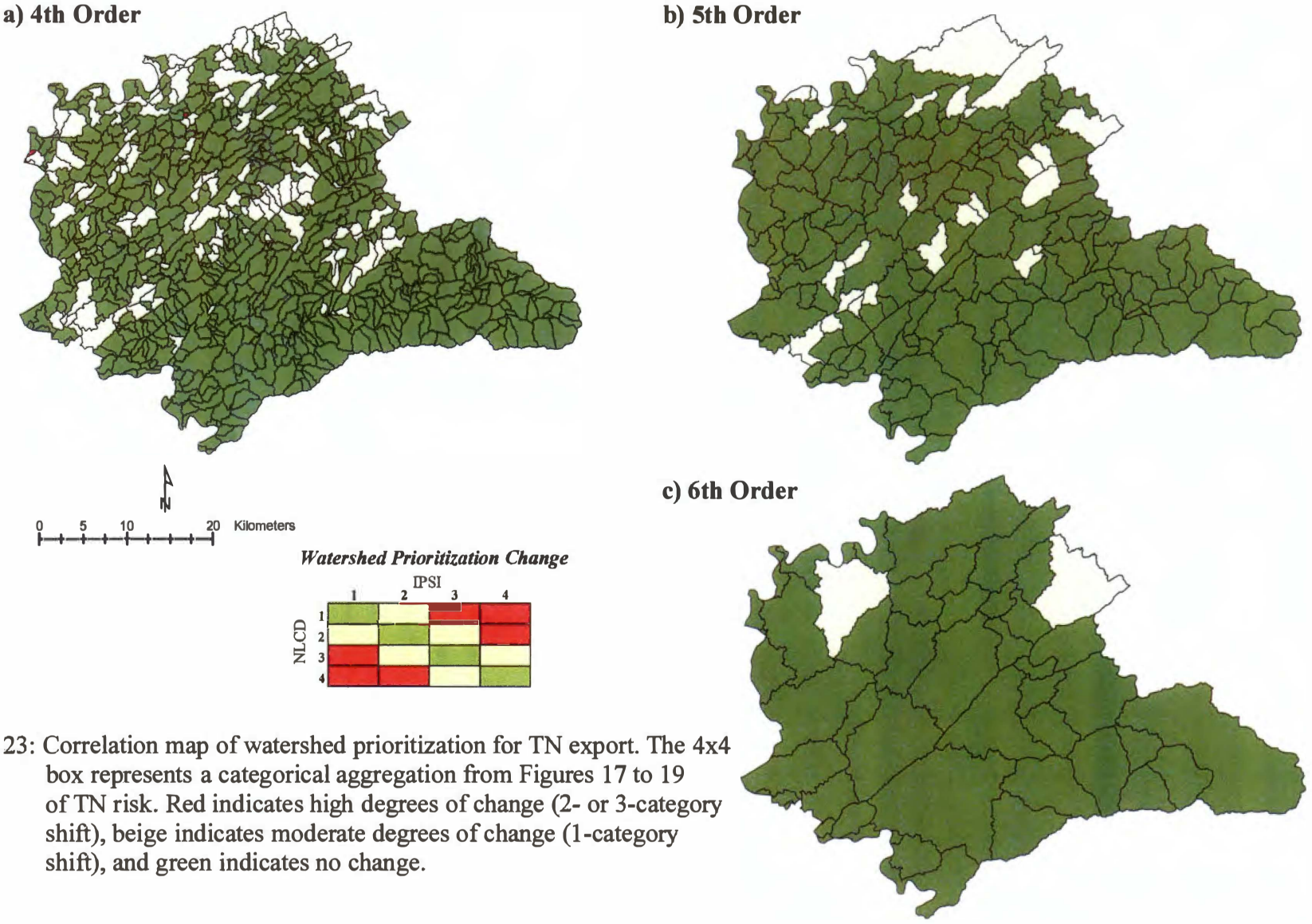


Figure 23: Correlation map of watershed prioritization for TN export. The 4x4 box represents a categorical aggregation from Figures 17 to 19 of TN risk. Red indicates high degrees of change (2- or 3-category shift), beige indicates moderate degrees of change (1-category shift), and green indicates no change.

6th order extents, differences in prioritization of watersheds for both TP and TN flux occur primarily in mixed land cover watersheds. Watersheds that include multiple types of land cover exhibit more variation in land cover identification and therefore more variation (within the dataset) in nutrient loadings.

Fourth-order watersheds exhibit the most difference in TP and TN watershed prioritization between IPSI- and NLCD-based simulations (Figures 22a and 23a). Roughly 26% of the 4th order watersheds modeled for TP changed prioritization category between the simulations, while 19% changed during TN model simulations. However, differences in prioritization classes for TN were only moderate, and differences in prioritization classes for TP were primarily moderate, with some areas of extreme change that occupied only 3% of all watersheds and were confined to areas averaging 1-km^2.

At the 5th order extent, the degree and frequency of prioritization difference decreased (Figures 22b and 23b), which indicates that as the spatial mapping scale increases, the degree and frequency of model differences simulated from IPSI and NLCD become less apparent. TP and TN both exhibit moderate degrees of change at the 5th order extent, in which 22% (TP) to 14% (TN) of all watersheds switched prioritization ranking between model simulations.

Correlations between 6th order watershed simulations reveal a continued decrease in the frequency of TN prioritization difference between IPSI-based and NLCD-based simulations (Figure 23c). Simulated TN export risks from 6th order watersheds differ in only 4% of all watersheds, which indicates that as spatial mapping scale increases the differences in the prioritization of watersheds for TN flux become less apparent between IPSI- and NLCD-based simulations. However, simulated TP export risks differ in

roughly 29% of all 6th order watersheds. It should be noted that most of 6th order TP change occurs along the Blount County border, which is not a natural hydrologic boundary and includes portions of drainage areas that extend beyond the study area. The difference in total watershed area from one 6th order watershed to the next is problematic for comparing the change in watershed prioritization categories between land cover dataset simulations and will be discussed further in Chapter VI.

The Weighted Export Coefficient Model Analysis

Unweighted ECM results suggest that the 5th order watershed extent is the threshold at which IPSI- and NLCD-based model results are statistically similar (Table 7). For modeling nutrient export within watersheds, I selected three 5th order sub-watersheds (Figure 24) as study sites because they (1) exemplify low, moderate, and high nutrient export areas, (2) occupy similar nutrient (TP and TN) load rankings between IPSI and NLCD-based simulations (Figures 14 and 19), and (3) do not change watershed prioritization between IPSI- and NLCD-based simulations (Figures 22 and 23). Figure 24 shows that each sub-watershed includes varying degrees of land cover and terrain; the low-risk watershed incorporates primarily forest cover, while moderate- and high-risk watersheds include a mix of primarily agricultural and urban cover.

Weighted ECM simulations within 5th order watersheds using both 10-m and 30-m data indicate that the greatest risk of nutrient loading occurs in areas characterized by gently rolling slopes, large upslope-contributing areas, and dispersal areas free of forest cover. Cornfields, grazing land, and urban land situated on concave landforms with few

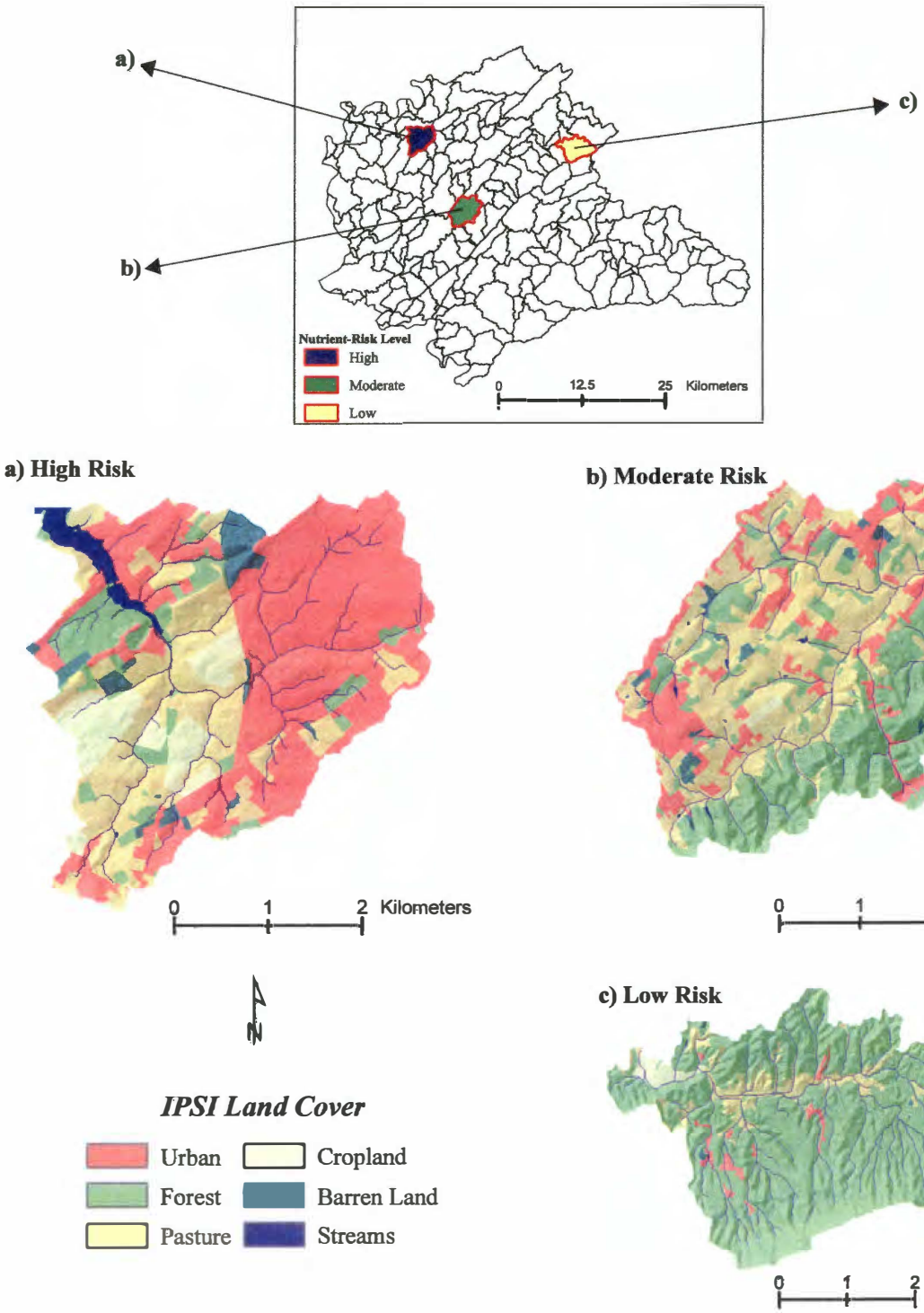


Figure 24: The weighted ECM study area. Selected watersheds shown with land cover composition. Watershed selection was based on overall prioritization levels of (a) high, (b) moderate, and (c) low risk.

vegetative buffers have high runoff potential (high TI values) and low nutrient trapping likelihood (low BI values) (Endreny and Wood 2003), thus assigning a more significant weight to the ECV. Two sets of data were used in this analysis: (1) ISPI land cover and 10-m National Elevation Data (NED) (fine scale) and (2) NLCD and 30-m NED (broad scale). I identify high nutrient-risk areas by extracting pixel (or loading) values, within each watershed's loading distribution, that are greater than the 25-percentile pixel value. TP- and TN-loading distributions within all three watersheds are highly variable between datasets and present negatively skewed distributions; hence, I could not choose a single pixel value as the *high* loading threshold for all three watersheds. Based on the natural breaks in each watershed's loading distribution, I noted within each distribution where pixel values began to exhibit high annual levels of TP and TN export compared to the lower distribution values. Within all three distributions the 25 percentile value (Table 8) provided a distinct break in the data. I used this break as a threshold and considered those nutrient values (or pixels) greater than the 25-percentile value to be *high* in export.

Several differences are apparent between the 10-m and 30-m weighted ECM simulations. I found that, in all three watersheds, weighted ECM simulations using 10-m data identify areas outside the riparian zone—which ranges from 100 m to 50 m in width depending on stream order—as the primary origins of nutrient flux. Conversely, simulations using 30-m data identify only high- and moderate-risk watersheds as having greater origins of nutrient flux outside the riparian zone (Table 9). When considering *absolute* nutrient fluxes, I found that weighted ECM simulations using 30-m data simulation does not compare well to the 10-m simulations. Within each watershed's riparian zones, simulations using 30-m data capture only 9% (TP) and 23% (TN) of the

Table 8: Twenty-fifth percentile nutrient loading values.

	TP (kg/pixel)		*TN (kg/pixel)*	
Watershed	**IPSI**	**NLCD**	**IPSI**	**NLCD**
Low Risk	0.05	1.18	0.32	3.79
Moderate Risk	0.06	0.31	0.30	1.81
High Risk	0.05	0.29	0.29	1.81

Table 9: Percentage of each risk-watershed's total area associated with a high nutrient loading.

a) TP Export

	Low-Risk		*Moderate-Risk*		*High-Risk*	
	IPSI (%)	**NLCD** (%)	**IPSI** (%)	**NLCD** (%)	**IPSI** (%)	**NLCD** (%)
Riparian Zone	0.45	0.16	0.47	0.47	1.80	0.97
All Other Areas	0.93	0.07	1.20	1.43	5.54	7.68

b) TN Export

	Low-Risk		*Moderate-Risk*		*High-Risk*	
	IPSI (%)	**NLCD** (%)	**IPSI** (%)	**NLCD** (%)	**IPSI** (%)	**NLCD** (%)
Riparian Zone	0.38	0.09	0.46	1.18	1.43	0.88
All Other Areas	0.40	0.03	2.56	1.99	4.00	4.48

total nutrient-risk-area load identified by simulations using fine-scale data. Similarly, throughout each watershed's entire area, 30-m data simulations capture only 9% (TP) and 11% (TN) of the nutrient-risk load identified by fine-scale data.

However, visual comparisons between 10-m and 30-m data simulations compare fairly well for prioritizing nutrient areas in the lowlands of each watershed (Figures 25 and 26). Figures 25 and 26 illustrate that simulations with 30-m data are less dispersed and do not capture smaller patches of nutrient risk in upland regions as do those modeled with 10-m data. Moreover, the low-risk watershed is the most problematic for 30-m data simulation (Figures 25c and 26c). Within the low-risk watershed, simulations using 30-m data do not capture urban and agricultural areas, which are potential producers of excessive nutrient flux, situated in rugged, upland terrain. Management teams using a nutrient-risk map created from 30-m ECM simulations (e.g., Figure 25c) would be directed to low-lying riparian zones as primary sources of nutrient risk, not considering the TP-export risk areas associated with upland portions of the watershed that are only identified simulations using 10-m data. Therefore, a management-team could presumably consider a different best management practice (BMP) if the decision-making process relied on 30-m ECM results. However, within moderate- and high-risk watersheds—which include low-lying terrain and mixed land cover types—differences in nutrient-area prioritization become less apparent and general patterns of nutrient flux are similar between 10-m and 30-m simulations (Figure 25a/b and 26a/b).

Watershed management implications from the analysis results presented are critical when considering the different types of data available for GIS/hydrologic

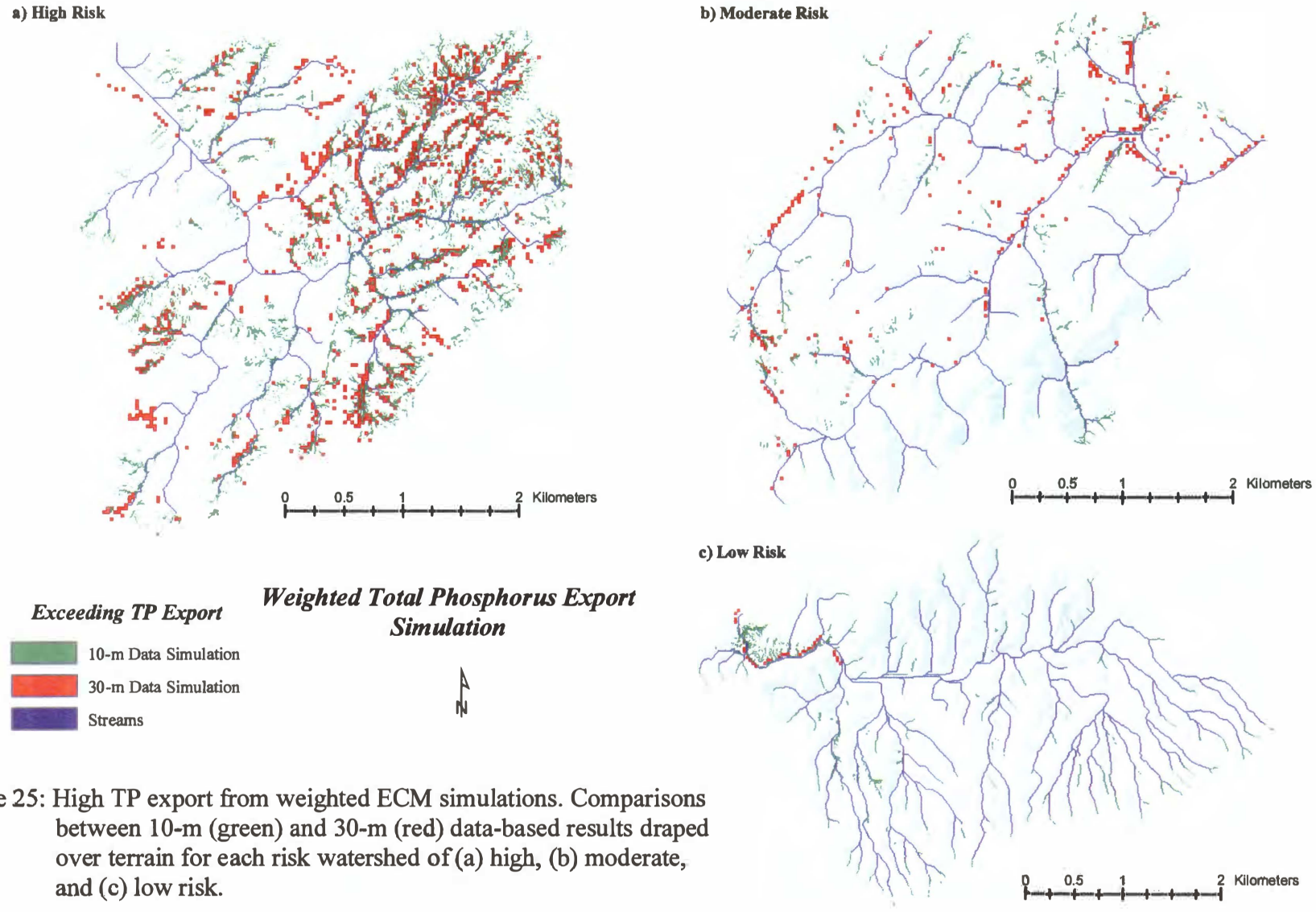


Figure 25: High TP export from weighted ECM simulations. Comparisons between 10-m (green) and 30-m (red) data-based results draped over terrain for each risk watershed of (a) high, (b) moderate, and (c) low risk.

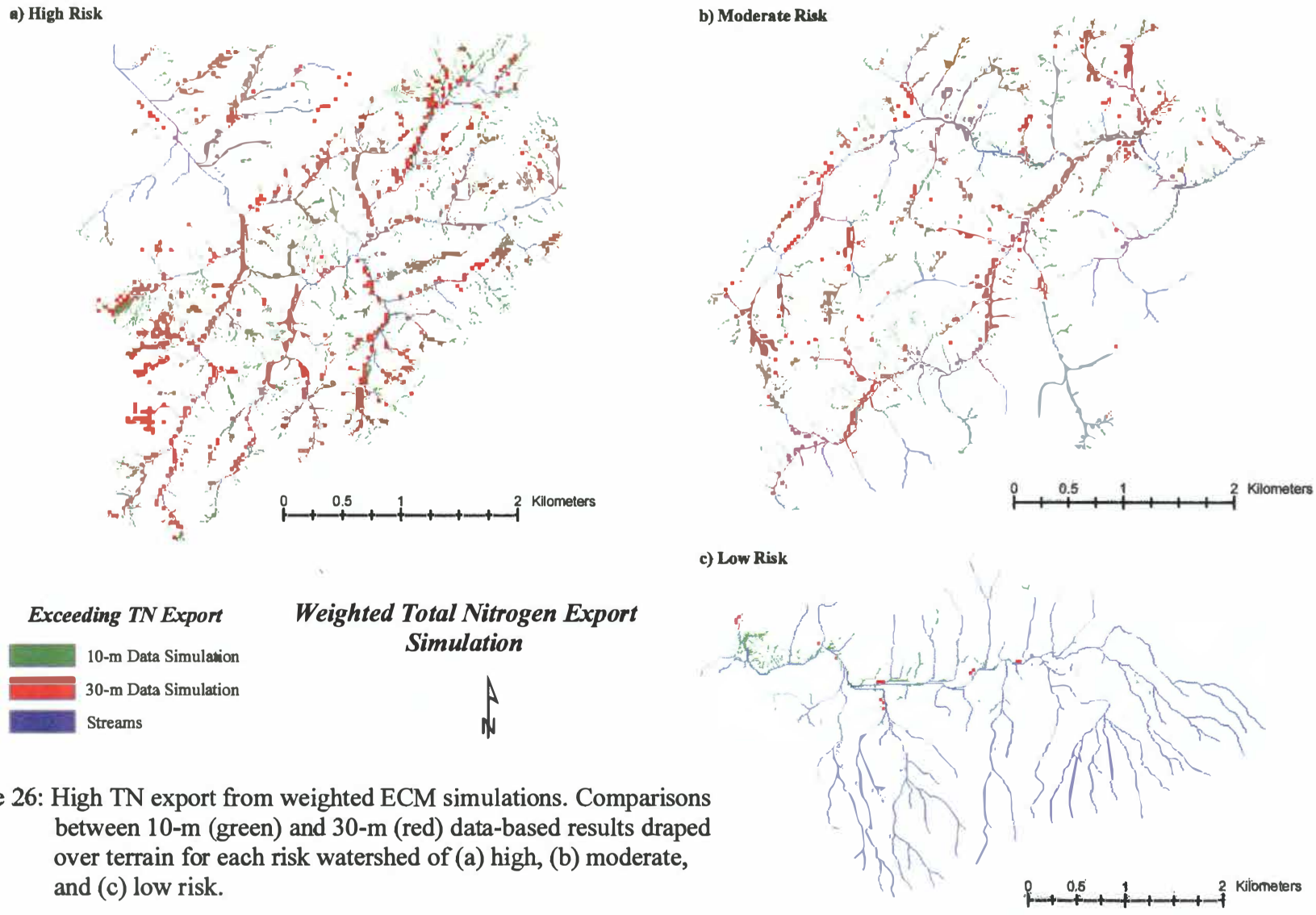


Figure 26: High TN export from weighted ECM simulations. Comparisons between 10-m (green) and 30-m (red) data-based results draped over terrain for each risk watershed of (a) high, (b) moderate, and (c) low risk.

modeling efforts. Chapter VI discusses important implications of the results obtained and limitations encountered in this research.

CHAPTER VI
DISCUSSION AND CONCLUSION

Research Implications

Scale and Data

The Blount County and Little River Watershed (BCLRW) unweighted export coefficient model (ECM) analysis supports the hypothesis that broad-scale land cover data (e.g., 30-m NLCD) are appropriate for spatial prioritization of nutrient-risk areas at the county-mapping scale. Findings from this research strongly suggest broad-scale data, such as NLCD (30-m), produce model results that can be used in decision making-processes. On the other hand, global-scale data, such as LULC-AVHRR (1-km), as expected, produce model results that do not capture general patterns (compared to NLCD and IPSI) of nutrient-risk at the county-mapping scale. Using freely available NLCD within a GIS-based ECM in study areas similar (terrain, climate, hydrology, etc.) to BCLRW, management teams can confidently prioritize sub-watersheds for remediation, and not incur the expenses associated with developing costly, fine-scale (e.g., 10-m IPSI) data.

This research suggests the 5^{th} order watershed extent is the threshold at which broad-scale data produce model results that are statistically ($\alpha = 0.05$) similar to results obtained from fine-scale (IPSI 10-m) simulations (Table 7); this will assist watershed managers in determining a minimal-mapping extent for modeling nutrient export with broad-scale data. Although modeling smaller watersheds (e.g., $< 4^{th}$ order) with NLCD is

not statistically appropriate, watershed prioritization differences between NLCD- and IPSI-based simulations (Figures 22 and 23) are moderate and apparent in only 22% (total phosphorus) to 19% (total nitrogen) of all 4th order watersheds. Fourth-order watersheds that were modeled for total nitrogen (TN) did not contain any extremely different prioritizations (those areas that exhibit a two- or three-category switch) between land cover simulations. Conversely, in 3% of the 4th order watersheds modeled for total phosphorus (TP), prioritization changes between simulations were great. While 3% is not an alarming amount, it should be noted the 4th order watersheds that exhibited great difference in prioritization for TP flux are relatively small (in area) compared to other 4th order watersheds (Figures 6), and small-area watershed delineation within GRID© is susceptible to erroneous stream ordering or flow path extraction. Prior to the analysis, I examined the stream network within these watersheds and found streams to be properly ordered; however, whether or not errors exist within the DEM is unknown. Systematic errors, although limited by NED (*See* Chapter III), may interrupt polygon construction during the watershed delineation calculations, creating smaller, unwanted polygons.

Findings from the unweighted ECM analysis reveal patterns of spatial data aggregation that could lead a researcher or watershed manager to different conclusions when modeling water quality at broad scales as opposed to fine scales. For example, Figures 12 and 13 show variation within each set of land cover-based nutrient loading results at the 4th, 5th, and 6th order watershed mapping extents. The box plots associated with each set of model results suggest that as watershed extent increases, for example, from 4th order (Figure 12a) to 6th order (Figure 12c), the variation within each set of simulated loadings also *increases*. This spatial phenomenon is characteristic of the

modifiable areal unit problem (MAUP), which is related to scale and which suggests that with each combination of similar areal data aggregated into several sets of larger areal units, different conclusions may be made (Jelinski and Wu 1996). For example, consider modeling watershed-cumulative-nutrient loadings for 6th order watersheds with the same nutrient export data used for 4th order watersheds: Model results at the 6th order extent will produce more varying nutrient loadings than those at 4th order extents because they cover a larger areal unit and include a variety of landscape variables (e.g., land cover) from one watershed to the next. On the other hand, 4th order watersheds cover smaller areal units and, presumably, do not include such a variety of landscape variables; therefore, their simulated values will not vary as much as the 6th order results. Watershed managers should consider the degrees of nutrient variation observed within each 4th and 6th order watershed simulation (Figures 12 and 13) because using these two areal units may lead to different overall conclusions of water quality health. Jelinski and Wu (1996) summarize different statistical and non-statistical methods for dealing with MAUP into four approaches: the "basic entity approach," "optimal zoning approach," "sensitivity analysis approach," and "visualization approach."

Correlation results presented in Figures 22 and 23 exhibited minor changes in the prioritization of watersheds for nutrient flux between IPSI- and NLCD-based unweighted ECM simulations. Correlations between these land cover datasets at broader extents (e.g., 8th order) across region-sized areas will presumably result in even less prioritization change, suggesting that fine-scale data development for a regional area would be unnecessary. Additionally, LULC-AVHRR-based model results do not reveal the same patterns of nutrient export as NLCD- and IPSI-based results. However, I expect that, at

the regional extent, unweighted ECM runs with LULC-AVHRR will better correlate to NLCD- and IPSI-based results, producing nutrient loading results that are more usable for decision-making processes. The scope of this research does not include regional analyses of LULC-AVHRR.

Differences in Nutrient Between Sub-Watersheds

Differences in the prioritization of watersheds for nutrient flux between IPSI- and NLCD-based unweighted ECM simulations (Figures 22 and 23) occurred primarily in mixed watersheds. Therefore, managers must consider which areas they are most interested in; if targeted watersheds incorporate mostly urban areas, for example, then using NLCD in simulations at the 4th order extent are appropriate. However, if the primary areas of concern are mixed land cover watersheds, then unweighted ECModeling with NLCD may produce undesirable results—those that exhibit the greatest changes (two- or three-category switch) in watershed prioritization compared to watershed prioritization produced from fine-scale land cover.

Change in risk categories from TP and TN simulations support the theory that as spatial scale broadens, fine-scale entities still exist but are not apparent (Allen *et al.* 1987). Model results reveal a decreasing trend in prioritization change as the spatial extent increases (Figures 22 and 23), which parallels this concept. For example, I calculated the percentage of watersheds from Figures 22 and 23 that changed prioritization class between IPSI- and NLCD-based unweighted ECM simulations. In the case of TN-export prioritization, the percent of watersheds that changed prioritization class between land cover simulations decreased from 19% (4th order) to 4% (6th order).

This suggests that as spatial extent is broadened, differences in fine- and broad-scale model results become less apparent.

However, in the case of TP-export prioritization, this pattern was not observed; the percent of watersheds that changed prioritization category decreased from 26% (4^{th} order) to 22% (5^{th} order), but, at the 6^{th} order extent, the percentage increased to 29%. One reason is that most 6^{th} order watershed prioritization (for TP) change occurred along the Blount County border, which is not a natural hydrologic boundary. I had to *clip* sub-watersheds that extended beyond the Blount County boundary (*See* Chapter III), leaving small, erroneous watersheds. The drastic difference in total area between these erroneous watersheds and fully developed 6^{th} order watersheds can be problematic for determining changes between model simulations. For example, small erroneous watersheds (< 5 km^2) are assigned cumulative-nutrient exports based on the number and type of underlying land cover pixels. Within smaller areas, 30-m land cover datasets will contain a lower pixel count and a lower diversity in land cover type. Finer-resolution (10-m) land cover datasets will contain higher pixel counts and may include more diversity in the land cover type, leading to differences in calculated nutrient loadings. In finer mapping extents, such as 4^{th} order watersheds, erroneous watersheds are still apparent; however, fully developed 4^{th} order watersheds are small, and differences between erroneous and fully developed watersheds are moderate. If all watersheds were fully developed, I would expect to see the percent of prioritization class change between IPSI- and NLCD-based simulations decrease as spatial extent increases—similar to the pattern observed in the TN prioritization change.

Differences in Nutrient Loading Within Sub-Watersheds

Broad-scale data used in the weighted ECM analysis included NLCD and the 30-m Nation Elevation Dataset (NED), whereas fine-scale data included ISPI and 10-m NED. In general, weighted ECM runs (within low-, moderate-, and high-risk 5th order watersheds) using 30-m and 10-m datasets show high nutrient originating areas to be associated with agricultural/urban cover situated on concave landscapes outside the riparian zone (Table 9). It should be noted that temporal differences exist between IPSI (*ca* 2000) and NLCD (*ca* 1992). The low-risk watershed incorporates primarily dense forest cover with few patches of agriculture and urban cover (Figure 24). Moving from low to high nutrient-risk watersheds, urban areas become the dominant land cover. Between 1992 and 2000, total population in Blount County increased 23% (U.S. Census 2000); because low-risk watersheds include primarily forest, small amounts of land cover change would have occurred during the intervening years. However, watersheds with mixed urban and agricultural land experienced the most change due to increasing urban growth and decreasing agricultural operations (USDA 1997), thus changing the conditions of nutrient loading.

Within all three watersheds, quantitative comparisons between *absolute* nutrient loadings of all high-risk areas identified by 10-m and 30-m based simulations are extremely different. Only 9% (TP) to 11% of the high-risk loadings modeled by 10-m data were captured by the broad-scale data. Moreover, within the riparian zones of each watershed, 30-m data simulations only captured 9% (TP) to 23% (TN) of the absolute loadings identified by fine-scale data. However, visual comparisons of nutrient risk (rather than absolute counts) (Figures 25 and 26) show that general patterns of

prioritization are maintained between 10-m and 30-m data simulations in gently-rolling, lowland terrain. Again, the ECM is a scoping model, which is intended for nutrient prioritization due to the high amount of uncertainty associated with export coefficient values (ECV) rather than absolute nutrient-load reports (Reckhow *et al.* 1980; Endreny and Wood 2003).

It should be noted that modeling with 30-m data in the low-risk watershed creates the most problems for capturing the similar patterns of nutrient prioritization produced by 10-m datasets. One reason is that BCLRW's low-risk watersheds incorporate rugged terrain with many concave and convex landforms (Figure 24c). Broad-scale NED (30-m)—included in TI and BI computations—do not contain the level of detail (compared to 10-m NED) necessary for capturing fine-scale hydrologic processes, such as upland flow paths. TI and BI computations rely on a flow direction algorithm that uses the D-8 method (or steepest decent) for determining flow pathways (O'Callaghan and Mark 1984; ESRI 2004).

In this research, I use flow direction and accumulation algorithms for (a) stream extraction, and (b) determining biophysical processes within pixel upslope-contributing and downslope-dispersal areas (explained in Chapter IV). In the TI and BI computations, the streams layer was used to identify areas within the watersheds that *do not* contribute to nutrient flux. I used only streams extracted from the 10-m NED in both the fine- and broad-scale computations for TI and BI to keep consistency between ordered streams and delineated watersheds. However, when determining pixel contributing and dispersal areas, I use the NED that corresponds with the fine- (10-m) or broad-scale (30-m) dataset. In other words, although I used the flow direction/accumulation algorithm to extract

streams from only the 10-m NED, I computed pixel contributing and dispersal areas (used in TI and BI computations) with 10- and 30-m NED, which had an effect on final nutrient export computations. Conversely, moderate- and high-risk watershed terrain includes gently-rolling slopes and less detail in concave and convex landforms; hence, less detail is needed for weighted nutrient modeling.

Because elevation data are a primary driving factor in the weighted ECM, integrating the 10-m NED and NLCD within the model could, presumably, produce model results closer to those produced with IPSI and the 10-m NED in rugged-terrain watersheds. For instance, one could resample NLCD (30-m) to a 10-m raster layer, and include the re-sampled NLCD and TI/BI created with the 10-m NED within the overall ECM. This alternative weighted ECM would produce results that compared better to the IPSI/10-m NED-based model (used above) because the 10-m NED would identify topographic characteristics (e.g., concave and convex landforms) with more detail. The scope of this research did not include an additional weighted analysis to test this scenario.

Overall, simulations using 30-m data capture the areas prioritized for remediation by simulations using 10-m data and suggest similar BMP consideration. However, as spatial extent is constricted to detailed areas of the watershed, such as the riparian zone, differences in model results become more apparent and may warrant different management strategies. For example, Figure 27a shows that model runs using both 10-m and 30-m datasets identify a lowland area (cropland patch) as a primary area of TP export, which could be mediated with riparian reconstruction (e.g., streamline fencing, livestock crossings, reforestation, etc.). The type of riparian BMP would depend on the situation and can only be confirmed by field verification. However, as the spatial scale

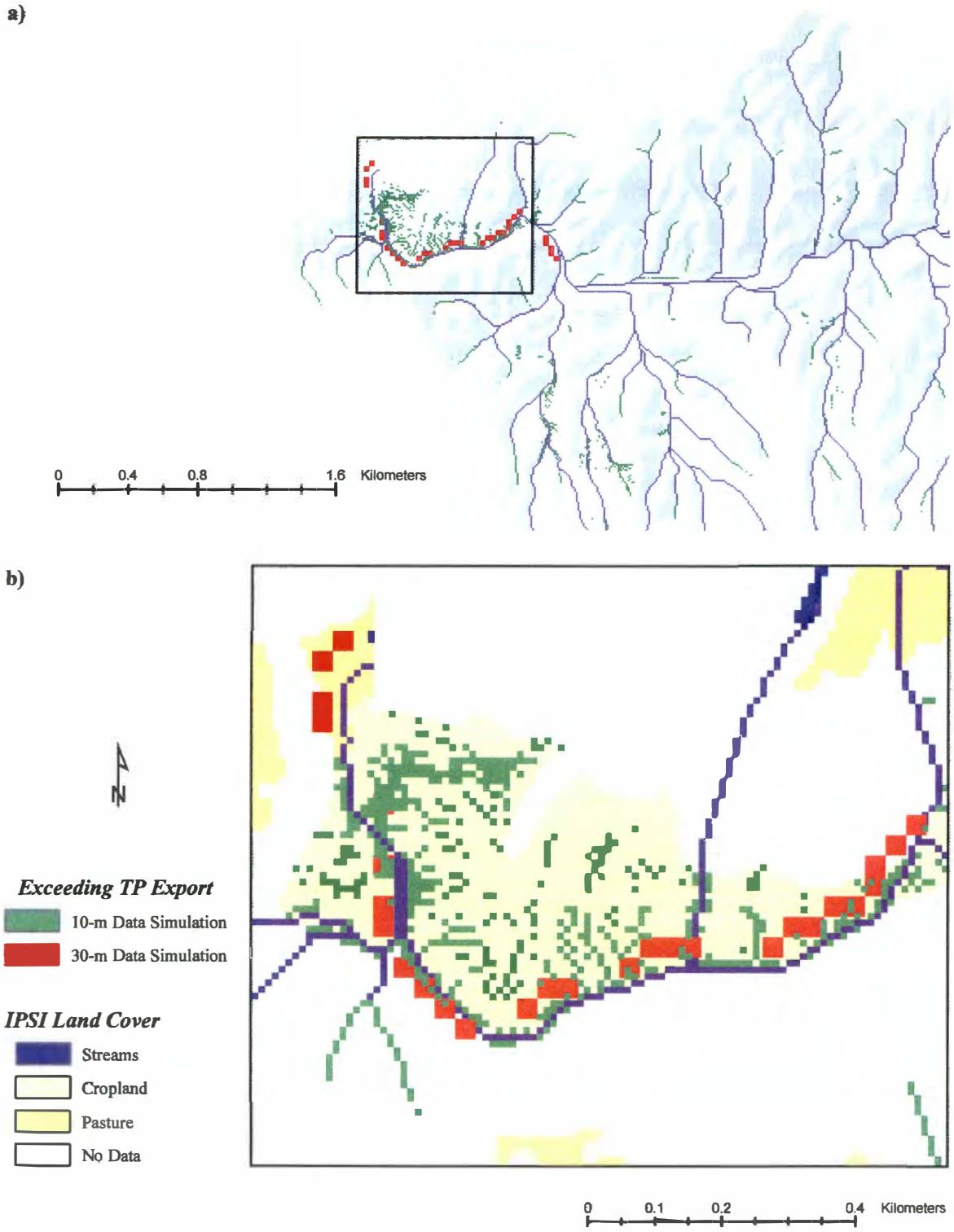


Figure 27: Detailed map of high TP fluxes produced from 10-m and 30-m data-based simulations. At (a) large extents differences are less apparent in lower stream reaches; whereas, (b) smaller extents reveal more differences between TP simulations.

becomes finer (Figure 27b), the stream reach that requires riparian reconstruction becomes less apparent in simulations based on 30-m data. Moreover, the 10-m data simulations also identify different areas within the cropland patch (upland from the stream) as potential remediation areas; whereas, 30-m data simulations do not recognize any upland cropland areas. Hence, the watershed manager must consider the degree of detail he/she is concerned with achieving.

Since a high level of uncertainty exists in ECModeling and model results should only be used for prioritization, field verification is crucial (Beaulac and Reckhow 1982; Johnes *et al.* 1996; Winter and Duthie 2000).

Model Limitations

General Limitations

In general, an important limitation of the ECModeling approach is the inability to predict in real-time; variations in available nutrient transport and uptake mechanisms over the annual cycle are not captured by the model (Johnes 1996; Winter and Duthie 2000). While the weighted ECM captures the spatial variation of nutrient export within the watershed, it does not consider detailed biophysical mechanisms, such as organic absorption, that alter nutrient concentrations once in the stream and affect exports from downstream watersheds. However, the broad-scale nature of ECModeling, discussed in Chapter II, suggests that detailed biophysical processes are less important at broad-scales (e.g., county- or state-sized regions) and that including these variables will make modeling efforts extremely complex (Meentemeyer 1989).

A further general limitation of the ECModeling approach is that literature-derived ECVs cannot be fully verified for the entire study area without extensive experimental fieldwork (Johnes 1996; Winter and Duthie 2000). The ECM extrapolates plot-sized empirical data to remote areas of the basin. As variation in the hydrologic, topographic, edaphic, and biological conditions between these areas increases, uncertainty also increases. Although model calibration attempts to minimize uncertainty surrounding literature-derived ECVs, full verification is still lacking. For example, the BCLRW-ECM was calibrated successfully using median ECVs derived from the distribution of literature reported ECVs (Table 5; Table A.4). This, however, does not suggest that each ECV associated with a given land cover type is an accurate nutrient export estimation for that land cover. Calibration was based on the ECM's performance for simulating *total* basin load and does not consider the proportional share of export from a specific land area within a total load estimate. Consider a scenario of implementing an ECM in which the ECVs underestimate TP in simulating forest loads and overestimate TP in simulating pasture loads. This scenario would allow individual exports from two land covers to offset one another and still portray the simulated total load to within ±0.5% of observed loads. In other words, while the cumulative-basin load may be accurate (±0.5%), the exact export from each land cover type remains uncertain.

The multiple regression approach (McFarland and Huack 2001) attempts to further minimize uncertainty and can verify ECVs derived from the literature by associating in-stream water quality measurements taken across the basin with surrounding land cover, building ECVs that are more indicative of the local region. In this research, the BCLRW multiple regression analysis was unsuccessful due to reasons

discussed in Chapter IV, and could not be used to verify the set of median ECVs that I selected for weighted and unweighted ECM analysis.

BCLRW-ECMs Limitations

The BCLRW-ECMs include several specific limitations. An important one is that calibration used water quality data for Ellejoy and Nails creeks that were only available for a six-month sampling period (June to November 2003) and did not include storm events. A more extensive water quality survey (e.g., 2-4 year period) that included storm events would better represent annual nutrient concentrations. Moreover, sampling was completed for a TMDL report, which will be submitted by TDEC; therefore, site selection and sampling schedule were decided by TDEC; a more spatially extensive water quality survey would better represent nutrient export across the study area. Because BCLRW crosses hydrologic boundaries, the calibration could not be implemented for the entire area, but could be implemented for the Little River watershed, which covers roughly 50% of BCLRW. Previous sampling conducted by TDEC (1998) did include locations along the Little River, but a single sample was not taken at the mouth of the watershed where a cumulative-basin load could have been captured. Furthermore, TDEC data collection was not complete (e.g., missing flow data) and did not include continuous month-to-month sampling; several winter and fall months were not represented in the samples.

Another calibration limitation was the lack of internal BCLRW data that could be used to verify calibration results. I selected ECVs from empirical studies that had climate regimes and soil characteristics similar to those of BCLRW and aggregated their

distributions into quartiles. However, each model run during the calibration analysis used an entire set of quartile ECVs (shown in Table 5) and did not randomize the ECVs within each set, mixing a 25% ECV of forest with a 75% ECV of pasture, for example. The lack of internal BCLRW data prevented me from conducting a randomized sensitivity analysis because there would have been no way to verify sensitivity results. For example, a randomized calibration analysis could potentially suggest a maximum quartile ECV for pasture and a 25% ECV for cropland. I would have no way to verify these results without specific fertilizer application (type and amount), livestock waste removal, or septic loading data.

Although no detailed internal BCLRW data are available, I was able to gather general information concerning BCLRW agriculture practices and land use. Overall, crop production and livestock operations are thought to be the primary contributors to excessive nutrient loading in BCLRW, with cropland export the higher of the two (Eric Henry, *personal communication).*

Croplands, which include corn, moderate amounts of soybeans, and limited amounts of tobacco, rely the most on nitrogen and phosphorus based fertilizer applications (Eric Henry, *personal communication).* Most cropland operations till during winter months, a practice that increases nutrient loading because of the lack of plants to prevent erosion and nutrient export (Beaulac and Reckhow 1982). On the other hand, pasture land in BCLRW is devoted to primarily cattle and dairy livestock operations that use continuous grazing practices. While rotational grazing is preferred for reducing nutrient exports (Beaulac and Reckhow 1982), the small patch farming distribution within BCLRW prevents this practice. Onsite waste storage facilities exist on some dairy

farms; however, most livestock operations do not incorporate on-site waste disposal. Although BCLRW livestock operations are environmentally undesirable and are thought to be a major determinate of stream quality, Blount County Soil Conservation District officials still associate higher nutrient loads with cropland (Eric Henry, *personal communication*). Such expert opinions confirm that cropland should be assigned higher ECVs than pasture, as is apparent in the set of median ECVs (Table 5); however, determining the sensitivity of ECVs would require detailed data that could only be acquired through extensive field experiments and questionnaires.

In addition to these limitations, the ECMs used in this research incorporate land cover, elevation, and buffer capacity variables, but do not include additional hydrologic variables that provide a more realistic representation of absolute loading in support of nutrient prioritization. Equations 1 and 5 could be calibrated with additional variables, including atmospheric deposition rates, soil type, septic loads, precipitation lost to runoff, livestock waster storage, and fertilizer applications. Examples of ECMs containing such additional variables can be found in Johnes (1996), Winter and Duthie (2000), and Endreny and Wood (2003). Once again, the lack of internal BCLRW data (e.g., fertilizer application, septic loads, and detailed soil characteristics) prevented me from including additional variables into these modeling efforts. For example, extensive soil data would have allowed me to verify runoff potential calculated by the TI. Moreover, Reckhow *et al.* (1980) offer septic-related nutrient ECVs for rural households (e.g., kg/capita). However, advancements in sewage disposal technology (e.g., septic systems) since 1980 create high levels of uncertainty in model results; thus, I did not include rural household

nutrient loads into the ECMs. Including these data would require an extensive survey of rural populations within BCLRW.

Application of BCLRW-ECMs to Other Regions

The ECMs presented in this research were developed and calibrated for areas similar to eastern Tennessee. While ECModeling relies on simplicity so that it can be distributed as a generic model, researchers should use caution when applying the models to other regions. Selection of literature-reported ECVs is critical for determining local nutrient export and should be accomplished with a calibration procedure (Beven 1993).

Calibration can be done with observed in-stream nutrient concentrations or extensive field experiments; if these data are not available, a simple examination of local climate, soil, and land use management will provide some model calibration. Caution should also be used when modeling different nutrients. By selecting TP and TN, the researcher must consider more variables—more nutrient source types, more transformation processes, more pathways, and more sinks—that affect the fate and transport of two nutrients rather than only one. The highly variable fate and transport of TN makes it difficult to comprehensively model absolute exports levels (Endreny and Wood 2003). In this research, however, I use TP and TN simulation results for nutrient prioritization at different mapping scales and between different geospatial-data scales; absolute nutrient export amounts were not reported.

The unweighted ECM is the more versatile of the two models, incorporating only land cover type, area measurements, and ECVs in the computation; thus, it can be applied in more regions compared to the weighted ECM. USEPA (2001b) distributes PLOAD,

which is a version of the unweighted ECM bundled within the multi-facetted BASINS architecture. PLOAD exploits the visualization power explicit to GIS applications for providing a graphical front-end to spreadsheet ECModeling. One limitation of PLOAD is its inability to model in raster, which is essential for certain broad-scale land cover data (e.g., NLCD). Vectorizing raster-based land cover data creates undesirably large datasets that will limit PLOAD's broad-scale modeling ability due to considerable amounts of computational payload. However, PLOAD has predefined parameters and is easy to implement, whereas raster-based GIS does not have predefined parameters for ECModeling and is less intuitive and more time-consuming to implement. Hence, the researcher must consider the size of his/her study area, and the time available for modeling in selecting raster- or vector-based ECModeling.

It should be noted that while USEPA (2001b) advertises PLOAD's ability to model several different water quality constituents—for example, Dissolved Oxygen (DO), Total Organic Content (TOC), Biochemical Oxygen Demand (BOD), *Fecal Coliform*, and *E. Coli*—most empirical studies have only included TP and TN in modeling efforts (Reckhow *et al.* 1980; Frink 1991; Soranno *et al.* 1996; Johnes 1996; Mattikalli and Richards 1996; Winter and Duthie 2000; Wickham and Wade 2002; Endreny and Wood 2003). I have not found existing literature that discourages modeling additional water quality constituents with ECMs; however, calibration will be difficult because the limited sources in the literature for other pollutant ECVs.

Compared to the unweighted ECM, the weighted ECM is limited in its applicability in other regions. Weighted ECMs use a topographic index (TI) (Beven and Kirkby 1979) to model the runoff-producing potential of specific watershed areas, which

is not applicable for all climatic regimes. The TI is based on the theory that as watershed areas become saturated, their soil's water storage capacity decreases, which will ultimately result in overland flow (or runoff). Studies conducted by Torch *et al.* (1993) support this theory for humid areas in the eastern United States, where water table levels follow the topography of the landscape; however, in contrasting climate regimes this theory is not valid. Moreover, the weighted ECM does not support vector data formats and can only be accomplished through raster-based GIS modeling. Hydrologic algorithms performed on a DEM are simply not possible for a vector elevation model.

Future Research

The purpose of this research was to determine whether broad-scale data (e.g., 30-m resolution) produce reliable water quality modeling results compared to fine-scale data (e.g., 10-m resolution) for making remediation decisions. Researchers and watershed managers can use this information in determining geographic scales *a priori* in future modeling projects. Knowledge that, for example, export coefficient modeling of 5^{th} order watersheds for nutrient export based on NLCD produces statistically similar results to modeling based on more detailed, fine-scale data will assist watershed managers in selecting the appropriate data for their modeling needs. It should be noted that my findings in this research are empirical and not based on existing theory. Hence, my findings may not be supported in other regions of the United States or beyond. For example, in different regions, the average size of a 5^{th} or 6^{th} order stream contributing areas may be different from those computed in BCLRW. Different size stream

contributing areas could be caused by different topographic characteristics (compared to BCLRW) or the resolution of the input DEM (i.e., 10 m vs. 30 m), which presumably will affect final results when comparing broad- and fine-scale data within an unweighted or weighted ECM.

Findings presented in this thesis are only one step in examining geographic scale in hydrologic modeling with broad- versus fine-scale data at the county-mapping scale. Future research could expand the unweighted ECM analysis study area to, for example, 8-digit HUCs across the southeastern United States. A larger study area would allow one to examine differences in broad- and global-scale datasets (e.g., NLCD and LULC-AVHRR) and determine whether or not similar patterns (to this research) of statistical difference and change in watershed prioritization between watersheds are observed. I chose the BCLRW study area based on the availability of IPSI data. NLCD and LULC-AVHRR are freely available for the entire United States. However, this future research scenario should include newer releases of NLCD, which will be available for the eastern United States in late 2004 (USEPA 2003b). Temporal differences in IPSI (*ca* 2000) and NLCD (*ca* 1992) were apparent during simulations within BCLRW watersheds containing mixed land cover types; BCLRW experienced a 23% growth in population between 1990 and 2000 (US Census 2000) and decreases in agricultural land (USDA 1997), creating urban infringement on forest and agriculture. I expect that, within BCLRW, differences in model results between fine-scale data (e.g., ISPI) and NLCD will decrease from those presented in this research as more up-to-date NLCD are used.

The development of ECVs using the multiple regression technique suggested by McFarland and Huack (2001) was unsuccessful in BCLRW primarily because of the

limited availability of water quality data. Future research with an extensive water quality survey (2 to 4 years) could better determine if this technique is applicable in regions similar to BCLRW and aim to improve this technique so that other research and watershed managers can benefit. An extensive water quality survey should include continuous sampling that captures a spatial representation of the entire basin.

Calculations of flow paths, upslope-contributing areas, and downslope dispersal areas rely on only one method for determining pixel accumulation—the D-8 method or steepest decent. Building upon and improving the TI and BI within the weighed ECM will help researchers understand differences in weighted ECM simulation in areas characterized by both gently rolling and rugged terrain. Research conducted by Quinn *et al.* (1991), Costa-Cabral and Burges (1994), and Tarboton *et al.* (1997) provide alternative flow path extraction methods.

Moreover, the weighted ECM analysis suggests that non-riparian zones were primary nutrient sources in BCLRW. The lack of internal BCLRW data and scope of this thesis prevented me from conducting field surveys to verify these findings. Endreny and Wood (2003) also were unable to validate weighted ECM results to detailed field surveys. Conducting extensive field surveys would provide future model applications a higher level of confidence for accurately locating BMP potential areas.

Finally, findings from this research do not suggest that fine-scale land cover data are unnecessary for modeling the hydrologic processes and water quality of a particular watershed, only that fine-scale data are unnecessary for prioritizing risk areas in a county-sized area similar to that of BCLRW. For example, on a client-by-client basis, TVA uses IPSI within propriety spreadsheet models to simulate several different water quality

constituents (e.g., nutrients, bacteria, zinc, and sediment loss). IPSI's ability to model detailed hydrologic processes is essential for isolating specific land cover types and reporting accurate NPS pollutant concentrations. Conversely, this research is suggesting that in regions that have the same hydrologic characteristics as BCLRW, and where IPSI or other fine-scale data are not available, local watershed managers can confidently use broad-scale data (e.g., NLCD and 30-m NED) to prioritize nutrient-risk areas. Simple and quick modeling allows managers to determine some level of risk for their study while retaining a good portion of their budget for other detailed modeling or monitoring needs.

WORKS CITED

Abt, S. R., C. I. Thornton, and T. L. Johnson, 1995. Estimating Drainage Area on Steep Uniform Slopes. *Water Resources Bulletin.* 31(1): 53-55.

Allen, T. F. H. and T. B. Starr, 1983. Hierarchy: Perspectives for Ecological Complexity. The University of Chicago Press.

_____, R. V. O'Neill, and T. W. Hoekstra, 1987. Interlevel Relations in Ecological Research and Management: Some Working Principles from Hierarchy Theory. *Journal of Applied Systems Analysis.* 14:63-79.

Anderson, J.R., Hardy, E.E., Roach J.T., and Witmer R.E., 1976, A Land Use and Land Cover Classification System for Use with Remote Sensor Data. USGS Professional Paper 964, 28.

Arnold, C. L. and C. J. Gibbons, 1996. Impervious Surface Coverage the Emergence of a Key Environmental Indicator. *Journal of American Planning Association.* 62(2): 243-258.

Arnold, J. G., R. Srinivasan, R. S. Muttiah, and J. R. Williams, 1998. Large Area Hydrologic Modeling and Assessment Part I: Model Development. *Journal of American Water Resources Association.* 34(1): 73-89.

_____, J. R. Williams, A. D. Nicks, and N. B. Sammons, 1990. SWRRB, A Basin Scale Simulation Model for Soil and Water Resources Management. College Station: Texas A&M University Press.

Beasley, D. B., L. F. Huggins, and E. J. Monke, 1980. ANSWERS: A Model for Watershed Planning. *Transactions of the American Society of Agricultural Engineers.* 23(4): 938-944.

Beaulac, M. N. and K. H. Reckhow, 1982. An Examination of Land Use—Nutrient Nutrient Export Relationships. *Water Resources Bulletin.* 18(6): 1013-1024.

Betson, R. P. 1978. Bulk Precipitation and Streamflow Quality Relationships in an Urban Area. *Water Resources Research.* 14(6): 1165-1169.

Beven, 1993. Prophecy, Reality and Uncertainty in Distributed Hydrological Modelling. *Advances in Water Resources.* 16(1): 41-51.

_____, 1995. TOPMODEL. *In:* Computer Models of Watersheds Hydrology. Water Resources Publication, CO, 627-668.

_____ and J. Kirkby, 1979. A Physically Based, Variable Contributing Area Model of Basin Hydrology. *Hydrologic Sciences Bulletin.* 24(1): 43-69.

Bradford, R. R, 1974. Nitrogen – Phosphorus Losses from Agronomy Plots in North Alabama. US EPA 660/2-74-033.

Burian, S. J., M. J. Brown, and T. M. McPherson, 2002. Evaluation of Land Use/Land Cover Datasets fro Urban Watershed Modeling. *Water Science and Technology*. 45(9): 269-276.

Burnash, R. J., R. L. Ferral, and R. A. McQuire, 1973. A Generalized Stream Flow Simulation System in Conceptual Modeling for Digital Computers. Sacramento, CA: U.S. National Weather Services.

Burt, T. P. and P. J. Johnes, 1997. Managing Water Quality in Agricultural Catchments. *Transactions Institute of British Geographers*. 22(1): 61-68.

Carrubba, L., 2000. Hydrologic Modeling at the Watershed Scale Using NPSM. *Journal of American Water Resources Association*. 36(6): 1237-1246.

Colby, J. D., K. A. Mulcahy, and Y. Wang, 2000. Modeling Flooding Extent from Hurricane Floyd in the Coastal Plains of North Carolina. *Environmental Hazards*. 2(4): 157-168.

Costa-Cabral, M.C. and S.J. Burges. 1994. Digital Elevation Model Networks (DEMON): A Model of Flow Over Hillslopes for Computation of Contributing and Dispersal Areas. *Water Resources Research*. 30(6): 1681-1692.

DeSelm H. R., 2001. Vegetation Results from Land Surveys in Three East Tennessee Counties, 1807-1887. Department of Botany, The University of Tennessee, Knoxville, TN.

Dillon, P. J. and W. B. Kirchner, 1975. The Effects of Geology and Land Use on the Export of Phosphorus from Watersheds. *Water Resources*. 9: 135-148.

Di Luzio, M., R. Srinivasan, and J. G. Arnold, 2002. Integration of Watershed Tools and SWAT Model into BASINS. *Journal of American Water Resources Association*. 38(4): 1127-1140.

Dunne, T. and L. B. Leopold 1978. Runoff Processes. *In:* Water in Environmental Planning. W. H. Freeman & Company Publishing, New York, NY pp. 255-278.

Endreny T. A. and E. F. Wood, 2003. Watershed Weighting of Export Coefficients to Map Critical Phosphorous Loading Areas. *Journal of the American Water Resources Association*. 39(1):165-180.

_____, C. Somerlot and J. M. Hassett, 2003. Hydrograph Sensitivity to Estimates of Map Impervious Cover: a WinHSPF BASINS Case Study. *Hydrological Processes*. 17:1019-1034.

ESRI, 2001. Understanding GIS: The ARC/INFO Method, Version 7.2. Environmental Systems Research Institute, Redlands, CA.

_____, 2004. Arc/Info 8.3 Online Help Documentation. Environmental Systems Research Institute, Redlands, CA.

Fisher, D. S., J. L. Steiner, D. M. Endale, J. A. Stuedemann, H. H. Schomberg, A. J. Franzluebbers, S. R. Wilkinson, 2000. The Relationship of Land Use Practices to Surface Water Quality in the Upper Oconee Watershed of Georgia. *Forest Ecology and Management*. 128: 39-48.

Frink, C. R., 1991. Estimating nutrient exports to estuaries. *Journal of Environmental Quality*. 20: 717-724.

Gale, J. A., D. E. Line, D. L. Osmond, S. W. Coffey, J. Spooner, J. A. Arnold, T. J. Hoban, and R. C. Wimberley, 1993. Evaluation of the Experimental Rural Clean Water Program, US EPA 841/R-93-005, Washington, D.C.

Garbrecht, J. and L. W. Martz, 2001. Digital Elevation Model Issues in Water Resources Modeling. *In:* Hydrologic and Hydraulic Modeling Support with Geographic Information Systems. ESRI Press, Redlands, CA pp 1-27.

Gburek, W. J. and G. J. Folmar, 1999. Flow and Chemical Contributions to Streamflow in an Upland Watershed: A Baseflow Survey. *Journal of Hydrology*. 217: 1-18.

Haith, D. A., 1976. Land Use and Water Quality in New York Rivers. *Journal of Environmental Engineering Division of American Society of Civil Engineers*. 102: 1-15.

_____, and Shoemaker, 1987. Generalized Watershed Loading Functions for Stream Flow Nutrients. *Water Resources Bulletin*. 23: 471-478.

Harden, C. P., 1992. Incorporating Roads and Footpaths in Watershed-Scale Hydrologic and Soil Erosion Models. *Physical Geography*. 13(4): 368-385.

Heng, H. H. and N. P. Nikolaidis, 1998. Modeling of Nonpoint Source Pollution of Nitrogen at the Watershed Scale. *Journal of the American Water Resources Association*. 34(2): 359-374.

Henderson, G. S. and W. F. Harris, 1975. An Ecosystem Approach to Characterization of the Nitrogen Cycle in a Deciduous Forest Watershed. *In:* Forest Soils and Forest Land Management. Proceedings of 4th North American Forest Soils Conference. Laval University Press, 179-193.

_____, A. Hunley, and W. Selvidge, 1977. Nutrient Discharge from Walker Branch Watershed. *In:* Watershed Research in Eastern North America. Vol. I.

Henry, Eric, October 15, 2003. Soil Conservation Specialist at the Blount County Soil Conservation District, Maryville, TN.

Hill, A. R., 1978. Factors Affecting the Export of Nitrate-Nitrogen from Drainage Basins in Southern Ontario. *Water Research*. 12:1045-1057.

Hodge, T. A. and L. J. Armstrong, 1993. Use of a Multiple Linear Regression Model to Estimate Stormwater Pollutant Loading. *In:* New Techniques for Modelling the Management of Stormwater Quality Impacts. Lewis Publishers, Boca Raton, FL, pp. 201-214.

Hornberger, G. M. and E. W. Boyer, 1995. Recent Advances in Watershed Modeling. *Reviews of Geophysics*. 33(Supp): 949-957.

Jelinski, D. E., and J. Wu, 1996. The Modifiable Areal Unit Problem and Implications for Landscape Ecology. *Landscape Ecology*. 11(3): 129-140.

Johanson, R. C., J. C. Imhoff, J. L. Kittle, and A. S. Donigian, 1984. Hydrological Simulation Program—FORTRAN (HSPF): Users Manual for Release 8.0. Athens, GA: Environmental Research Laboratory, U.S. EPA.

Johnes, P. J., 1996. Evaluation and Management of the Impact of Land Use Change on the Nitrogen and Phosphorus Load Delivered to Surface Waters: The Export Coefficient Modeling Approach. *Journal of Hydrology*. 183: 323-349.

_____ and A. L. Heathwaite, 1997. Modeling the Impact of Land Use Change on Water Quality in Agricultural Catchments. *Hydrological Processes*. 11:269-286.

Jones, B. K., A. C. Neale, M. S. Nash, R. D. Van Remortel, J. D. Wickham, K. H. Ritters, and R. V. O'Neill, 2001. Predicting Nutrient and Sediment Loadings to Streams from Landscape Metrics: A Multiple Watershed Study from the United States Mid-Atlantic Region. *Landscape Ecology*. 16(4): 301-312.

_____, K. H. Riitters, J. D. Wickham, R. D. Tankersley, R. V. O'Neill, D. J. Chaloud, E. R. Smith, and A. C. Neale, 1997. An Ecological Assessment of the United States Mid-Atlantic Region: A Landscape Atlas. US EPA /600/r-97/130, Washington, D.C.

Kilmer, V. J., J. W. Gilliam, J. F. Lutz, T. R. Joyce, and C. D. Eklund, 1974. Nutrient Losses from Fertilized Grassed Watersheds in Western North Carolina. *Journal of Environmental Quality*. 3(3): 214-219.

Konarska, K. M., P. C. Sutton, and M. Castellon, 2002. Evaluating Scale Dependence of Ecosystem Service Valuation: A Comparison of NOAA-AVHRR and Landsat TM Datasets. *Ecological Economics*. 41: 491-507.

Konrad, J. G., J. S. Baumann, and S. E. Bergquist, 1985. Nonpoint Pollution Control: The Wisconsin Experience. *Journal of Soil and Water Conservation*. 40(1): 55-61.

Krebs, J. E. and F. B. Golley, 1977. Budget of Selected Mineral Nutrients for Two Watershed Ecosystems in the Southeast Piedmont. NTIS Publication 272-286.

Krysanova, V. and H. Luik, 1989. Simulation Modeling of a System Watershed-River-Sea Bay. Tallinn, Valgus.

Laroche, A. J. Gallichand, R. Lagace, and A. Pesant, 1996. Simulating Atrazine Transport with HSFP in an Agricultural Watershed. *Journal of Environmental Engineering*. 122(7): 622-630.

Lee, K. H., T. M. Isenhart, and R. C. Schultz, 2003. Sediment and Nutrient Removal in an Established Multi-Species Riparian Buffer. *Journal of Soil and Water Conservation*. 58(1): 1-7.

Leonard, R. A., W. G. Knisel, and D. A. Still, 1987. GLEAMS: Groundwater Loading Effects on Agricultural Management Systems. *Transactions of the American Society of Agricultural Engineers*. 30(5): 1403-1428.

Lin, S., 1972. Nonpoint rural sources of water pollution. Circular III, State of Illinois Department of Registration and Education.

Likens, G. E. and F. H. Bormann, 1974. Linkages between terrestrial and aquatic ecosystems. *Bioscience* 24: 447-456.

Loehr, R. C., 1974. Characteristics and Comparative Magnitude of Non-point Sources. *Journal of Water Pollution Control*. 46(8): 1849-1872.

_____, S. O. Ryding, and W. C. Sonzogni, 1989. Estimating the Nutrient Load to a Waterbody. *In:* The Control of Eutrophication of Lakes and Reservoirs. The Parthenon Publishing Group, Park Ridge, NJ, pp. 115-146.

Loveland, T. R. and D. M. Shaw, 1996. Multi-resolution land characterization: building collaborative partnerships. *In*: Gap Analysis: A Landscape Approach to Biodiversity Planning Proceedings of the ASPRS/GAP Symposium. July 15-19, Charlotte, N.C., National Biological Service, Moscow, ID, pp. 83-89.

Maas, R. P., S. L. Brichford, M. D. Smolen, and J. Spooner, 1988. Agricultural Nonpoint Source Control: Experiences from the Rural Clean Water Program. *Lake and Reservoir Management*. 4(1): 51-56.

McFarland, A. S. and L. M. Hauck, 2001. Determining Nutrient Export Coefficients and Source Loading Uncertainty Using In-Stream Monitoring Data. *Journal of the American Water Resources Association*. 37(1): 223-236.

Mander, U, A. Kull, LV. Tamm, V. Kuusemets, and R. Karjus, 1998. Impact of Climatic Fluctuations and Land Use Change on Runoff and Nutrient Losses in Rural Landscapes. *Landscape and Urban Planning*. 41:229-238.

Mark, D. M. 1984, Automatic Detection of Drainage Networks from Digital Elevation models. *Cartographica*. 23: 168-178.

Mattikalli, N. M. and K. S. Richards, 1996. Estimation of Surface Water Quality Changes in Response to Land Use Change: Application of the Export Coefficient Model Using Remote Sensing and Geographical Information System. *Journal of Environmental Management*. 48: 263-282.

McDowell, L. L., M. E. Ryan, K. C. McGregor, and J. D. Greer. Nitrogen and Phosphorus Losses in Runoff from No-till Soybeans. Presented Paper #78-2508. 1978 Winter Meeting ASAE, Chicago, IL.

Meentemeyer, V., 1989. Geographic Perspectives of Space, Time, and Scale. *Landscape Ecology*. 3:163-173.

_____ and E. O. Box, 1987. Scale Effects in Landscape Studies. *In* Landscape Heterogeneity and Disturbance. Ecological Studies, Vol. 64 pp. 15-34. Ed. M. G. Turner, Springer-Verlag, New York.

Miller, S. N., W. G. Kepner, M. H. Mehaffey, M. Hernandez, R. C. Miller, D. C. Goodrich, K. K. Devonald, D. T. Heggern, and W. P. Miller, 2002. Integrating Landscape Assessment and Hydrologic Modeling for Land Cover Change Analysis. *Journal of American Water Resources Association*. 38(4): 915-929.

Muir, J., E. C. Seim, and R. A. Olson, 1973. A study of Factors Influencing the Nitrogen and Phosphorus Contents of Nebraska Waters. *Journal of Environmental Quality*. 2: 466-470.

Nerbonne, B. A., and D. Vondracek, 2001. Effects of Local Land Use on Physical Habitat, Benthic Macroinvertebrates, and Fish in the Whitewater River, Minnesota, USA. *Environmental Management*. 28(1): 87-99.

Northeast Florida Water Management District, 1994. S. Marks and Wakulla Rivers Resource Assessment and Greenway Protection Plan. Appendix 4.

Noss, R. F., M. A. O'Connell and D. D. Murphy, 1997. The Science of Conservation Planning. Island Press, Washington, D.C.

Novotny, V., and G. Chesters, 1989. Delivery of Sediment and Pollutants from Nonpoint Sources: A Water Quality Perspective. *Journal of Soil and Water Conservation*. 44: 568-576.

O'Callaghan, J. F. and D. M. Mark, 1984. The Extraction of Drainage Networks from Digital Elevation Data. *Computer Vision, Graphics, and Image Processing*. 28(3): 232-344.

Omernik, J. M., 1976. The Influence of Land Use on Stream Nutrient Levels. EPA-600/3-76-014 U.S. Environmental Protection Agency, Washington, D.C.

Preston, E. M. and B. L. Bedford, 1988. Evaluating Cumulative Effects on Wetland Functions: A Conceptual Overview and Generic Framework. *Environmental Management*. 12(5): 565-583.

Quinn, P., K. Beven, P. Chevallier, and O. Planchon, 1991. The Prediction of Hillslope Flow Paths for Distributed Hydrological Modeling Using Digital Terrain Models. *Hydrological Processes*. 5(1): 59-79.

Reckhow, K. H., M. N. Beaulac, and J. T. Simpson, 1980. Modeling Phosphorus Loading and Lake Response Under Uncertainty: A Manual and Compilation of Export Coefficients. US EPA 440/5-80-011, Washington, D.C.

Rodgers, J., 1953. Geologic Map of East Tennessee. Tennessee Division of Geology. Nashville, TN.

Scepan, J., 1999. Thematic Validation of High-Resolution Global Land-Cover Data Sets. *Photogrammetric Engineering and Remote Sensing*. 65(9): 1051-1060.

Sliva, L, and D. D. Williams, 2001. Buffer Zone Versus Whole Catchment Approaches to Studying Land Use Impact on River Water Quality. *Water Resources*. 35(14): 3462-3472.

Smith, C. N., R. A. Leonard, G. W. Langdale, and G. W. Bailey, 1978. Transport of Agricultural Chemicals from Small Upland Piedmont Watersheds. US EPA 600/3-78-056.

Smith, J. H., J. D. Wickham, S. V. Stehman, and L. Yang, 2002. Impacts of Patch Size and Land-Cover Heterogeneity on Thematic Image Classification Accuracy. *Photogrammetric Engineering and Remote Sensing*. 68(1): 65-70.

Smith, K .E., 2000. Physiography of Tennessee. Tennessee Archaeology Net. *www.mtsu.edu/~kesmith/tnarchnew/physio.html.*

Soranno, P. A., S. L. Hubler and S. R. Carpenter, 1996. Phosphorus Loads to Surface Waters: A Simple Model to Account for Spatial Pattern of Land Use. *Ecological Applications*. 6(3): 865-878.

Springer, M. E. and J. A. Elder, 1980. Soils of Tennessee. The University of Tennessee, Knoxville, TN.

SPSS for Windows, 2001. Online Help Documentation. SPSS, Inc.

Syvitski, J. P., M. D. Morehead, and M. Nicholson, 1988. HYDROTREND: A Climate-Driven Hydrologic-Transport Model for Predicting Discharge and Sediment Load to Lakes or Oceans. *Computers and Geosciences*. 24(1): 1-110.

Tennessee Valley Authority, 2002. Integrated Pollutant Source Identification (IPSI). *http://www.tva.gov/environment/pdf/ipsi.pdf.*

_____, 2003. Blount County and Little River Basin Nonpoint Source Pollution Inventories and Pollutant Load Estimates. Lenoir City, TN. pp1-5.

Tarboton, D. G., 1997. A New Method for the Determination of Low Directions and Upslope Areas in Grid Digital Elevation Models. *Water Resources Research*. 33: 309-319.

Taylor, A. W., W. M. Edwards, and C. E. Simpson, 1971. Nutrients in Streams Draining Woodland and Farmland Near Coshocton, Ohio. *Water Resources Research*. 7(1): 81-89.

Tong, S. and W. Chen, 2002. Modeling the Relationship Between Land Use and Surface Water Quality. *Journal of Environmental Management*. 66(4): 377-393.

Torch, P A., M. Mancini, C. Paniconi, and E. F. Wood, 1993. Evaluation of a Distributed Catchment Scale Water Balance Model. *Water Resources Research*. 29(6): 1805-1817.

U.S. Department of Agriculture, 1997. Census of Agriculture. National Agricultural Statistics Service. *http://www.nass.usda.gov/census/.*

U.S. Census Bureau. Blount County, Tennessee Population Statistics. *http://www.census.gov/.*

U.S. Environmental Protection Agency, 2001a. Better Assessment Science Integrating Point and Nonpoint Sources: BASINS User's Manual. pp 329-335. *http://www.epa.gov/waterscience/basins/bsnsdocs.html*

_____, 2001b. PLOAD Version 3.0 User's Manual. pp1-44. *http://www.epa.gov/waterscience/basins/b3docs/PLOAD_v3.pdf*

_____, 2002. Clinch and Powell Valley Watershed Ecological Risk Assessment. National Center for Environmental Assessment, EPA/600/R-01/050, Washington, D.C.

_____, 2003a. National Pollutant Discharge Elimination System. *http://cfpub.epa.gov/npdes/.*

_____, 2003b. 1992 NLCD Accuracy. *http://www.epa.gov/mrlc/accuracy.html.*

_____, 2003c. Laws and Regulations: The Clean Water Act. *http://www.epa.gov/r5water/cwa.htm*

United States Geological Survey and National Aeronautics Space Administration, 2003. National Land Cover Characterization. *http://landcover.usgs.gov/natllandcover.html.*

Uusi-Kamppa, J., E. Turtola, H. Hartikainen, and T. Ylaranta, 1997. The Interactions of Buffer Zones and Phosphorous Runoff. *In:* Buffer Zones: Their Processes and Potential in Water Protection. Quest Environmental, Hertfordshire, UK, pp. 43-53.

Uttormark, P. D., J. D. Chapin, and K. M. Green, 1974. Estimating Nutrient Loading of Lakes from Nonpoint Sources. US EPA 660/12-74-020.

Vogelmann, J. E., S. M. Howard, L. Yang, C. R. Larson, B. K. Wylie, and N. Van Driel, 2001. Completion of the 1990s National land Cover Data Set for the conterminous United States from Landsat Thematic Mapper data and ancillary data sources. *Photogrammetric Engineering & Remote Sensing.* 63(1): 45-57.

Wang, L., J. Lyons, and P. Kanehl, 2002. Effects of Watershed Best Management Practices on Habitat and Fish in Wisconsin Streams. *Journal of American Water Resources Association.* 38(3): 663-680.

Watson, I. and A. D. Burnett, 1995. Streamflow. *In*: Hydrology – An Environmental Approach. Lewis Publishers, Boca Raton, FL, pp. 457-477.

Whittemore, R C., and J. Beebe, 2000. EPA's BASINS Model: Good Science or Serendipitous Modeling? *Journal of American Water Resources Association*. 36(3): 493-499.

Wickham, J. D., R. V. O'Neill, K. H. Riitters, E. R. Smith, T. G. Wade, and B. K. Jones, 2002. Geographic Targeting of Increases in Nutrient Export Due to Future Urbanization. *Ecological Applications*. 12(1) 93-106.

_____ and T. G. Wade, 2002. Watershed Level Risk Assessment of Nitrogen and Phosphorus Export. *Computers and Electronics in Agriculture*. 37: 15-24.

Wischmeier, W. H. and D. D. Smith, 1978. Predicting Rainfall Erosion Loss: A Guide to Conservation Planning *In:* Agricultural Handbook 537. USDA, Washington, D.C.

Winter, J. G. and H. C. Duthie, 2000. Export Coefficient Modeling to Assess Phosphorus Loading in an Urban Watershed. *Journal of American Water Resources Association*. 36(5): 1053-1061.

Yang, L., S. V. Stehman, J. H. Smith, and J. D. Wickham, 2001. Thematic Accuracy of MRLC Land Cover for the Eastern United States. *Remote Sensing of the Environment*. 76(3): 418-422.

Yarbro, L. A., E. J. Kuenzler, P. J. Mulholland, and R. P. Sniffen, 1984. Effects of Stream Channelization on Exports of Nitrogen and Phosphorus from North Carolina Coastal Plain. *Environmental Management*. 8(2):151-160.

Young, R. A., C. A. Onstad, D. D. Bosch, and W. P. Anderson, 1989. AGNPS: A Non-Point Source Pollution Model for Evaluating Agricultural Watersheds. *Journal of Soil and Water Conservation*. 44(2): 168-173.

APPENDIX

Table A.1: IPSI and NLCD original land cover classification schemes with generalized and detailed categories.

ISPI		*NLCD*	
Generalized	***Detailed Description***	***Generalized***	***Detailed Description***
Residential	Single family, medium density (2-5 per acre)	***Developed***	Low Intensity Residential
	Subdivision under construction		High Intensity Residential
	Single family, low density (fewer than 2/acre)		High Intensity Comm./Ind./Trans.
	Subdivision under construction (roads and some house construction)	***Barren***	Bare Rock/Sand
	Apartment/condominium complex		Quarries/Strip Mines/Gravel Pits
	Apartment/condominium complex under construction		Transitional
	Mobile home park	***Forest***	Deciduous Forest
	Farmstead with accompanying structures		Evergreen Forest
Commercial	Commercial, service, institutional		Mixed Forest
	Auto junkyard	***Shrubland***	Deciduous Shrubland
	Golf course		Evergreen Shrubland
	Race course		Mixed Shrubland
	Campground	***Non-Natural Woody***	Planted/Cultivated (orchards, vineyards, groves)
	Boat ramp	***Herbaceous Upland***	Grassland/Herbaceous
	Athletic field	***Planted/Cultivated***	Pasture
	Commercial, service, institutional		Row Crops
	Park		Small Grains
	Scenic overlook		Barren Land
	Landfill		Other Grasses (Urban/recreational)
	Water treatment	***Wetlands***	Woody Wetlands
	Sewage treatment		Herbaceous Wetlands
	Educational	***Water***	Water
	Religious		Perennial Ice/Snow
	Cemetery		
	Archaeological site		

Table A.1: Continued.

ISPI		*NLCD*	
Generalized	***Detailed Description***	***Generalized***	***Detailed Description***
Industrial	Industrial		
	Saw mill		
	Industry under construction		
Transportation	Transportation, Communication, Utility		
	Airport		
	Airport runway		
	Major highway right of way		
	Dam		
	Electric transmission right of way		
	Transmission facility, substation		
Crops/Pasture	Row crop: no residue, (0 to 10%)		
	Row crop: with residue, (>30%)		
	Strip cropped: alternating strips of cultivated and non-cultivated		
	Row crop: medium residue (10 to 30%)		
	Good pasture: well maintained		
	Fair pasture: uneven growth and condition, minimal maintenance		
	Heavily overgrazed pasture		
	Feedlot or loafing areas		
Forested	Orchards, vineyards, and nurseries		
	Forest land		
	Forest land: clear cut		
Rangeland	Shrub and brush: old field with volunteer woody growth		
Water	Water		
Disturbed land	Mining, quarries and borrow areas		
	Disturbed area		
National Park	Great Smoky Mountains National Park - Forest		

Table A.1: Continued.

ISPI		*NLCD*	
Generalized	***Detailed Description***	***Generalized***	***Detailed Description***
Wetland	Palustrine emergent		
	Palustrine forested/scrub-shrub		
	Palustrine scrub-shrub		
	Palustrine scrub-shrub/emergent		

Table A.2: IPSI, NLCD, and LULC-AVHRR reclassification into the six-class scheme.

IPSI		*NLCD*		*LULC-AVHRR*	
Re-class	**Description**	**Re-class**	**Description**	**Re-class**	**Description**
Urban	Commercial/Service/Institutional	***Urban***	Low Intensity Residential	***Urban***	Urban and Built-Up Land
	Industrial		High Intensity Residential		
	Transportation/Communication/ Utility		High Intensity Commercial		
	Single family: medium density - 2-5/acre		Other Grasses (Urban/recreational)		
	Single family: low density - < 2/acre				
	Apartment/Condominium complex				
	Mobile home park				
	Farmstead				
	Industry under construction				
	Airport				
	Major highway right of way				
	Dam				
	Electric transmission right of way				
	Auto junkyard				
	Golf course				
	Race course				
	Campground				
	Boat ramp				
	Athletic field				
	Park				
	Water treatment				
	Sewage treatment				

Table A.2: Continued.

IPSI		*NLCD*		*LULC-AVHRR*	
Re-class	**Description**	**Re-class**	**Description**	**Re-class**	**Description**
Urban	Educational	***Urban***		***Urban***	
	Religious areas				
	Cemetery				
	Archaeological site				
	Saw mill				
	Airport runway				
	Subdivision under construction				
	Subdivision under construction				
	Transmission facility/Substation				
Forest	Scenic overlook	***Forest***	Deciduous Forest	***Forest***	Deciduous Broadleaf Forest
	Forest land		Evergreen Forest		Deciduous Needleleaf Forest
	Palustrine emergent		Mixed Forest		Evergreen Broadleaf Forest
	GSMNP - Forest		Woody Wetlands		Evergreen Needleleaf Forest
	Palustrine scrub-shrub		Herbaceous Wetlands		Mixed Forest
	Palustrine forested/scrub-shrub				Herbaceous Wetland
	Palustrine scrub-shrub/emergent				Wooded Wetland
	Shrub and brush				Shrubland
					Mixed Shrubland/Grassland
Pasture	Pasture/Woodland	***Pasture***	Pasture	***Pasture***	Dryland Cropland and Pasture
	Feedlot or loafing areas				Irrigated Cropland and Pasture
	GSMNP - Grassland				Savanna
	Good pasture: well maintained				Grassland
	Fair pasture: uneven growth				
	Heavily overgrazed pasture				

Table A.2: Continued.

IPSI		*NLCD*		*LULC-AVHRR*	
Re-class	**Description**	**Re-class**	**Description**	**Re-class**	**Description**
Cropland	Orchards/Vineyards/Nurseries	**Cropland**	Row Crops	***Cropland***	Cropland/Grassland Mosaic
	Row crop: no residue (0 to 10%)				Cropland/Woodland Mosaic
	Row crop: with residue (>30%)				
	Row crop: medium residue (10 to 30%)				
	Alternating stripped crops				
Barren Land	Mining/Quarries/Borrow areas	***Barren Land***	Bare Rock/Sand	***Barren Land***	Barren or Sparsely Vegetated
	Disturbed area		Quarries/Strip Mines/Gravel Pits		
	Landfill		Transitional		
	Forest land: clear cut				
Open Water	Open Water	***Open Water***	Water	***Open Water***	Water Bodies

Table A.3: IPSI land cover composition associated with drainage area above each sampling site.

Site	*Urban* (%)	*Forest* (%)	*Pasture* (%)	*Cropland* (%)	*Barren Land* (%)	*Open Water* (%)	*Total Area* (ha)
EC1	5.8	51.9	37.2	3.5	0.6	0.6	9,940
EC2	5.5	49.8	39.3	3.8	0.6	0.6	8,551
EC3	8.5	16.5	63.9	8.1	2.2	0.8	1,890
EC4	3.6	61.4	32.2	1.5	0.1	0.4	5,384
EC5	4.7	54.5	38.4	0.8	0.1	0.3	3,509
EC6	1.7	91.0	7.2	0.0	< 0.1	0.0	1,110
EC7	7.5	27.9	60.7	1.0	< 0.1	0.6	1,612
EC8	2.8	88.9	7.8	0.0	0.1	0.1	1,233
LR1	0.9	96.5	2.4	< 0.1	< 0.1	0.1	31,678
LR10	4.7	80.1	13.4	1.2	0.3	0.3	69,673
LR11	56.2	13.7	24.1	2.4	3.2	0.4	9,820
LR12	5.9	75.1	16.4	1.8	0.3	0.4	77,717
LR13	21.0	36.8	35.3	5.7	0.8	0.3	3,721
LR14	11.7	67.9	17.4	1.9	0.6	0.4	88,305
LR2	0.0	99.9	0.1	0.0	0.0	0.0	27,448
LR3	0.9	96.0	2.8	< 0.1	0.1	0.1	33,352
LR4	1.3	94.8	3.6	< 0.1	0.1	0.1	37,026
LR5	1.8	92.4	5.3	0.1	< 0.1	0.4	6,978
LR6	1.3	93.1	5.5	0.0	0.1	0.1	3,257
LR7	1.8	93.2	4.3	0.3	0.1	0.2	49,726
LR8	16.3	50.0	31.1	2.1	0.3	0.3	8,195
LR9	5.8	51.9	37.2	3.5	0.6	0.6	9,938
LT1	14.8	35.6	43.4	5.4	0.6	0.2	2,627
LT2	6.7	80.8	11.8	0.1	0.2	0.4	5,071

Table A.3: Continued.

Site	*Urban* (%)	*Forest* (%)	*Pasture* (%)	*Cropland* (%)	*Barren Land* (%)	*Open Water* (%)	*Total Area* (ha)
NC1	2.8	88.9	7.8	0.0	0.1	0.1	3,739
NC2	21.5	37.2	34.3	5.7	0.8	0.3	3,605
NC3	29.4	31.6	33.6	3.7	1.2	0.3	2,259
NC4	29.4	31.6	33.6	3.7	1.2	0.3	558

Table A.4: Literature survey of TP and TN export coefficient values.

Land Cover	*TP (kg/ha/yr)*	*TN(kg/ha/yr)*	*Source*
Forest			
Forest[1]	0.01	0.10	Haith and Shoemaker (1987)
Deciduous Hardwood[2]	0.35	2.82	Taylor *et al.* (1971)
Mixed Pine and Hardwood[2]	0.43	0.28	Krebs and Golley (1977)
Mixed Pine and Hardwood[2]	1.50	0.20	Krebs and Golley (1977)
Oak-Hickory forest[2]	2.00	0.03	Henderson *et al.* (1977)
Woodland[3]	0.15	3.12	Northeast Florida Water Mngt Dis. (1994)
Urban			
Urban[1]	1.00	5.00	Rast and Lee (1983)
Industrial[2]	4.17	14.95	Betson (1978)
Industrial[3]	5.35	11.13	Northeast Florida Water Mngt Dis. (1994)
Commercial[2]	4.85	12.78	Betson (1978)
Commercial[3]	2.30	10.63	Northeast Florida Water Mngt Dis. (1994)
Low Density Urban[1, 4]	2.20	28.00	Haith and Shoemaker (1987)
Suburban/Residential[2]	0.43	1.56	Betson (1978)
Multi-family Residential[3]	2.21	7.92	Northeast Florida Water Mngt Dis. (1994)
Pasture			
Moderate dairy grazing[2]	0.14	3.46	Kilmer *et al.* (1974)
Heavy Dairy grazing[2]	0.16	10.99	Kilmer *et al.* (1974)
Pasture for brood cattle[2]	1.35	9.23	Krebs and Golley (1977)
Continuous grazing[2]	3.80	13.00	Krebs and Golley (1977)
Pasture[3]	0.56	6.28	Northeast Florida Water Mngt Dis. (1994)
Cropland			
Corn/Soybeans; no till[2]	3.70	19.30	McDowell *et al.* (1978)
Corn[2]	2.21	12.42	Smith *et al.* (1978)
Corn[2]	0.40	3.29	Bradford (1974)
Soybeans; conventional tillage[2]	17.64	46.50	McDowell *et al.* (1978)
Soybeans; no tillage[2]	2.60	5.10	McDowell *et al.* (1978)
Soybeans; no tillage[2]	7.20	23.00	McDowell *et al.* (1978)
Soybeans; no tillage[2]	3.70	19.30	McDowell *et al.* (1978)
Tobacco and Corn[2]	1.40	3.70	Krebs and Golley (1977)
Millet[2]	0.44	3.04	Bradford (1974)
Agricultural Crops[3]	1.05	17.54	Northeast Florida Water Mngt Dis. (1994)
Barren Land			
Inactive Ag. Land[1]	0.52	2.00	Haith and Shoemaker (1987)
Idle Land[4]	0.05	0.50	Loehr *et al.* (1989)
Idle Land[4]	0.25	6.00	Loehr *et al.* (1989)

[1] Compiled by Frink (1991).
[2] Compiled by Reckhow *et al.* (1980).
[3] Compiled by EPA (2001b).
[4] Complied by McFarland and Hauck (2001).

Table A.5: Calibration loading values. Nutrient loadings produced from ECM simulations at each ECV quartile.

	Unweighted ECM		*Weighted ECM*	
ECV Quartile	**TP***	**TN***	**TP***	**TN***
Minimum	1,750.5	23,424.3	1,695.3	20,365.2
Lower	5,817.8	48,828.7	5,541.7	45,693.3
Median	10,600.4	82,458.6	10,146.0	73,228.1
Upper	24,391.1	107,470.6	23,641.6	101,880.1
Maximum	52,988.2	164,585.1	52,125.6	155,268.3
Observed Loadings	10,704.1	87,235.6	10,704.1	87,235.6

* Nutrient loadings are represented as kg/year.

Table A.6: Categorical breaks in unweighted ECM results produced using all three land cover datasets. The natural break values in (a) TP and (b) TN distributions are used to define the four categories of nutrient risk.

a) TP (kg/ha/year)

	IPSI			***NLCD***			***LULC-AVHRR***		
Watershed Extent	**4th**	**5th**	**6th**	**4th**	**5th**	**6th**	**4th**	**5th**	**6th**
Low Value	0.08	0.31	0.31	0.09	0.26	0.26	0.00	0.00	0.00
1	0.59	0.57	0.50	0.53	0.51	0.50	2.27	2.72	0.97
2	0.94	0.89	0.74	0.81	0.73	0.53	7.83	7.26	5.24
3	1.42	1.34	1.15	1.20	1.06	0.80	16.38	14.84	8.55
High Value	2.19	1.96	1.65	1.93	1.49	1.25	32.03	23.98	14.12

b) TN (kg/ha/year)

	IPSI			NLCD			***LULC-AVHRR***		
Watershed Extent	4th	5th	6th	4th	5th	6th	4th	5th	6th
Low Value	0.05	0.24	0.24	0.08	0.23	0.20	0.00	0.00	0.00
1	1.81	1.57	1.72	1.46	1.16	1.07	21.61	17.07	14.24
2	4.60	4.04	4.17	3.78	2.99	2.78	63.64	54.50	36.59
3	7.45	6.70	6.84	6.27	5.43	5.10	109.86	94.29	60.96
High Value	11.08	10.14	9.06	11.39	8.66	7.64	199.52	149.34	91.77

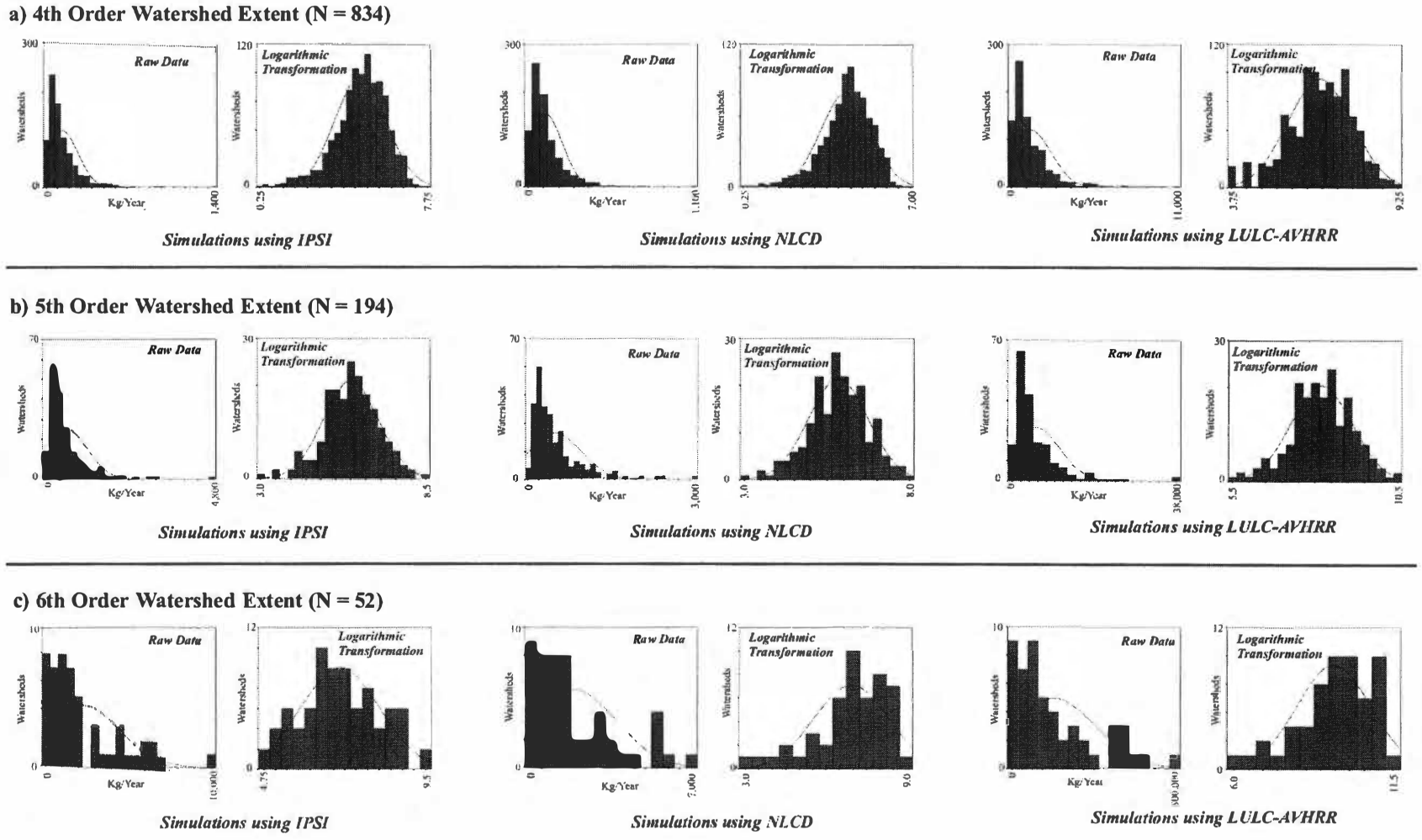
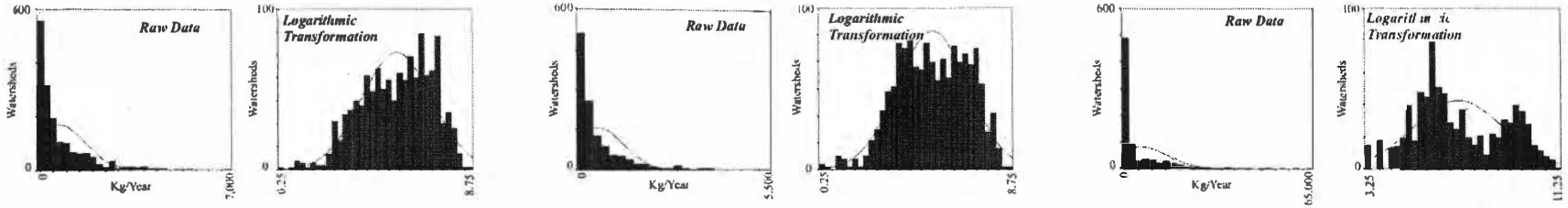
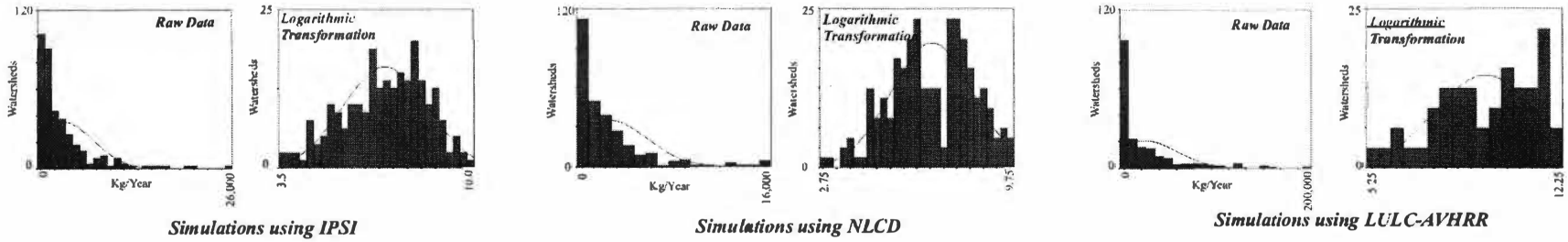


Figure A.1: Logarithmic transformation of TP results produced from ECM simulations. Unweighted simulations were conducted at the (a) 4th, (b) 5th, and (c) 6th order watershed extent using IPSI, NLCD, and LULC-AVHRR.

a) 4th Order Watershed Extent (N = 834)



b) 5th Order Watershed Extent (N = 194)



c) 6th Order Watershed Extent (N = 52)

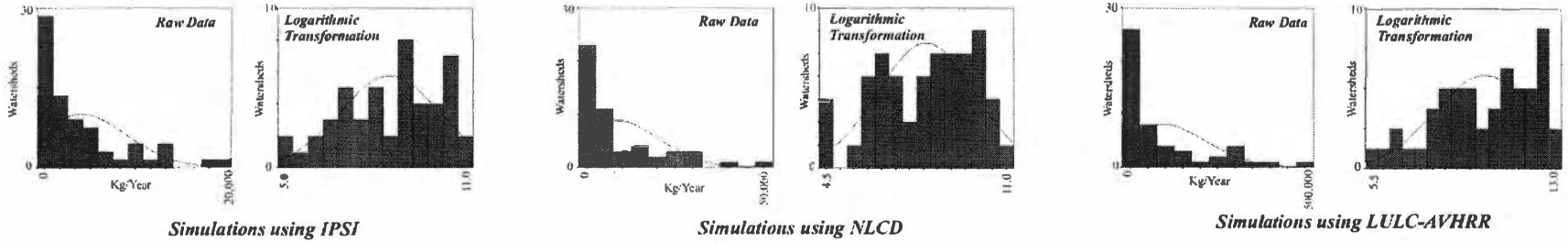


Figure A.2: Logarithmic transformation of TN results produced from ECM simulations. Unweighted simulations were conducted at the (a) 4th, (b) 5th, and (c) 6th order watershed extent using IPSI, NLCD, and LULC-AVHRR.

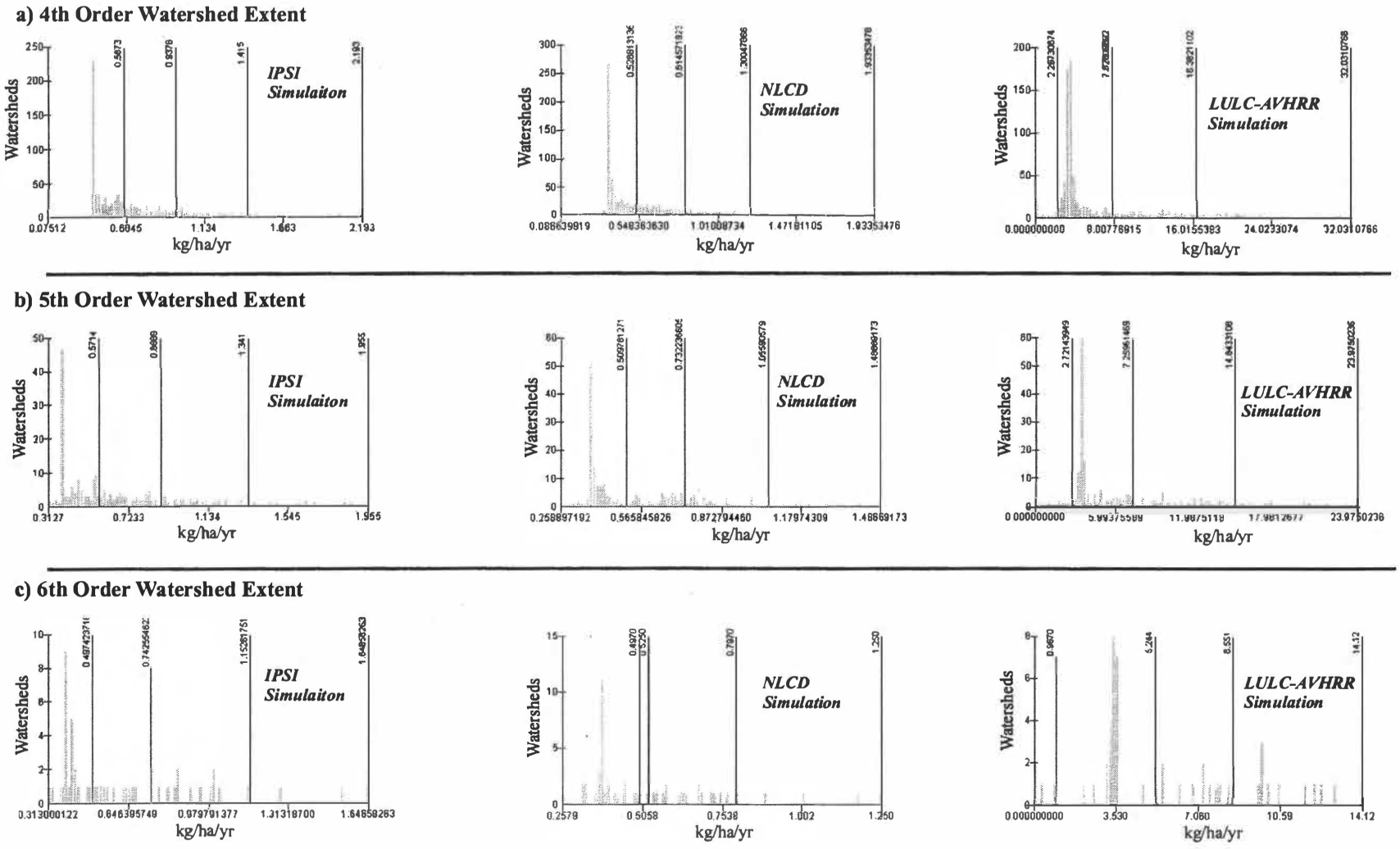


Figure A.3: TP flux by sub-watershed with natural-break values. Simulations were conducted at (a) 4th, (b) 5th, and (c) 6th order watershed extents using IPSI, NLCD, and LULC-AVHRR.

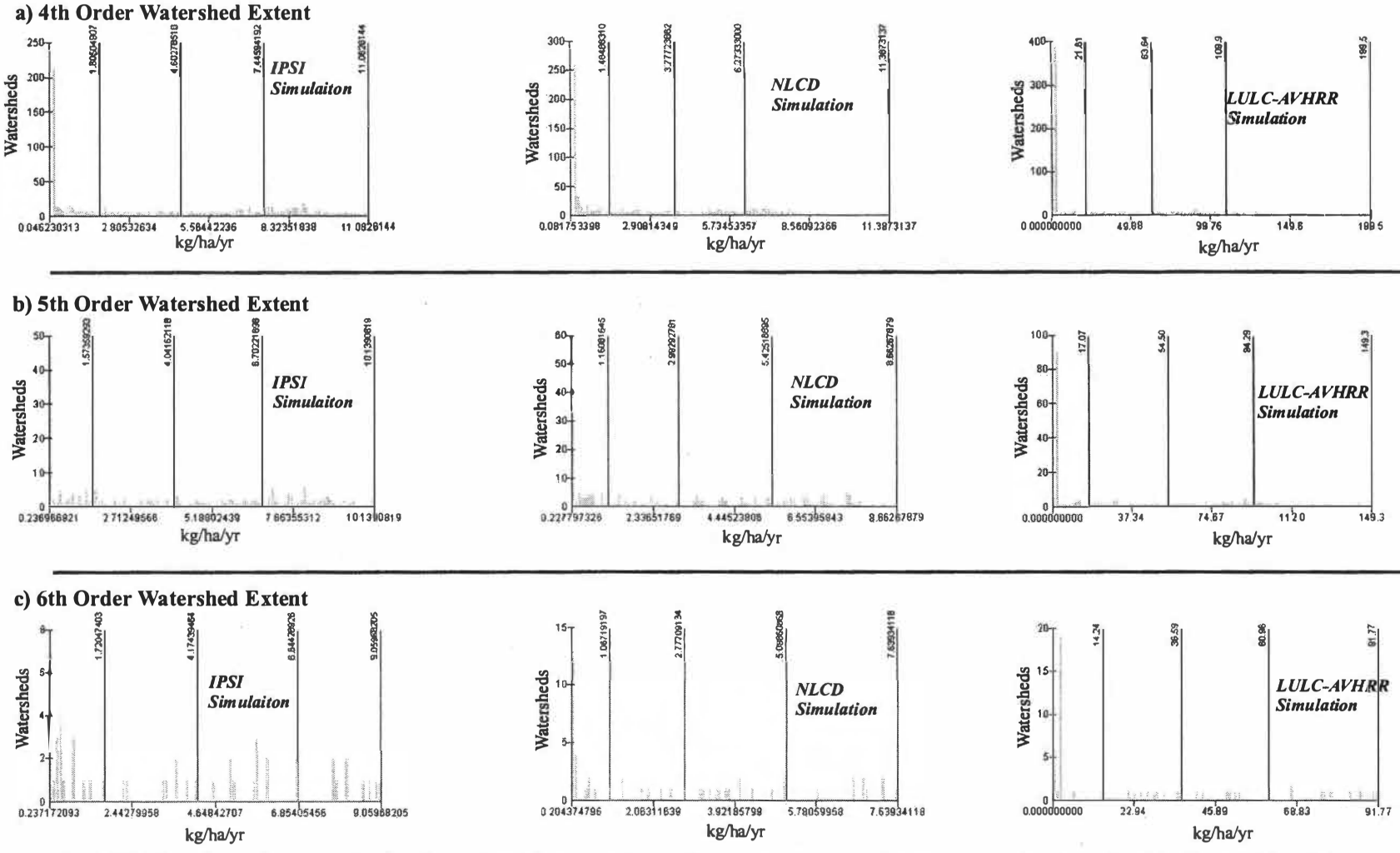


Figure A.4: TN flux by sub-watershed with natural-break values. Simulations were conducted at the (a) 4th, (b) 5th, and (c) 6th order watershed extent using IPSI, NLCD, and LULC-AVHRR.

VITA

Christopher Moniodes was born in Pittsburgh, Pennsylvania. He graduated from Chartiers Valley High School in 1996, then from Indiana University of Pennsylvania in 2000 with a B.S. in Regional Planning. After working as a GIS analyst in Pittsburgh for a year, he moved to Deerfield Beach, Florida, where he began graduate school at Florida Atlantic University in Geography. In fall 2002, Chris transferred to the Geography Department at the University of Tennessee in Knoxville and received a research assistantship from the Tennessee Valley Authority working in GIS and environmental assessment. Following the completion of the M.S. degree in Geography in May 2004, he plans to return to the northeast and continue working in the GIS industry.

5989 2949 6
06/23/04 MAB